

**From Research Center Borstel  
Leibniz-Center for Medicine and Biosciences  
Department of Immunochemistry and Biochemical Microbiology  
Director: Prof. Dr. Stefan Ehlers**

Division of Structural Biochemistry  
Head: Prof. Dr. Otto Holst

**Structural and biological characterization  
of the cell envelope components  
of bovine mastitis bacterial strains  
*Streptococcus agalactiae* 0250 and *S. dysgalactiae* 2023**

Dissertation  
For Fulfillment of  
Requirements  
for the Doctoral Degree  
of the University of Lübeck  
from the Department of Natural Sciences

Submitted by  
Olga Neiwert  
from Tomsk, Russia  
Lübeck, October 2013



First referee:	Prof. Dr. Otto Holst
Second referee:	Prof. Dr. Tamás Laskay
Date of oral examination:	25.02.2014
Approved for printing. Lübeck,	05.03.2014



# List of contents

<b>A</b>	<b>List of tables .....</b>	<b>V</b>
<b>B</b>	<b>List of figures .....</b>	<b>V</b>
<b>C</b>	<b>List of abbreviations .....</b>	<b>IX</b>
<b>1</b>	<b>Introduction.....</b>	<b>1</b>
	<b>1.1 Bovine mastitis - infectious disease in the dairy cattle .....</b>	<b>1</b>
	<b>1.2 Causes of mastitis .....</b>	<b>2</b>
	<b>1.3 Genus <i>Streptococcus</i> .....</b>	<b>3</b>
	1.3.1 Characteristics of <i>Streptococcus agalactiae</i> .....	3
	1.3.2 Characteristics of <i>Streptococcus dysgalactiae</i> .....	5
	<b>1.4 Cell envelope of Gram-positive bacteria .....</b>	<b>6</b>
	<b>1.5 Immunological background of infections.....</b>	<b>10</b>
	1.5.1 Innate immune recognition / TLR signaling .....	10
	1.5.2 HEK293 cells .....	12
	1.5.3 NKT cells .....	13
	1.5.4 Immunological and inflammatory processes in the bovine mammary gland.....	14
	<b>1.6 Surveillance, hygiene, vaccine development .....</b>	<b>16</b>
<b>2</b>	<b>Aims of the project .....</b>	<b>17</b>
<b>3</b>	<b>Materials and Methods .....</b>	<b>19</b>
	<b>3.1 Materials.....</b>	<b>19</b>
	3.1.1 Chemicals and reagents.....	19
	3.1.2 Buffers, solutions and media .....	20
	3.1.3 Cell lines .....	21
	3.1.4 Equipment and materials for chromatography.....	22
	3.1.5 Equipment and plastic material.....	23
	<b>3.2 General methods.....</b>	<b>24</b>
	3.2.1 Microorganisms and growth conditions .....	24
	3.2.2 Photography of bacterial species.....	24
	3.2.3 Transmission electron microscopy (TEM) .....	24
	<b>3.3 Isolation of bacterial components .....</b>	<b>25</b>
	3.3.1 Isolation of the LTA.....	25
	3.3.2 Isolation of glycolipids.....	25
	3.3.2.1 Bligh and Dyer extraction.....	25
	3.3.2.2 Visualization of the glycolipids.....	26
	3.3.3 Isolation of the WTA .....	27
	3.3.3.1 WTA isolation using 5% TCA .....	27
	3.3.3.2 WTA isolation via enzymatic treatment .....	27
	3.3.4 Acetone precipitation of EPS.....	28
	3.3.4.1 Enzymatic treatment of the supernatants .....	28
	3.3.5 Isolation of capsular polysaccharide .....	29
	3.3.6 Isolation of rhamnan .....	29
	<b>3.4 Analytical methods.....</b>	<b>30</b>
	3.4.1 Chromatographic methods.....	30
	3.4.2 Neutral sugar analysis .....	30
	3.4.3 Amino sugar analysis .....	31
	3.4.4 Fatty acids analysis .....	31
	3.4.5 Methanolysis .....	31
	3.4.6 Determination of the phosphate content.....	32
	3.4.7 Methylation analysis .....	33
	3.4.8 Determination of the absolute configuration .....	33
	<b>3.5 Preparative methods .....</b>	<b>33</b>
	3.5.1 Hydrofluoric acid treatment.....	33
	3.5.2 Hydrazinolysis .....	34

## II List of tables

---

<b>3.6 Structural analysis</b> .....	<b>34</b>
3.6.1 NMR spectroscopy .....	34
3.6.2 Mass spectrometry .....	35
3.6.2.1 ESI FT-ICR MS.....	35
3.6.2.2 MALDI FT-ICR MS .....	35
<b>3.7 Immunological methods</b> .....	<b>35</b>
3.7.1 Preparation of bacteria for stimulation of HEK293 cells .....	35
3.7.2 Transfection of HEK293 cells .....	36
3.7.3 Stimulation of HEK293 cells by cell envelope components.....	36
3.7.3.1 Dealanylation of LTA samples .....	37
3.7.3.2 Hydrogen peroxide treatment of LTA samples .....	37
3.7.4 hMNC assay .....	37
3.7.5 Phagocytosis assay.....	38
3.7.5.1 Separation of bovine leukocytes .....	38
3.7.5.2 Phagocytosis capacity assay .....	38
3.7.6 Stimulation of splenocytes by glycolipids.....	39
3.7.6.1 Assay with murine spleen cells.....	39
<b>4 Results</b> .....	<b>41</b>
<b>4.1 Morphology and growth of the bacteria</b> .....	<b>41</b>
4.1.1 Growth of streptococci.....	41
4.1.2 Transmission electron microscopy analyses.....	42
<b>4.2 Stimulation of HEK293 by <i>Streptococcus</i> cells</b> .....	<b>44</b>
<b>4.3 Structural analysis of LTA</b> .....	<b>45</b>
4.3.1 Isolation and compositional analysis of LTA .....	45
4.3.2 NMR investigation of the LTA.....	46
4.3.3 ESI/MS investigation of the LTA .....	48
4.3.4 Isolation and NMR investigation of the lipid anchor of the LTA .....	49
<b>4.4 Biological activity of the LTA</b> .....	<b>53</b>
4.4.1 HEK293 assay with native LTA.....	53
4.4.2 Stimulation of hMNC by LTA .....	54
4.4.3 Effect of Ala on biological activity of LTA in HEK293 cells .....	55
4.4.4 Phagocytosis capacity of the leukocytes in the presence of LTA .....	56
<b>4.5 Investigation of the glycolipids of <i>Streptococcus</i> species</b> .....	<b>57</b>
4.5.1 Isolation of the glycolipids .....	57
4.5.2 ESI FT-ICR MS and MALDI FT-ICR MS analysis of the glycolipids .....	59
4.5.3 NMR spectroscopy of the glycolipids .....	59
4.5.4 Immunological activity of the glycolipids in HEK293 cells.....	62
4.5.5 Stimulation of splenocytes by glycolipids.....	64
<b>4.6 WTA</b> .....	<b>65</b>
4.6.1 Isolation and investigation of the WTA from streptococci.....	65
4.6.2 NMR spectroscopy of WTA.....	67
4.6.3 WTA isolation by enzymatic treatment.....	70
<b>4.7 Rhamnose-rich polysaccharides</b> .....	<b>70</b>
4.7.1 Determination of the rhamnan structure of <i>S. agalactiae</i> 0250 .....	70
4.7.2 Determination of the rhamnan structure of <i>S. dysgalactiae</i> 2023 .....	76
<b>4.8 EPS</b> .....	<b>80</b>
4.8.1 EPS isolation and compositional analysis .....	80
<b>5 Discussion</b> .....	<b>83</b>
<b>5.1 Structural investigation and biological characterization of the LTA</b> .....	<b>83</b>
<b>5.2 Influence of LTA on phagocytosis</b> .....	<b>85</b>
<b>5.3 Structural investigation and biological characterization of the glycolipids</b> .....	<b>86</b>
<b>5.4 Structural investigation of the WTA</b> .....	<b>87</b>
<b>5.5 CPS</b> .....	<b>88</b>
<b>5.6 Rhamnose-rich polysaccharides</b> .....	<b>89</b>
5.6.1 Rhamnose-rich polysaccharide of <i>S. agalactiae</i> 0250.....	89
5.6.2 Rhamnose-rich polysaccharide of <i>S. dysgalactiae</i> 2023 .....	90
<b>5.7 Mannose-rich polysaccharides</b> .....	<b>91</b>
<b>5.8 Conclusion</b> .....	<b>91</b>

<b>6 Deutsche Zusammenfassung .....</b>	<b>93</b>
<b>7 References.....</b>	<b>95</b>
<b>Curriculum vitae .....</b>	<b>XIII</b>
<b>List of publications contributing to this study.....</b>	<b>XV</b>
<b>Acknowledgements.....</b>	<b>XVII</b>



## A List of tables

Table 1.1 Examples of different WTA structures from selected Gram-positive bacterial species. ....	7
Table 3.1 Chemical products .....	19
Table 3.2 Nutrient media .....	21
Table 3.3 Cell lines.....	21
Table 3.4 Materials and equipment for chromatography .....	22
Table 3.5 Equipment .....	23
Table 4.1 Calculated approx. molecular ratios of the FA from the LTA of <i>S. agalactiae</i> 0250 and <i>S. dysgalactiae</i> 2023.....	45
Table 4.2 <sup>1</sup> H and <sup>13</sup> C chemical shift data (in ppm) of the native LTA isolated from <i>S. dysgalactiae</i> 2023.....	47
Table 4.3 The assigned and calculated mass peaks from the LTA of <i>S. dysgalactiae</i> 2023.....	49
Table 4.4 <sup>1</sup> H and <sup>13</sup> C chemical shift data (in ppm) of the <i>O</i> -deacylated lipid anchor isolated from LTA of <i>S. dysgalactiae</i> 2023.....	51
Table 4.5 <sup>1</sup> H and <sup>13</sup> C chemical shift data (in ppm) of the aqueous phase components obtained after HF treatment of LTA isolated from <i>S. dysgalactiae</i> 2023.....	51
Table 4.6 Summary of fatty acid composition of the glycolipids from <i>S. agalactiae</i> 0250 and <i>S. dysgalactiae</i> 2023.....	59
Table 4.7 <sup>1</sup> H and <sup>13</sup> C chemical shift data (in ppm) of glycolipid G1 of <i>S. dysgalactiae</i> 2023.....	60
Table 4.8 <sup>1</sup> H and <sup>13</sup> C chemical shift data (in ppm) of G2 of <i>S. dysgalactiae</i> 2023 .....	61
Table 4.9 <sup>1</sup> H and <sup>13</sup> C chemical shift data (in ppm) of G3 of <i>S. dysgalactiae</i> 2023 .....	61
Table 4.10 Glycolipid structures .....	62
Table 4.11 Calculated molecular ratios of the neutral sugar analysis of the WTA preparations: fractions P1, P2 and P3.....	66
Table 4.12 <sup>1</sup> H and <sup>13</sup> C chemical shift data (in ppm) of the WTA preparation of <i>S. dysgalactiae</i> 2023.....	68
Table 4.13 Methylation analysis data of the rhamnose-rich polysaccharide of <i>S. agalactiae</i> 0250.....	72
Table 4.14 <sup>1</sup> H and <sup>13</sup> C chemical shift data (in ppm) of the rhamnan of <i>S. agalactiae</i> 0250 .....	74
Table 4.15 <sup>1</sup> H and <sup>13</sup> C chemical shift data (in ppm) of the GlcNAc in the rhamnan of <i>S. agalactiae</i> 0250.....	75
Table 4.16 Methylation analysis data of the rhamnose-rich polysaccharide of <i>S. dysgalactiae</i> 2023. ..	76
Table 4.17 <sup>1</sup> H and <sup>13</sup> C chemical shift data (in ppm) of the rhamnan of <i>S. dysgalactiae</i> 2023 .....	79

## B List of figures

Figure 1.1 General architecture of the cell envelope of the Gram-positive bacteria. ....	6
Figure 1.2 Type I LTA from <i>Staph. aureus</i> with gentiobiose in the lipid anchor [95]. .....	8
Figure 1.3 Examples of different polysaccharide capsules of Gram-positive bacteria. ....	9

## VI List of figures

---

Figure 1.4 Schematic structures of CPSs of <i>S. pneumoniae</i> Type 14 and <i>S. agalactiae</i> Type III.....	9
Figure 1.5 TLR signaling in conventional dendritic cells, macrophages and plasmoid dendritic cells. .....	11
Figure 1.6 Activation of CD1d-restricted NKT cells.....	13
Figure 4.1 Growth curves of <i>S. agalactiae</i> 0250 (A) and <i>S. dysgalactiae</i> 2023 (B). ....	41
Figure 4.2 Colonies of <i>S. agalactiae</i> 0250 (A) and <i>S. dysgalactiae</i> 2023 (B) grown on THB agar plate at 37°C for 48 h.....	42
Figure 4.3 Transmission electron micrograph of ultrathin sections of fixed <i>S. agalactiae</i> 0250 after 24 h of growing on THB medium (A) and BHI medium (B).....	43
Figure 4.4 Transmission electron micrograph of ultrathin sections of fixed <i>S. dysgalactiae</i> 2023 after 24 h of growing on THB medium (A) and BHI medium (B) supplemented with 2% of casein hydrolysate. ....	43
Figure 4.5 Stimulation of HEK293 <i>in vitro</i> by whole cells of <i>S. agalactiae</i> 0250 (AG, unfilled) and <i>S. dysgalactiae</i> 2023 (DG, fasciated) and activation of HEK293 cells transfected with boTLR2 + NF-κB (blue) and with NF-κB (brown). ....	44
Figure 4.6 <sup>1</sup> H NMR spectra of the native LTA from <i>S. agalactiae</i> 0250 and <i>S. dysgalactiae</i> 2023. ....	46
Figure 4.7 Exerpt of <sup>1</sup> H, <sup>13</sup> C HSQC-DEPT spectrum of the native LTA of <i>S. dysgalactiae</i> 2023.....	47
Figure 4.8 Part of the ESI FT-ICR mass spectrum from the native LTA of <i>S. dysgalactiae</i> 2023. ....	48
Figure 4.9 Exerpts of the overlaid <sup>1</sup> H, <sup>13</sup> C HSQC-DEPT spectra of <i>O</i> -deacylated lipid anchors of both <i>Streptococcus</i> species. ....	50
Figure 4.10 The structure of the LTA from <i>S. agalactiae</i> 0250 and <i>S. dysgalactiae</i> 2023.....	52
Figure 4.11 Activation either of TLR2- (A) or TLR4- (B) transfected HEK293 cells by LTA of <i>S. agalactiae</i> 0250 (AG, not filled) and <i>S. dysgalactiae</i> 2023 (DG, fasciated). ....	53
Figure 4.12 Stimulation of hMNC by H <sub>2</sub> O <sub>2</sub> -treated LTAs of <i>S. agalactiae</i> 0250 (AG, blue, not filled) and <i>S. dysgalactiae</i> 2023 (DG, blue, fasciated). ....	54
Figure 4.13 Activation of TLR2-transfected HEK293 cells by native LTA of <i>S. agalactiae</i> 0250 (AG, not filled) and <i>S. dysgalactiae</i> 2023 (DG, fasciated).....	55
Figure 4.14 Influence of LTA from <i>S. agalactiae</i> 0250 and <i>S. dysgalactiae</i> 2023 on the phagocytosis capacity of neutrophils. ....	56
Figure 4.15 Influence of LTA from <i>S. agalactiae</i> 0250 and <i>S. dysgalactiae</i> 2023 on the phagocytosis capacity of monocytes.....	57
Figure 4.16 TLC with overview of recovered lipids and glycolipids of <i>S. agalactiae</i> 0250 and <i>S. dysgalactiae</i> 2023.....	58
Figure 4.17 Purified glycolipids G1, G2, G3 of <i>S. agalactiae</i> 0250 and <i>S. dysgalactiae</i> 2023.....	58
Figure 4.18 The <sup>1</sup> H NMR proton spectra of the glycolipids from <i>S. agalactiae</i> 0250. ....	60
Figure 4.19 Activation of HEK293 cells transfected with NOD1, NOD2, TLR2 or TLR4 by G1 (blue), G2 (dark pink) and G3 (dark cyan) from <i>S. agalactiae</i> 0250 (AG, not filled) and <i>S. dysgalactiae</i> 2023 (DG, fasciated).....	63
Figure 4.20 Release of IL-4 and IFN-γ by murine splenocytes after incubation with 20 μg/ml of G1, G2 and G3 of <i>S. agalactiae</i> 0250 (AG) and <i>S. dysgalactiae</i> 2023 (DG) for 72 h.....	64
Figure 4.21 Phosphate content of the Q Sepharose fractions. ....	65
Figure 4.22 <sup>1</sup> H NMR spectra of P1, P2 and P3 isolated from <i>S. dysgalactiae</i> 2023.....	66
Figure 4.23 Exerpt of the <sup>1</sup> H, <sup>13</sup> C HSQC-DEPT spectrum of the WTA from <i>S. dysgalactiae</i> 2023.....	67
Figure 4.24 The proposed structure of the WTA from <i>S. agalactiae</i> 0250 and <i>S. dysgalactiae</i> 2023....	69
Figure 4.25 Exerpt of <sup>1</sup> H and overlaid <sup>1</sup> H, <sup>1</sup> H TOCSY and <sup>1</sup> H, <sup>1</sup> H ROESY NMR spectra of the rhamnose-rich polysaccharide preparation from <i>S. agalactiae</i> 0250.....	71

---

Figure 4.26 Excerpt of the $^1\text{H}$ , $^{13}\text{C}$ HSQC-DEPT spectrum of the rhamnose-rich polysaccharide of <i>S. agalactiae</i> 0250.....	73
Figure 4.27 Proposed structure of the rhamnose-rich molecule of <i>S. agalactiae</i> 0250.....	75
Figure 4.28 Excerpt of overlaid $^1\text{H}$ and overlaid $^1\text{H}$ , $^1\text{H}$ COSY and $^1\text{H}$ , $^1\text{H}$ TOCSY NMR spectra demonstrate the chemical shifts of the rhamnose-rich polysaccharide of <i>S. dysgalactiae</i> 2023.....	77
Figure 4.29 Excerpt of $^1\text{H}$ , $^{13}\text{C}$ HSQC-DEPT spectrum of rhamnan of <i>S. dysgalactiae</i> 2023.....	78
Figure 4.30 Proposed structures of the rhamnose-rich polymers of <i>S. dysgalactiae</i> 2023. ....	80
Figure 4.31 $^1\text{H}$ NMR spectra of the supernatant preparations after growth of <i>S. agalactiae</i> 0250 and <i>S. dysgalactiae</i> 2023 and without growth of bacteria (blank).....	81
Figure 5.1 The structure of GBS antigen. ....	90



## C List of abbreviations

μl	microliter
1D	one-dimensional
2D	two-dimensional
Ala	alanine
APC	antigen presenting cell
BHI	Brain-Heart Infusion
BMDC	bone marrow dendritic cells
ca.	circa
CAMP	cationic antimicrobial peptide
CFSE	carboxyfluorescein succinimidyl ester
COSY	correlation spectroscopy
CPS	capsular polysaccharide
d	day
DC	dendritic cell
DGlcDAG	diglucosyldiacylglycerol
DMSO	dimethyl sulfoxide
ELISA	enzyme-linked immunosorbent assay
EPS	exopolysaccharide
ESI FT-ICR MS	electrospray ionization Fourier-transform ion cyclotron resonance mass spectrometry
<i>et al.</i>	<i>et alii</i> , and others
FA	fatty acid(s)
FACS	fluorescence assisted cell sorting
FPLC	fast protein liquid chromatography
GalNAc	<i>N</i> -acetylgalactosamine
Galp	galactopyranose
GBS	Group B streptococci
GCS	Group C streptococci
GLC/MS	gas liquid chromatography/mass spectrometry
GlcNAc	<i>N</i> -acetylglucosamine
GlcP	glucopyranose
Gro	glycerol
h	hour
HEK293	human embryonic kidney cells 293

## X List of abbreviations

---

Hex	hexose
HIC	hydrophobic interaction chromatography
HMBC	heteronuclear multiple bond correlation
HMQC	heteronuclear multiple quantum coherence
HPLC	high-performance liquid chromatography
HSQC-DEPT	heteronuclear single quantum coherence distortionless enhancement by polarization transfer
iE-DAP	$\gamma$ -D-glutamyl- <i>meso</i> -diaminopimelic acid
IFN	interferon
IL	interleukin
iNKT cells	invariant NKT cells
l	liter
LGT	lateral gene transfer
LPS	lipopolysaccharide
LTA	lipoteichoic acid
MALDI FT-ICR MS	matrix-assisted laser desorption/ionization Fourier-transform ion cyclotron resonance mass spectrometry
MDP	muramyl dipeptide ( <i>N</i> -acetylmuramyl-L-alanyl-D-isoglutamine)
MEC	mammary epithelial cells
MGlcDAG	monoglucosyldiacylglycerol
MHC	major histocompatibility complex
min	minute
ml	milliliter
moDC	monocytes-derived dendritic cells
ms	millisecond
MurNAc	<i>N</i> -acetylmuramic acid
n. d.	not determined
NF- $\kappa$ B	nuclear factor kappa B
NKT cells	natural killer cells
NMC	National Mastitis Council
NMR	nuclear magnetic resonance
NOD	nucleotide-binding oligomerization domain
NOE	nuclear Overhauser enhancement
OD <sub>600</sub>	optical density, light absorbance measured at 600 nm
Pam <sub>3</sub> C-SK <sub>4</sub>	<i>N</i> -Palmitoyl- <i>S</i> -[2,3-bis(palmitoyloxy)-(2 <i>RS</i> )-propyl]-[ <i>R</i> ]-cysteinyl-[ <i>S</i> ]-seryl-[ <i>S</i> ]-lysyl-[ <i>S</i> ]-lysyl-[ <i>S</i> ]-lysyl-[ <i>S</i> ]-lysine
PAMP	pathogen-associated molecular pattern
pbMEC	primary bovine mammary epithelial cells

PBS	phosphate buffered saline
PGN	peptidoglycan
PGro-DGlcDAG	glucero-phosphoryl diglucosyldiacylglycerol
PMN	polymorphonuclear neutrophil leucocytes
PRR	pattern recognition receptor
Rbo	ribitol
Rha	rhamnose
ROESY	rotational nuclear Overhauser enhancement spectroscopy
RPMI	Roswell Park Memorial Institute
SCC	somatic cell count
SD	standard deviation
SDS	sodium dodecylsulfate
sp.	species
ssp.	subspecies
TA	teichoic acid
TEM	transmission electron microscopy
TFA	trifluoroacetic acid
THB	Todd Hewitt Broth
TLC	thin-layer chromatography
TLR	Toll-like receptor
TMS	tetramethylsilan
TNF- $\alpha$	tumor necrosis factor alpha
TOCSY	total correlation spectroscopy
TRAF	TNF-receptor associated factor
UK	United Kingdom
vol.	volume
WT	wild type
WTA	wall teichoic acid
$\alpha$ GalCer	$\alpha$ -galactosylceramide



# 1 Introduction

## 1.1 Bovine mastitis - infectious disease in the dairy cattle

Definition of the word mastitis literally comes from *mastos* (greek), the breast and *-itis* (greek), the suffix used always for inflammation [1]. Thus, the bovine mastitis is an inflammatory disease of the cow's mammary gland, which can vary from self-cure or easily treated local infection of the udder to a systemic infection in the worst case [2]. Mastitis is one of the most common and most costly infectious diseases for the dairy industry [3] and estimates for example at £300 million annually in the UK [4] or 118€ million annually in the Dutch dairy sector [5].

Briefly, in case of clinical mastitis a high grade of the bacterial infection is observed. The cow gets fever, a hot and swollen udder, flacks, gloats in the milk, and can even die if the infection becomes systemic [4]. On the contrary the sub-clinical mastitis proceeds without visible signs of the disease, the bacteria persist in the mammary tissue and the immune system of the cow does not react efficient enough to the presence of bacteria [6]. The problem in this case is the not identified and therewith untreated infection.

Generally, the differentiation between healthy and infected gland is possible by monitoring the changes in the somatic cell count (SCC) of the milk. Whereas the milk from the uninfected gland has a cell count of about 200,000 cells/ml, the sub-clinically infected gland contains ~250,000 cells/ml and clinically infected gland even in excess of ~2,000,000 cells/ml [7]. Healthy cow produces milk, which contains losted epithelial cells, leucocytes, macrophages, and neutrophils. With the invasion of bacteria in the mammary gland, SCC, especially the number of neutrophils increases dramatically [7]. This inflammatory response affects the milk quality and the milk yield, the latter of which is well investigated [8]. The quality deteriorates due to loss of protein and lipid amount in the milk. Decrease of proteins was monitored for example in infections with bovine *Streptococcus agalactiae* species [9], and SCC in the milk have negative effects on the yield and quality of Cheddar cheese [10]. Beside the unmarketable milk products and the loss of usual milk yield, the consequences of the mastitis infected cow are veterinary services and drug treatment of the cow – all of them lead to an economy loss [4, 11]. Antibiotic treatment is one of successful therapies against bovine mastitis. However this therapy accompanies the risk of the development of various antimicrobial resistance responses of bacteria [12–14] and of the drug residues in the milk. Additionally, bovine mastitis is a painful disease and a high cytokines activity leads to changes not only in the milk but in cows` blood, and to adverse effects like tissue destruction,

hormone disorders or affection of the reproduction organs [15]. Thus, the increase of the disease outbreaks contributes to the welfare and care of animals in cattle.

A preventive five-point-plan was developed in the 1960ies with recommendations and requests like disinfection of dipping teats after every milking, culling of chronic mastitis cases and treating and strict recording of all clinical cases [16]. In the 1970ies the relative merits of hygiene procedures were determined. It became clear, that the level of infections in a herd is dependent from the new infection rate and the duration of infection, and that it is important to made the duration of infection shorter [17]. In the last 40-50 years the implementation of this guide rules helped the dairy cattle to minimize constantly the transmission of infection. In the 1960ies the clinical mastitis incidence was detected of more than 140 cases /100 cows/ year [4], and in the studies since 1980 and 2008 incidence account varies between 17 and 65 cases/ 100 cows/ year [18–20]. At the end of the last century the five-point-plan was extended by the National Mastitis Council (NMC) to a ten-point-plan points with more guide lines to control the disease [21]. In consideration of the fact that the inflammation of the cows` mammary gland is still a big problem in the cattle the pharmaceutical industry, variable research branches and the veterinary medical care still quest for better knowledge of bovine mastitis pathogenesis and for better effective treatment solutions.

### 1.2 Causes of mastitis

Bovine mastitis can be caused by more than 135 different microorganisms, most of which are bacteria, but fungi and algae were also detected [22]. Worldwide *Staphylococcus aureus* [23], *Streptococcus uberis* [24], *S. agalactiae* [25, 26], *Streptococcus dysgalactiae* and *Escherichia coli* [23] represent the five common pathogen types of bacterial bovine mastitis. Other bovine mastitis Gram-negative bacteria are further present *Klebsiella* spp., *Serratia* spp. and *Enterobacter* spp. species [27], and representative Gram-positive bacteria are e. g. coagulase-negative staphylococci (CNS) or *Mycobacterium bovis* [21].

In the most causes of clinical mastitis *S. uberis*, *E. coli*, and coagulase-positive staphylococci (CPS) are still observed. In the cases of subclinical mastitis comprise a big cause CPS, CNS, and streptococci like *S. uberis*, *S. agalactiae*, *S. dysgalactiae* [28, 29].

### 1.3 Genus *Streptococcus*

Molecular biological investigations such as DNA-DNA reassociation experiments and 16S RNA sequencing improved the taxonomy of streptococci noticeably during the last 20 years. Thus, *Enterococcus* and *Lactococcus* split off from the genus *Streptococcus* and became own genera [30]. Today the genus *Streptococcus* belonging to the *Streptococcaceae* family contains of over 50 species, which are catalase-negative Gram-positive cocci, tending to form chains in liquid medium [31, 32]. Streptococci can be differentiated by the hemolysis reaction which is helpful for their clinical identification. Beta-hemolytic streptococci were subdivided in 1933 by Lancefield into defined antigen groups A, B, C, E, F, and G [33]. Based on serogrouping the current division and identification of the streptococci remain Lancefield groups [31]. Pyogenic streptococci are closely related to each other and include beta-hemolytic *S. agalactiae*, *S. canis*, *S. dysgalactiae* [subdivided in *S. dysgalactiae* subsp. *dysgalactiae* (zoonotic pathogens) and *S. dysgalactiae* subsp. *equisimilis* (human pathogens)], *S. equi*, and *S. pyogenes*. Thereby *S. dysgalactiae* subsp. *dysgalactiae* represents an exception of the pyogenic streptococcal group as non-hemolytic species [30, 31].

Streptococci are characterized by their incapability of respiratory metabolism due to the lack of heme compounds. Bacteria of the genus *Streptococcus* are facultative anaerobic, their temperature optimum is around 37°C and some of them like viridans streptococci and *S. pneumoniae* require 5% CO<sub>2</sub> for an adequate growth [30].

#### 1.3.1 Characteristics of *Streptococcus agalactiae*

*S. agalactiae* is non-motile coccus, it possesses the Lancefield Group B carbohydrate. A peptidoglycan-anchored antigen in their cell envelope, which assigns it to the Group B streptococci (GBS) [31], and is a common human as well as zoonotic pathogen. In humans *S. agalactiae* can persist often asymptotically in genitourinary tract of woman [34], is capable to cause meningitis, sepsis and respiratory infections of neonates and infants in the first 3 months of life [35, 36]. Furthermore, the infections by *S. agalactiae* of elderly people are known [37].

*S. agalactiae* was at first identified as bovine mastitis pathogen in 1887 [38]. It has been detected as agent of clinical mastitis [29], but causes mostly subclinical mastitis in ruminants [9] and in sheep [39]. This bacterial species is associated with a high SCC (> 700,000 cells/ml) in the clinical mastitis cases [40]. *S. agalactiae* persists mainly in the udder and hardly survives in the environment. It was defined by A. Biggs as the most contagious (transfer from cow to cow) of the

contagious bovine mastitis causative agents [2]. In the 1970ies-1980ies this bacterial strain was very common in dairy herds [17]. Especially the contagious character of *S. agalactiae* helped to minimize its eradication by cleaning and disinfection sanctions as well as successful antibiotic treatments, and in 1998 it was described even as eliminated [41, 42]. Nevertheless *S. agalactiae* is still common in dairy industry and has been frequently isolated in several countries [28, 29, 43]. Determination of pathogens and their resistances of ca. 1% samples from all bavarian milk suppliers identified 1.7% *S. agalactiae* strains in 1997-1998 and 4.3% *S. agalactiae* pathogens in 2008-2009 [44]. Penicillin resistance possessed 2.5% of isolated *S. agalactiae* species of this study, resistances of bovine GBS against other antimicrobials are also described [28, 29, 44].

In mouse and rat models different virulence factors of *S. agalactiae* have been identified, like laminin-binding protein (*lmb*), fibronectin-binding protein (*pavA*), fibrinogen-binding protein (*fnb*, *fnbA*),  $\alpha$ -C protein,  $\beta$ -C protein (*cba*), C5a peptidase (*scp*),  $\beta$ -hemolysin/cytolysin [45], and capsule [46]. Bovine *S. agalactiae* isolates were identified to be positive for the *cfb*, and negative for the *pavA* (16 of 17), *fnb*, *lmb*, *scpB*, and *cba* genes, whilst the human *S. agalactiae* pathogen species were positive for all these mentioned virulent factors. Thus, the bovine *S. agalactiae* isolates were discussed either to be less virulent than human strains or to possess otherwise adherence and invasion facilities [47]. Another study sequenced for the presence of laminin-binding protein and the C5a peptidase genes in GBS, which were present in all human isolates. The *scp* gene was identified in all bovine species, but laminin-binding protein was produced only by 32% of bovine *S. agalactiae* [48].

Strain-variable genes of surface proteins are putative virulent factors, which can be used as marker for serotyping of *S. agalactiae* species. This are the  $\alpha$ -like proteins Alp (*bca*), Alp1 (*alp1*), Alp2 (*alp2*), Alp3 (*alp3*), Alp4 (*alp4*), R4 (*rib*), non-Alp proteins C $\beta$  (*bac*), protein R3 and recently recognized proteins Z1 and Z2 [49, 50].

CAMP factor (*cfb*) is an extracellular protein of GBS, which renders streptococci haemolytic reaction, a lysis of erythrocytes by growing on agar media supplemented with blood [51]. It was established as a useful characteristic for GBS identification in the clinical laboratory, and the cationic antimicrobial peptide CAMP factor was presumed to be also a virulent factor of GBS [52]. Later this protein was observed in the mouse model, and was postulated to be non virulent [53]. A new CAMP factor II of *S. agalactiae* was characterized in 2012, it may confere co-hemolytic activity in case of loss of genomic CAMP factor. This toxin can be transferred by conjugation (ICEs – Integrative and Conjugative Elements) to other *Streptococcus* species and lead to the result, that hemolytic properties possess not only GBS [54, 55]. Further discussed pathogenic factors of GBS are pili proteins from human *S. agalactiae* species which were shown to be relevant for adherence and invasion of lung and cervical epithelial cells [56].

Beside of the virulence of the veterinary and human GBS isolates molecular biologists attempt to find out the transmission routes and the origin lineage of virulent species. Multilocus sequence typing (MLST) was used to screen humans and cows from the farms for virulent and nonvirulent GBS species, in which the species were symptomatic or asymptomatic in one or in both groups. The investigation demonstrated the transmission of the genes between human and bovine isolates [57]. Bisharat *et al.* proved by MLST that hyperinvasive neonatal GBS has arisen from a bovine lineage [58], however investigations of GBS genes applying multiple-locus variant-repeat assay (MLVA) could not confirm this [59]. In 2011 the first complete sequenced genome of bovine clinical mastitis *S. agalactiae* FSL S3-026 was published. The comparison of 8 recognized novel islands between 20 human and 20 bovine GBS isolates revealed a strong differentiation, especially in fermentation of lactose of both pathogenic groups [60]. Additionally, the same study demonstrated 99% of similarity of lactose and fructose operon sequences of bovine *S. agalactiae* with bovine mastitis isolate *S. dysgalactiae* subsp. *dysgalactiae* and the similarity of nisin U operon with bovine mastitis isolate *S. uberis* and proved therewith the lateral gene transfer (LGT) of streptococci in the udder. The authors refer to published tetracycline resistance genes of *S. pneumoniae* and *S. dysgalactiae* subsp. *equisimilis* associated with LGT and warn of transmission of antibiotic resistances between bovine mastitis streptococci in the same environment [60].

### 1.3.2 Characteristics of *Streptococcus dysgalactiae*

*S. dysgalactiae* subsp. *dysgalactiae* was first described 1932 by Diernhofer as an udder pathogen. It belongs to the Lancefield group C *Streptococcus* (GCS) and is non-hemolytic [61]. It is exclusively a zoonotic pathogen, and is reported to be a contagious as well as an environmental bacterium. *S. dysgalactiae* was identified to be transmitted from cow to cow during milking processes and was identified in reservoirs like cow's tonsils, mouth and vagina, and in herds during the nonlactating period (reviewed in [39, 62]). *S. dysgalactiae* subsp. *dysgalactiae* is mostly associated with subclinical bovine mastitis [63, 64], but it was also isolated from clinical infected udder [65]. *S. dysgalactiae* represents one of 5 causative agents of summer mastitis, a bacteriological inflammation and udder sepsis of non-lactating cows and heifers, which occurs in particular during the summer months [16, 66].

The bacterium was additionally described to cause subcutaneous cellulitis with toxic shock-like syndrome in a cow [67], ovine subclinical mastitis [39], piscine granulomatous inflammatory disease, and septicemia and bacteremia in puppies [68].

In case of *S. dysgalactiae* a variety of surface proteins has been identified acting as virulence factors such as plasminogen activator PadA [63, 69], the proteins Mig and Mag with  $\alpha_2$ -

macroglobulin-, albumin- and IgG- binding domains [70, 71], receptors binding host-derived proteins fibronectin, fibrinogen, vitronectin, und collagen [62]. Sequencing of GCS genes revealed a range of virulence genes coding for Mig [72], Mag [70] and M-like protein [73], antibiotic resistances, especially against tetracycline of all investigated *S. dysgalactiae* species, or bacteriophage-associated virulence genes [74].

## 1.4 Cell envelope of Gram-positive bacteria

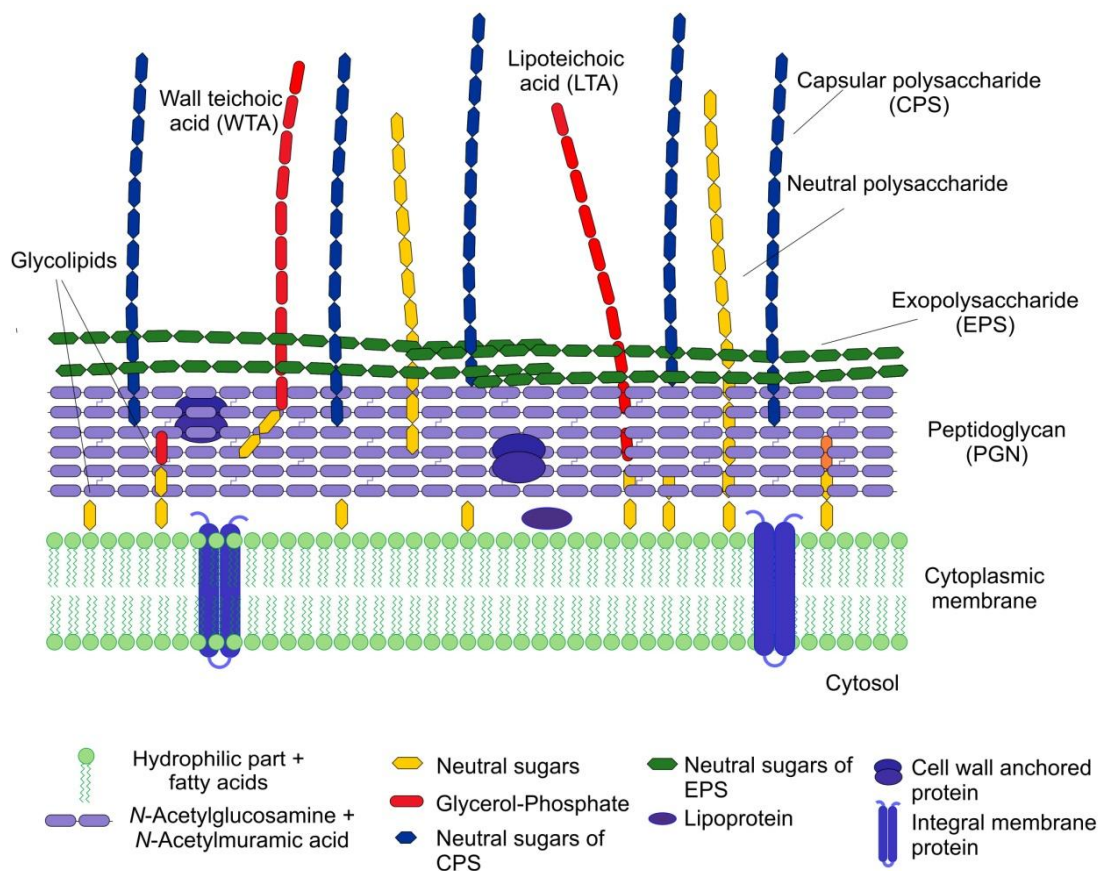


**Figure 1.1** General architecture of the cell envelope of the Gram-positive bacteria.

The names of the proteins were taken from [75].

The cell surface of Gram-positive bacteria (Figure 1.1) consists of one cytoplasmic membrane, and up to 70% of peptidoglycan (PGN) with repeating disaccharide  $\beta$ -D-MurNAc(1 $\rightarrow$ 4)- $\beta$ -D-GlcNAc, which is cross-linked by short peptides to many layers [76]. The peptidoglycan peptides linkage vary in their composition and contain either four L- and D- amino acids, or meso-diaminopimelic acid (DAP), as the third amino acid (DAP-type PGN) or L-lysine as the third amino acid (Lys-type PGN) [77]. The PGN itself can be decorated by addition of teichoic acids, phosphorylation or carbohydrates attachment [78, 79].

Further typical anionic polymers of Gram-positive bacterial cell wall are teichoic acids. Wall teichoic acids (WTA) are covalently attached to the PGN by distinct linkages and consist of repetitive polyol phosphate, glucosylpolyol phosphate units (Table 1.1) [80–82] or even the mixture of both [83]. Additionally, the repeating units of the WTA hydrophilic backbone can be substituted by carbohydrates or esterified by D-alanine (D-Ala) [84]. The mutation of the first synthesis enzyme was shown to be not essential for the viability of *Bacillus subtilis*. The WTA was reported to be important for maintenance of the cell shape and cell form [85], adherence to host cells and colonization of the host tissue [86] and to contribute to lysozyme [87] as well to antibiotic resistance [88].

**Table 1.1 Examples of different WTA structures from selected Gram-positive bacterial species.**

Strain	Teichoic acid	Linkage unit	PGN	Ref.
<i>Staphylococcus aureus</i>	$\begin{array}{c} \text{R} \\   \\ \text{-[Rbo-P]}_n\text{-Rbo-P-} \end{array}$	[Gro-P] <sub>2</sub> -β-ManNAc-(1→4)-GlcNAc-P-	-GlcNAc-(1→4)-MurNAc	[80]
<i>Bacillus subtilis</i>	$\begin{array}{c} \text{R} \\   \\ \text{-[Gro-P]}_n\text{-[Gro-P]}_a\text{-} \end{array}$	-β-ManNAc-(1→4)-GlcNAc-P-	-GlcNAc-(1→4)-MurNAc	[81]
<i>Bacillus coagulans</i> AHU 1366	[→6)-α-Gal-(1→2)-Gro-P-(1→] <sub>n</sub> -	-[Gro-P] <sub>2</sub> -β-Glc-(1→4)-GlcNAc-	-GlcNAc-(1→4)-MurNAc	[82]

R =, in *Staph. aureus* –H, D-Ala, N-acetylglucosamine (-GlcPNAc); in *B. subtilis* –H, D-Ala, -GlcPNAc.

Lipoteichoic acids are produced by low G+C Gram-positive bacteria, and represent amphiphile molecules with a hydrophilic backbone and a glycolipid anchor, which is localized in the cytoplasmic membrane [89, 90]. Type I LTA contains repetitive units of glycerol phosphate (Gro-P) or ribitol phosphate (Rbo-P) substituted by D-Ala, sugars or amino sugars, and is linked to a lipid anchor containing kojibiose or gentiobiose (Figure 1.2). It is the most common LTA type. Type II LTA is made up of two galactose residues linked to GroP (Gal-Gal-GroP) repeats and type III of Gal-GroP repeating units. The tetrasaccharide repeating units of *S. pneumoniae* species are substituted by phosphorylcholine and connected by RboP, and represent the LTA polymer of type IV [91–94].

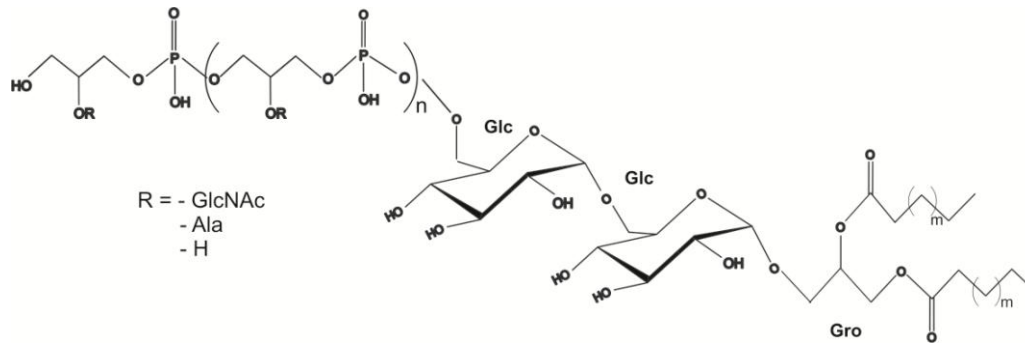


**Figure 1.2** Type I LTA from *Staph. aureus* with gentiobiose in the lipid anchor [95].

Lipoteichoic acid was discussed to be indispensable for bacterial viability [96], but to play a role in cell division and separation [97], adhesion capacity to host cells [98, 99] and to be relevant in the inflammatory response of the host [89]. Moreover, mutations in LTA as well as in WTA expression genes in *Staph. aureus* lead to synthetic lethality and demonstrated that the bacteria need at least one of both polymers for the growth [97].

Some Gram-positive bacteria produce teichuronic acids in low amount beside teichoic acid (TA), while under phosphate-limiting conditions they are capable to build them in higher quantities instead of TA. These polymers consist of uronic acids and amino sugars in the repeating unit part and are also covalently attached to the peptidoglycan [100].

Long-chain polymers of all TA extend through and beyond PGN layers. Their long chains of repetitive glycerolphosphates as long as negative charges of anionic cell wall polysaccharides (CWPs) of some bacteria result in a negatively charged cell envelope of Gram-positive bacteria [101]. On the contrary, D-alanyl esters of TAs are protonated, positive charged and rende teichoic acids zwitterionic. The negative charges of TA are described to be capable to assimilate the cations and to function as a kind of biophysical barrier [91].

Gram-positive bacteria are capable to produce a hydrated layer around the cell, which is rich of carbohydrates, so called capsular polysaccharide (CPS) or K-antigen [102]. The attachment of the capsule to the cell wall is poorly understood. Covalent linkages between capsular polysaccharide and the PGN are known for *Staph. aureus*, *S. pneumoniae* and *S. agalactiae* [103–105]. Gram-positive bacteria are classified into serotypes according to the variability of capsule polysaccharides [102]. The diversity of CPS of Group A streptococci *S. pneumoniae* is very high (93 different types) and the differences between the species are also remarkable [106]. The typical component of all 10 different types (Ia, Ib, II-IX) of *S. agalactiae* is *N*-acetylneuraminic acid (NeupNAc) [107, 108] (Figure 1.3). Group C and D streptococci possess hyaluronic acid as CPS component [109]. Prevention of cell dehydration and entrance of unfavorable factors as well as the regulation of the water regime are believed to be the important functions of the capsule. The

cases, where the capsules of different species are identical or are different only in one molecule are known and are investigated with great interest for their immunological properties [110] (Figure 1.4). Due to the immunogenicity of the capsules, the induction of specific antibodies against this polysaccharide by the immune system of humans and animals, CPS conjugate vaccines have been developed [111].

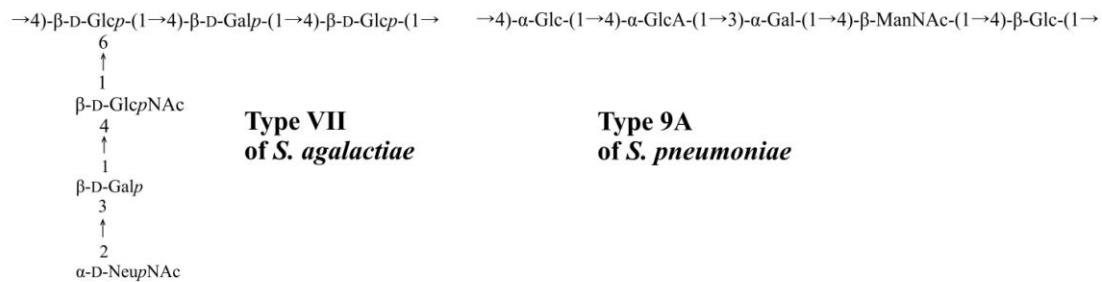


**Figure 1.3 Examples of different polysaccharide capsules of Gram-positive bacteria.** GlcA stands for glucuronic acid, ManNAc for mannosamine. From [106, 108].

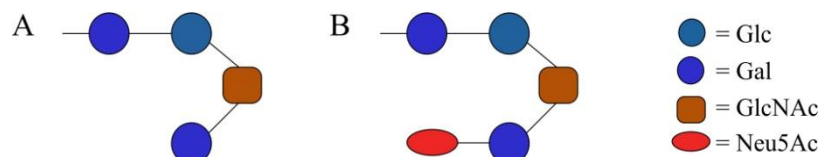


**Figure 1.4 Schematic structures of CPSs of *S. pneumoniae* Type 14 and *S. agalactiae* Type III.** From [110], modified.

Some Gram-positive bacteria produce so called S-layer, a crystalline layer of surface proteins with considered functions to be a protective layer, a setting up for enzymes, a virulent factor, and other more [112, 113]. Furthermore, the Gram-positive cell envelope is rich of inner membrane proteins, glycoproteins, and of phospholipids and glycolipids. The proteins can be associated with the membrane, anchored in the membrane, covalently linked to the PGN or reside only for a while in the outer leaflet of the cytoplasmic membrane and act as superantigens, or present protein systems, which influence the protein folding and help to transfer other proteins across the cell wall [75, 114].

The glycolipids or glycoglycerolipids are composed of fatty acids covalently linked to the mono- or disaccharideglycerol. The phosphoglycolipids contain GroP groups linked to one, two or three pyranoses. Their distribution across the Gram-positive bacteria and the different types are well investigated, but their function needs elucidation. Some glycolipids were demonstrated to anchor the LTA in the membrane [98], to play a role in biofilm formation [115], and to act as immunostimulating agents [116].

## 1.5 Immunological background of infections

### 1.5.1 Innate immune recognition / TLR signaling

The conserved Toll-Dorsal pathway in *Drosophila* discovered first in the 90ies has a great similarity to the interleukin-1 receptor (IL-1R) pathway of mammals and even to innate immune pathway of plants [117]. The sequencing of the *Drosophila* and mammalian genes identified a common Toll-like pathway. Innate immunity is not antigen-specific, but essential for organisms having the task to alert them in case of infections, to initiate the protective signaling cascades and to stimulate the adaptive immune response in vertebrates [118]. Microbial pathogens invading a host carry a variety of conserved toxins or pathogen-associated molecular patterns (PAMPs), which have three basic properties. PAMPs are build only by a microbe and not by the host, they are invariant in a given pathogen class, and they are essential for the pathogen [118]. These characteristics allow the detection of PAMPs by pattern recognition receptors (PRR), especially by the family of Toll-like receptors (TLRs), and to initiate the signaling pathways of the early innate immune response [119]. Altogether 13 TLRs are described [120]. Briefly, there are ten human and twelve murine TLRs - TLR1 to TLR10 in humans, and TLR1 to TLR13 in mice, in which TLR13 is the homolog of TLR10 being a pseudogen. Every TLR subfamily identifies specific PAMPs, and most of these ligands are already characterized. For example, TLR2 recognizes lipopeptides, TLR3 recognizes dsRNA, TLR4 is responsible for the identification of lipopolysaccharide (LPS), TLR5 recognize flagellin and TLR 7-9 detect nucleic acid and heme motifs [120]. TLRs reside on the surface of a rash of innate immune cells capable to interact with conserved bacterial molecules during the inflammation process. These are macrophages, dendritic cells, neutrophils, eosinophils, mast cells and Natural Killer cells [121]. Finally, innate immunity is necessary not only for the instant elimination of the pathogen, but also for the development of the adaptive immune response.

TLRs are type I transmembrane glycoproteins. They consist of the conserved extracellular N-terminal domain, the transmembrane helix domain and an intracellular C-terminal toll-interleukin-1 receptor (TIR) homology domain [122]. The  $\alpha$ -helices and  $\beta$  sheets of TLR glycoproteins build horseshoe-like tertiary structures. The polypeptide chain above the plasma membrane contains 16-28 leucine-rich repeats (LRRs), and bind as recognition domain to the ligands or PAMPs on the concave site of the horseshoe-like loop of TLRs [123, 124]. The twist of the tertiary structure is dependent from the amount and place of the leucine and other amino acids. TLRs initiate the signaling cascades as dimers. TLR4 and TLR3 form homodimers whereas TLR2 forms heterodimers with either TLR6 or TLR1 in order to recognize the agonists [125]. For example, the interaction of TLR1 and TLR2 is supported by hydrogen bonds and by hydrophobic interaction of the region nearby the binding pockets of both TLRs [126]. The binding pockets of TLR 1 and 2

are decorated with hydrophobic residues and together in a complex they are capable to accommodate tri-acetylated lipopeptides [126]. On the basis of the hydrophobicity of one pocket from TLR2 and one pocket from TLR6, the TLR2/TLR6 complex binds di-acetylated lipopeptides [127]. Some TLRs such as TLR3, TLR7, TLR8 and TLR9 are located in intracellular vesicles, like endosome and ER, whilst the other TLRs are expressed in the cell surface. Nevertheless of the expression of TLRs in different cellular compartments, nearly all signaling cascades are MyD88 (myeloid differentiation primary – response gene 88) -dependent except of endosomal TLR3 [124].

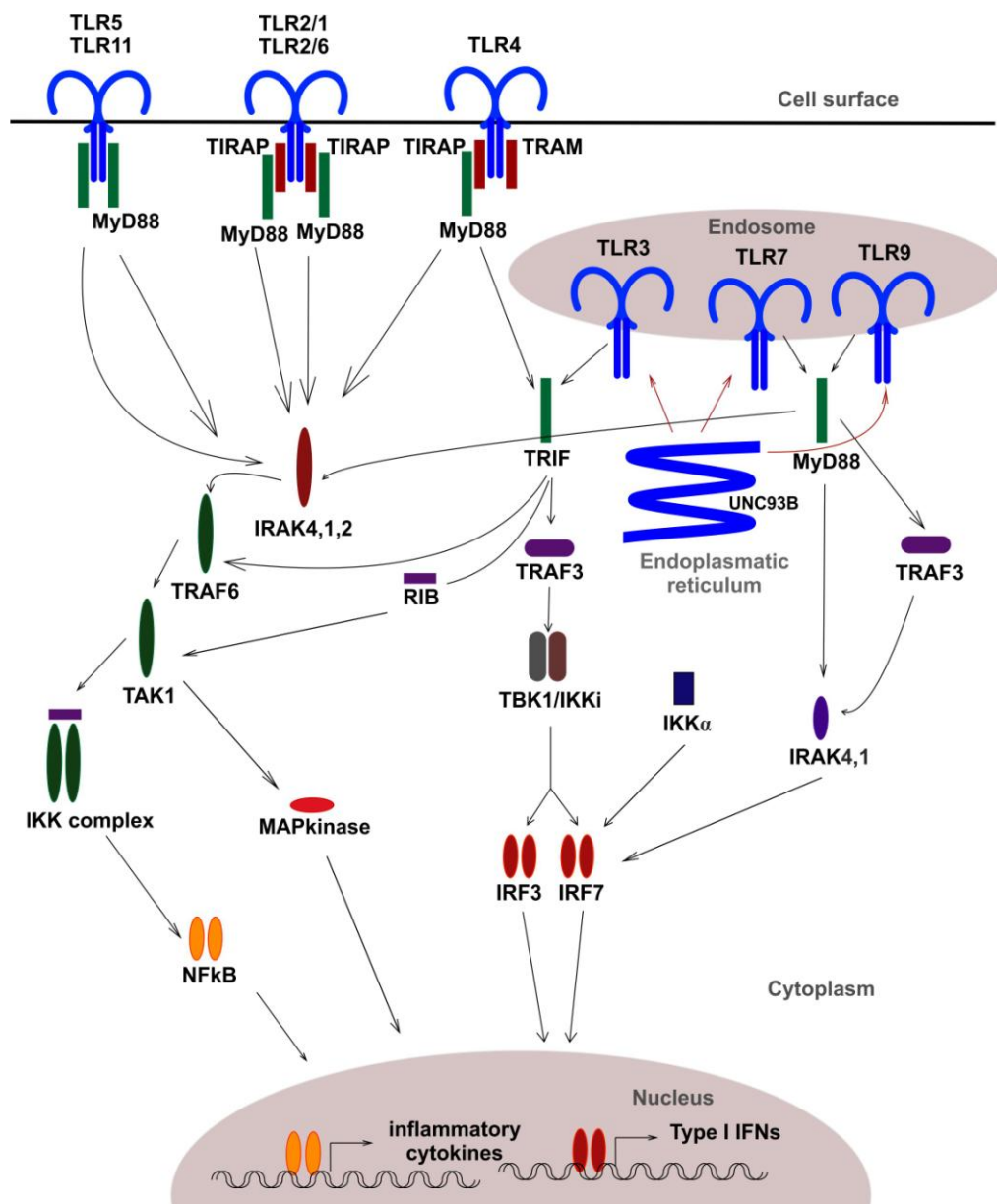


**Figure 1.5 TLR signaling in conventional dendritic cells, macrophages and plasmoid dendritic cells.** MyD88, myeloid differentiation primary response gene; TIRAP, TIR adaptor protein; TRAM, TRIF-related adaptor molecule; IRAK, interleukin-1 receptor associated kinase; TRAF, TNF receptor associated factor; TAK, transforming growth factor beta-activated kinase 1; IKK, kinase complex; NF-κB, nuclear factor κB; IRF, interferon regulatory factor. From [122], modified.

The TLR dimerization process and agonist recognition leads to recruitment of the adaptor proteins like MyD88, TIRAP (or Mal), TRAM and TRIF, which possess TIR domains for TLR binding. The crystal structures and the binding sites of some signaling complexes formed by adaptor proteins are published. Thus, the investigation of the human adaptor protein MyD88 by NMR spectroscopy revealed a protein with a TIR domain consist of 4 helices, which surround 5 central parallel  $\beta$ -sheets with the most structure similarity with the TLR2 TIR domain [128]. For TLR4 signaling required TIR domain of Mal adaptor protein binds to the sites II and III of MyD88 TIR [128]. The 6 MyD88, 4 IRAK4 and 4 IRAK2 death domains form Myddosome (MyD88-IRAK4-IRAK2) complex, which represents a left-handed helical oligomer. The Myddosome complex leads to the phosphorylation of IRAK2 and triggers TLR/IL-1R signaling pathway in mammals [129]. The phosphorylation of IRAK2 is the beginning of the signaling cascade, which initiates the expression of inflammatory cytokines and type I IFN (Figure 1.5).

The immunological investigations of the PAMPs from Gram-positive bacteria revealed the LTA to be capable to activate the release of IL-8, IL-1 $\beta$ , IL-10, IFN- $\gamma$  and TNF- $\alpha$  in innate immune cells and to be agonist of TLR2 and TLR4 [90, 130, 131]. The *in vitro* tests of the synthetic LTA revealed the release of IL-8, but TLR4 or TLR2 activity could not be determined [132]. Even little amounts of lipoproteins can contaminate the LTA preparations. The elegant solution of hydrogen peroxide (H<sub>2</sub>O<sub>2</sub>) treatment of the purified LTA samples and putative lipoproteins inside lead to the oxidation of the thioether group of the N-terminal cysteine to the sulfoxide and inactivates the lipoproteins [133]. The receptor of LTA still has to be identified.

### 1.5.2 HEK293 cells

Immunologists established different methods to work with different cells *in vitro* for the elucidation of immune processes. The generation of the HEK293 cell line from primary human embryonic kidney cells (HEK) and the transformation of HEK293 cells with sheared adenovirus 5 DNA has been developed in 1973 [134]. HEK293 cells are since then a widespread useful tool in cell biology and biotechnology. The neuronal kidney cells are published to be the cellular origin of HEK293 cells [135]. The cells are very easy to handle, to grow and to transfect with different genes. The transfected gene of the HEK293 is overexpressed and demonstrate in case of positive stimulation the identification of the antagonist by the receptor [136].

### 1.5.3 NKT cells

Natural killer T (NKT) cells were discovered in early 1980ies and originally described as a subset of the T cells, presenting some characteristics of T cells and of NK cells [137]. Mice, humans and other mammalian species possess NKT cells. The cells are classified in three groups: “T<sub>H</sub>1-like”, dedicated “T<sub>H</sub>2-like” and “T<sub>H</sub>17-like” invariant (iNKT) cells [138].

NKT cells play a role both in innate and adaptive immunity. They are involved during bacterial infections, in autoimmune diseases and in rejection of tumor cells [139–141]. NKT cells produce cytokines like IFN- $\gamma$ , IL-1, IL-2, IL-4, IL-5, IL-9, IL-10, IL-13, IL-17, IL-21 and GM-CSF and express molecules like CD4 (mouse NKT), CD8 (human NKT), IL-15 receptor, IL-17RB or CC-chemokine receptor 6 (CCR6) in order to perform their immunomodulatory activities [138]. iNKT cells recognize glycolipids presented by CD1d tetramer, a major histocompatibility complex (MHC) class I-like molecule [142]. CD1d accommodates the lipid part of the glycolipids in the hydrophobic pockets A' and F' and present it to the TCR of NKT cells [143]. Antigen presenting cells (APC) can be B lymphocytes or dendritic cells (DC), thereby the work of Im *et al.* demonstrated CD11c<sup>+</sup> DC as predominant APC for iNKT cells [144].

A characteristic features of iNKT cells are expression of the invariant variable region 14-joining region 18 (V $\alpha$ 14-J $\alpha$ 18) T cell antigen receptor (TCR)  $\alpha$ -chain in mice and V $\alpha$ 14 T cell antigen receptor in humans, and their preference for the glycolipid  $\alpha$ -galactosylceramide ( $\alpha$ -GalCer) restricted by CD1d molecule [137]. NKT cell with invariant recognition region V $\alpha$ 10-J $\alpha$ 50<sup>+</sup> belong neither to type I NKT cells nor to type II NKT cells. They are also CD1d-restricted, but beside  $\alpha$ -GalCer glycolipids they recognize bacterial  $\alpha$ -glucuronic acid-containing glycolipids  $\alpha$ -glucuronosyl ceramide (GSL-1) and  $\alpha$ -glucuronosyl diacylglycerol [142].

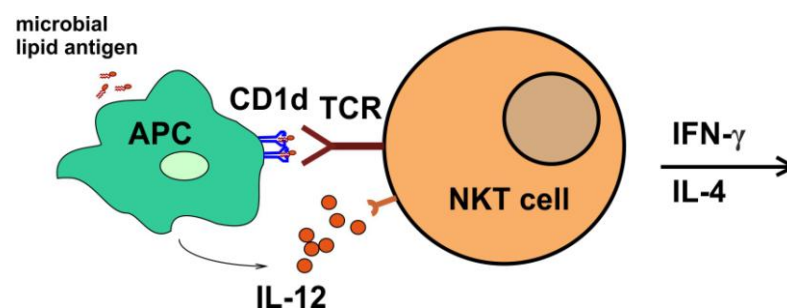


**Figure 1.6** Activation of CD1d-restricted NKT cells.

APC: antigen presenting cell, NKT: natural killer cell, TCR: T cell receptor. From [138], modified.

The *in vitro* tests with stimulation of mouse and human NKT cells by co-cultivation of antigen presenting cells (APC) have shown that NKT cells recognize a variety of microbial and synthetic

antigens [145]. These assays help to find out the relevance of NKT cells in innate and adaptive immunity and the possible antigens, which can be recognized during infections.

### 1.5.4 Immunological and inflammatory processes in the bovine mammary gland

The udder of the dairy cow is capable to produce on average 40 to 50 l milk per day. The udder blood volume of a lactating cow is about 8% of the total blood volume, which is a requirement for the udder to be adequately supplied with nutrients. The teats of the cow have a thin, keratinized epidermis with normal epithelium cell layer beneath it and a deeper dermis with blood vessels and nerves as long as two muscle layers. The innermost muscle layer covers the lumen of the teat cistern and is lined by a double layer of cuboidal epithelium, which acts as a barrier between the milk and the blood immune mediators. A disruption of this blood-milk barrier can occur after infection of the udder with pathogens and subsequent inflammation (mastitis) which damages the epithelium. The streak canal of the cow's teat builds on one side a barrier between the environment and the mammary gland tissue, and on the other hand it functions like a connector between them. Especially 20 - 30 min after milking, when sphincter muscles of the teat are relaxed and the canal is open, microorganisms have a very high possibility to enter the udder [2]. Thus, bacteria like *S. agalactiae* and *Staph. aureus* enter the teat duct and the udder's cisternal spaces, adhere to tissues and grow in the milk collecting interior [7]. In the case of infection the bovine mammary gland tissue is protected by mechanisms of innate and adaptive immunity [146].

In the healthy mammary gland macrophages and some lymphocytes predominate. The important task of the macrophages is to engulf and to eliminate the entered microorganisms. They are able to release pro-inflammatory cytokines for neutrophil recruitment and to multiply the innate immune response [146]. For example, in a murine model of mastitis mammary alveolar macrophages produce tumor necrosis factor (TNF)- $\alpha$ , IL-1 $\beta$ , IL-8 and nitrate oxide (NO) for LPS/TLR4 signaling, and trigger the migration of neutrophils from the blood to the infected area [147]. The polymorphonuclear neutrophil leucocytes (PMN) have an essential role in the ruminant innate immune response. Phagocytes like neutrophils and macrophages express glycosylphosphatidylinositol anchored protein CD14, which was shown to be required for the activation of the TRAM-TRIF-dependent signaling induced by LPS [148]. CD14 positive (CD14+) neutrophils and macrophages were found in the ruminant's mastitis infected udder in presence of Gram-positive bacteria like *Staph. aureus* und *S. uberis* [149]. Beside their initiative role in the inflammatory response, macrophages are capable to ingest apoptotic neutrophils and to resolve inflammation [150].

PMN possess a convoluted surface, phagocytize bacteria and kill them by producing of bactericidal effector molecules like the lingual antimicrobial peptide  $\beta$ -defensin or enzymes: peroxidase and alkaline phosphatase, or PMN take control over the growth of bacteria by releasing lactoferrin [151]. Beside the increased number of milk somatic cells in the acute phase of the udder inflammation several other molecules are detectable in blood and in milk like increasing concentrations of the acute phase proteins serum amyloid A and haptoglobin, secreted by the liver, but also locally by the tissues of the mammary gland [152]. Furthermore, the actions of neutrophils are reflected by their release of lysosomal enzyme *N*-acetyl- $\beta$ -D-glucosaminidase during phagocytosis and cell lysis [153].

During the time some days before and after parturition the immune healthy state of the cow is imbalanced and the animal is most susceptible to get mastitis [154]. The reasons for that are the open and leaking teat canal, colostrogenesis, low numbers of mature neutrophils in blood and milk around calving, and the neutrophil susceptibility to apoptosis around that time [151].

Clinical mastitis caused by Gram-negative *E. coli* in ruminants is characterized by obvious characteristic signs of acute inflammation and by strong immune reactions in the cow's body. *In vivo* experiments demonstrated the up-regulation of the  $\beta$ -defensin gene BNBD5 as well as of the PRR genes TLR2 and TLR4 in udder tissue and in local udder lymph nodes after the first 24 h of infection [155, 156]. In cows, TLR signal transduction leads to NF- $\kappa$ B-dependent induction of cytokines in case of infection with Gram-negative bacteria [157]. The pro-inflammatory cytokines CXCL8, TNF- $\alpha$ , IL-1 $\beta$  are expressed in primary mammalian epithelial cells as demonstrated by Bannerman *et al.* after the stimulation of pbMECs with LPS [158].

The infection of the mammary gland infection with *Staph. aureus* is less invasive and the disease can be classified as subclinical mastitis. In the first 24 h after bacteria inoculation inflammatory signs are not detectable, and further bacterial inoculations are necessary to evoke tissue inflammation [156]. The transcriptional profiles of mammary gland tissue infected with *Staph. aureus* showed gene up-regulations associated with response to stress, the expression of inflammatory TNF- $\alpha$ , CD14, of the chemokines CXCL1, CXCL2, CXCL10, and IL-1 $\beta$ , IL-6, IL-8 [156, 159, 160]. Indeed, the cytokine expression activated by NF- $\kappa$ B is low in case of infection with *Staph. aureus*. The NF- $\kappa$ B activation in bMECs is even described to be inhibited by the strain itself [161], presuming to evoke not sufficient strong host immune response and subclinical mastitis with persistent infection.

Streptococcal bovine mastitis infections may cause clinical mastitis, but usually infections are subclinical [162]. The innate immune responses proceed slowly and with delay. The first comprehensive study of mastitis by *S. agalactiae* in a mouse model demonstrated the increase of neutrophils in infected tissue as early as 6 h after infection as well as the increase of the pro-

inflammatory cytokines, however the infection was not under control until 24 h after bacteria injection. At the timepoint of 72 h after infection the early immune response cytokines decreased, and IL-12 and IL-10 increased. The highest level of CD4+ and CD8+ production was observed on the fifth day, and 10 days after infection anti-*S. agalactiae* antibodies were detectible. Thus, the infection triggers an adaptive immune response against this strain.

The biofilm formation of bacteria, their adherence to epithelial cells as long as their invasion are helpful processes for establishment of infection, which have been determined for different pathogens, including bovine mastitis isolates [163]. Processes of the receptor- and caveolae-mediated endocytosis in bMECs of bovine *S. uberis* enhanced by binding of host collagen, lactoferrin, or fibronectin are well investigated [164]. Intracellular trafficking in bMECs was shown for *Staph. aureus*, *S. dysgalactiae*, and pathogenic human and bovine *S. agalactiae* isolates, but also their ingestion by macrophages without losing their viability [165, 166]. Bacterial survival in the phagocytizing cells and the reinfection of the tissue have been discussed to be a possible cause of persistent ruminant intramammary infections [62, 167].

### 1.6 Surveillance, hygiene, vaccine development

Due to the development of guide lines and preventive measures in the cattle the incidence of mastitis infection was reduced successfully [25] worldwide in the last 40 years. On the contrary, in countries with bad hygiene standards and poor experiences in the farmer's cattle like Vietnam [168], Ethiopia [169], and India [47] the infection rate of the clinical and subclinical mastitis is high, and results in the mentioned consequences.

The bacterial ability to acquire antimicrobial resistance leads to the requirement of other antimicrobial strategies. The research efforts in vaccine development for bovine mastitis strains are immense. Vaccination of cows were performed for example by injections of live or killed cells of *S. uberis* and with the antigen plasminogen activator (PauA), a protein released by all *S. uberis* strains in the culture medium for protein hydrolysis of the milk [170–172]. Vaccines for bovine mastitis obtained from *Staph. aureus* were tested *in vivo* in cows between 1984 and 2010, compared and investigated for their efficacy [173]. Especially vaccines that apply new technologies like DNA and/or recombinant protein vaccines and some bacterins demonstrated better protection and control of mastitis [173]. This implies to apply these technologies in combination with two or more yet not tested virulence factors to obtain an efficient vaccine [173]. However, natural bacterial infections of the ruminant mammary gland showed that the adaptive immunity of the cow is relatively short-lived, thus, the development of an efficient vaccine represents a big challenge [157].

## 2 Aims of the project

The diversity and high number of bovine mastitis causative agents, which are constantly in the cow's environment, make it likely that this disease may never be eliminated. Nevertheless the ruminant health and the economically important high-quality milk are the motives for the fight against this infection disease.

At first, in case of the infection the bacterial cell envelope components have to be identified by the immune system agents of the host. Different structures often present different inflammatory potential. Therefore, the objectives of this thesis were to outline the structural characteristics of the cell envelope components from two bovine mastitis bacterial strains *S. agalactiae* 0250 and *S. dysgalactiae* 2023 by using biochemical isolation and structural investigation methods. It was aimed to determine possible structural differences in the cell envelope components of closely related streptococci and to investigate their biological importance.

CPS, LTA, WTA and glycolipids were demonstrated to be immunomodulatory active in murine innate immunity. Hence, these components were aimed to be structural elucidated applying compositional analysis, gas chromatography (GC), electrospray-ionization Fourier-transformed ion cyclotron mass spectrometry (ESI FT-ICR-MS), matrix-assisted laser desorption/ionization Fourier-transformed ion cyclotron mass spectrometry (MALDI FT ICR-MS) and high-resolution nuclear magnetic resonance (NMR) spectroscopy. For the determination of immunological activities it was planned to apply *in vitro* tests using pbMECs, HEK293 cells and/or splenocytes.



## 3 Materials and Methods

### 3.1 Materials

#### 3.1.1 Chemicals and reagents

**Table 3.1** Chemical products

Product	Company
( <i>R</i> )-(-)-2-Butanol	Sigma-Aldrich, Germany
( <i>S</i> )-(+)-2-Butanol	Sigma-Aldrich, Germany
( <i>R</i> )-(-)-2-Octanol	Sigma-Aldrich, Germany
( <i>S</i> )-(+)-2-Butanol	Sigma-Aldrich, Germany
1-Butanol	Sigma-Aldrich, Germany
1-Propanol	Sigma-Aldrich, Germany
Acetic acid	Merck, Darmstadt, Germany
Acetic anhydride	Fluka, Germany
Acetone	Merck, Darmstadt, Germany
Ammonium acetate	Merck, Darmstadt, Germany
Ammonium heptamolybdate tetrahydrate	Merck, Darmstadt, Germany
Chloroform	Merck, Darmstadt, Germany
Citric acid	Merck, Darmstadt, Germany
Dimethyl sulfoxide	Merck, Darmstadt, Germany
Di-sodium hydrogenphosphate dihydrate	Merck, Darmstadt, Germany
DNase	Sigma-Aldrich, Germany
Ethanol	Merck, Darmstadt, Germany
Hexane	Merck, Darmstadt, Germany
Hydrazine	Kodak
Hydrochloric acid	Merck, Darmstadt, Germany
Hydrofluoric acid	Merck, Darmstadt, Germany
Hydrogen peroxide 30%	Merck, Darmstadt, Germany
Iodmethan	Sigma-Aldrich, Germany
L-Ascorbic acid	Sigma-Aldrich, Germany
Lysozyme	Sigma-Aldrich, Germany

Table 3.1 continued	
Magnesium chloride	Merck, Darmstadt, Germany
Methanol	Merck, Darmstadt, Germany
Natrium chloride	Merck, Darmstadt, Germany
Perchloric acid	Merck, Darmstadt, Germany
Phenol	Merck, Darmstadt, Germany
Potassium chloride	Merck, Darmstadt, Germany
Potassium dihydrogenphosphate	Merck, Darmstadt, Germany
Proteinase K	Roche
Pyridine	Merck, Darmstadt, Germany
Pyridine, distilled	Fluka
RNase	Roche
Silica gel	Merck, Darmstadt, Germany
Sodium borodeuteride	Sigma-Aldrich, Germany
Sodium borohydride	Merck, Darmstadt, Germany
Sodium dodecylsulfate	Roth, Karlsruhe, Germany
Sodium hydroxide	Merck, Darmstadt, Germany
Sulfuric acid	Merck, Darmstadt, Germany
Trichloroacetic acid	Roth, Karlsruhe, Germany
Trifluoroacetic acid	Merck, Darmstadt, Germany
Tri-sodium citrate dihydrate	Merck, Darmstadt, Germany
Water Aqua B. Braun	Ecotainer, Melsungen, Germany
Water, pyrogen-free	Millipore, Darmstadt, Germany
$\alpha$ -Naphthol	Sigma-Aldrich, Germany

### 3.1.2 Buffers, solutions and media

All experiments were performed in a LPS-free laboratory. The pyrogen-free deionized water (Milli-Q<sup>®</sup> Integral Water Purification Systems device) was used for all solutions of structural analysis experiments. All glass vials, round flasks and bottles were heated at 240°C for 4 h to avoid endotoxin contamination. All washing steps in the experiments were performed with water Aqua B. Braun.

**Table 3.2 Nutrient media.**

Medium, buffer, component	Company
Agar	Bacto™ Agar, BD, USA
Brain Heart Infusion (BHI)	Roth, Germany
Todd Hewitt Broth (THB)	Bacto™ Todd-Hewitt Broth, BD, USA
Casein hydrolysate	Fluka, Sigma-Aldrich, Germany
Citric buffer, 0.1 M, pH 4.7	460 ml 0.1 M citric acid monohydrate
	540 ml 0.1 M trisodium citrate dihydrate
	sterile filtered (0.22 µm filter, Millipore, USA)
Phosphate buffer saline (PBS)	1.5 l of 37.5 mM Na <sub>2</sub> HPO <sub>4</sub> × 2 H <sub>2</sub> O and 102.7 mM NaCl
	0.4 l of 12.5 mM KH <sub>2</sub> PO <sub>4</sub> and 34.2 mM NaCl
	1 and 2 were given together, adjusted to pH 7.2 and to volume of 2 l with water, and sterile filtered (0.22 µm filter, Millipore, USA)

### Brain Heart Infusion

BHI used as liquid medium in the cultivation of a variety of bacterial species as well of yeasts and molds. The major constituents of BHI are calf brain infusion, beef heart infusion and peptone of digested animal tissue, including 5% sodium chloride [174].

### Todd Hewitt Broth

THB was designed in 1932 by Todd and Hewitt for production of hemolysin by *Streptococcus* species [175]. The liquid THB medium is still most commonly used for growing of streptococci. The major constituents of THB are heart infusion as a nitrogen source, yeast enriched peptone providing vitamins and essential minerals, dextrose as a carbon supplier and as activator of hemolysin production and sodium chloride for support of osmotic balance in the medium [176].

### 3.1.3 Cell lines

**Table 3.3 Cell lines**

Cell type	Abbreviation	Culture medium
Human mononuclear cells	hMNC	RPMI 1640 PAA, Pasching, Austria
Human embryonic kidney cells	HEK293	DMEM, Biochrom AG, Berlin, Germany
Murine spleen cells	-	RPMI 1640/15% FBS, Biochrom AG, Berlin, Germany

## RPMI

RPMI was developed by scientists of Roswell Park Memorial Institute in 1966. It is very useful for growing of various mammalian and hybrid cells. RPMI is often mixed with 10-20% fetal bovine serum (FBS) depending on the aim and cells. NaCl, NaHCO<sub>3</sub>, Na<sub>2</sub>HPO<sub>4</sub> × 7 H<sub>2</sub>O, amino acids and vitamins belong to the constituents of RPMI [177].

## Dulbecco's Minimal Essential Medium (DMEM)

Different mammalian cells can grow on modified Dulbecco's MEM. Beside usual major constituents of NaCl, NaHCO<sub>3</sub>, Na<sub>2</sub>HPO<sub>4</sub> × 7 H<sub>2</sub>O, the medium contains amino acids and vitamins four times higher concentrated compared to Minimal Essential Medium (MEM). Additionally, non-essential amino acids, trace elements and bicarbonate are included [178].

### 3.1.4 Equipment and materials for chromatography

**Table 3.4 Materials and equipment for chromatography**

Method, Matrices:	Company	Detection	Software
Thin-layer chromatography (TLC)			
TLC Silica Gel 60W F <sub>254</sub> S, aluminum sheets 20 × 20 cm	Merck, Darmstadt, Germany		
TLC Silica Gel 60 F <sub>254</sub> , glass plates 20 × 20 cm	Merck, Darmstadt, Germany		
Gel filtration			
BioGel P60	BioRAD, USA	RI Detector K-2301 KNAUER Smartline RI Detector 230 KNAUER	Clarity Chromatography station for Windows
Sephadex G10	GE Healthcare Life Science		
Hydrophobic interaction chromatography (HIC)			
HiPrep column (16 × 100 mm, bed volume 20 ml) of octyl- sepharose	GE Healthcare Life Science	HPLC device; Gilson, Detector 15X Series of UV/VIS	Trilution® LC
Anion-exchange chromatography			
HiTrap Q Sepharose HP 5 ml	GE Healthcare Life Science	ÄKTA FPLC UPC 900, Detector P-920, Amersham Pharmacia Biotech	Unicorn Version 4

### 3.1.5 Equipment and plastic material

**Table 3.5 Equipment**

Equipment	Company
Acrodisc <sup>®</sup> syringe filter with GHP membrane, 0.45 $\mu\text{m}$	Pall Life Sciences Corporation
Agar plates	Sarstedt
Analytical balance	Sartorius, Kern
Autoclave V 150	Systec
Cell homogenizer	B. Braun
Centrifuges	Beckmann Coulter, Hereaus, Hettich
CO <sub>2</sub> incubator for cell cultures	Hereaus Instruments
Filter for organic and watery solutions, 0.45 $\mu\text{m}$	Dionex
Gas chromatograph	7890 A GS System; 689011 Network System, Agilent Technologies
Glass beads	Roth, Karlsruhe, Germany
Long pasteur pipettes for NMR tubes	Deutero, Roth
Lyophilizator	Christ, Osterode, Germany
MALDI-TOF MS Reflex II	Bruker Daltonics, USA
Membrane tubing 3.5 ku	Spectra/Por, Spectrum Laboratories, Inc., USA
NMR Shigemi tubes	Shigemi Inc.
NMR tubes 5 mm, 3 mm	Deutero
Pasteur pipettes	Brand
UV/VIS spectrometer	Helios $\beta$ , Thermo; Helios $\epsilon$ , Thermo Spectronic, Electron Corporation
Pipette tips	Sarstedt
Steritop <sup>™</sup> Filter Units 22 $\mu\text{m}$	Millipore, USA
Transmission electron microscope	Zeiss
Vibrogen cell mill	Edmund Bühler, Hechingen, Germany

## 3.2 General methods

### 3.2.1 Microorganisms and growth conditions

*S. agalactiae* 0250 and *S. dysgalactiae* 2023 were isolated from cases of bovine mastitis in the UK [63] and are included in the National Institute for Research in Dairying (NIRD) culture collection (Prof. Dr. James Leigh, University of Nottingham, UK, kindly provided both isolates for this study).

Both *Streptococcus* species were cultivated on THB medium at 37°C with for 8 h without shaking. The growth curves of the bacteria were obtained by measuring the light absorbance at 600 nm (OD<sub>600</sub>). Additionally, the growth of bacteria was examined by supplying 5% CO<sub>2</sub>.

For the isolation of the capsular polysaccharide the bacteria were grown on BHI and on BHI supplemented with (2%, w/v) of casein hydrolysate. Liquid cultures were inoculated with bacterial colonies grown on agar plates (1.5%, w/v) with the medium states above mentioned. Purity of the culture was determined by plating on THB agar.

### 3.2.2 Photography of bacterial species

Both, *S. agalactiae* 0250 and *S. dysgalactiae* 2023 were grown for 48 h at 37°C on THB agar. The photos were taken under the clean bench using the camera Canon IXUS 210 (14.1 megapixels).

### 3.2.3 Transmission electron microscopy (TEM)

For the microscopy, the osmium fixation protocol [179] was used. *S. agalactiae* 0250 and *S. dysgalactiae* 2023 were grown on agar plates at 37°C (THB, BHI or BHI supplemented with 2% casein hydrolysate) for 24 h. The cell were resuspended in liquid media, transferred to falcon tubes, centrifuged (6,000 g, 4°C, 30 min; rotor JA 14, model Avanti J-26 XP, Beckman Coulter, USA), and the pellet was taken for fixation. First, the pellet was embedded in a soft agar. A 2% solution of osmium tetroxide (ChemPur, Karlsruhe, Germany) was applied for 1.5 h in order to fixate the preparations, which were washed afterwards three times with water. The post fixation positive stain was performed with 2% uranyl acetate solution (Serva, Heidelberg, Germany) for 1 h at 22°C, followed by washing of the preparations three times with water. Subsequently, a dehydration was achieved with a series of ethanol washing steps (30%, 50%, 70%, 90%, 100%), 15 min each. The 15 min incubation of the preparations in propylene oxide (Serva, Heidelberg,

Germany) followed. The preparations were impregnated at 4°C for 16 h with a mixture of propylene oxide/Epon resin (1:1, by vol.) (Serva, Heidelberg, Germany). The polymerization was achieved by transferring the material to Epon resin and incubation at 60°C for 20 h. The embedded preparations were cut with a diamond knife on a pyramyotom (ultrathin slices 80 - 100 nm) and placed on copper grids. The counter staining was achieved with lead citrate (Serva, Heidelberg, Germany) in CO<sub>2</sub> free environment. The cells were investigated and analyzed using a combined scanning/transmission electron microscope Zeiss EM910.

### 3.3 Isolation of bacterial components

#### 3.3.1 Isolation of the LTA

LTA was isolated from wet cell pellets as published by Morath *et al.* [180], with few modifications. Briefly, *Streptococcus* cultures (20 l) were harvested after 12 h, bacterial cells (~30 g of wet mass) were washed once with citric buffer (0.1 M, pH 4.7). The bacterial cells were disrupted with the Vibrinogen cell mill. An equal volume of glass beads (0.1 mm) was given to ~30 g of biomass resuspended in 100 ml citric buffer. The disruption process took 3 min. Afterwards, the glass beads were separated from the debris by centrifugation (5,000 g, 10 min., 4°C) and by two additional washing steps with citric buffer. Collected supernatants were subjected for butan-1-ol – water extraction (20-22°C, 30 min).

LTA was recovered from the aqueous phase after butan-1-ol – water extraction. The water phase-containing LTA was dialyzed (3.5 ku cut off) against 50 mM ammonium acetate for 7 d and lyophilized. Next, the dried water phase-containing LTA was dissolved in buffer A (15% propan-1-ol/ 0.1 M ammonium acetate), filtrated (0.45 µm), and loaded on HiPrep column (100 × 16 mm, bed volume 20 ml) of octyl-sepharose [181]. Bound material was eluted with a gradient from 100% buffer A to 100% buffer B (60% propan-1-ol/ 0.1 M ammonium acetate) over 60 min. Phosphate-containing fractions were combined after their characterization by a photometric phosphate assay [182]. The purified LTA was washed repeatedly with water and freeze-dried to remove residual buffer.

#### 3.3.2 Isolation of glycolipids

##### 3.3.2.1 Bligh and Dyer extraction

The butanol phase left after butanol/water extraction of LTA isolation method was used for the isolation of streptococci glycolipids. The glycolipids of *S. agalactiae* and *S. dysgalactiae* were

obtained by Bligh and Dyer extraction (CHCl<sub>3</sub>/MeOH/sodium acetate buffer 2:2:1.8, by vol.) [183]. Subsequently, the glycolipid crude extracts of both *Streptococcus* species were separated by column chromatography (silica gel, 7 × 1 cm) with an increased gradient of MeOH in CHCl<sub>3</sub>/MeOH solutions (3% - 50%).

### 3.3.2.2 Visualization of the glycolipids

The glycolipids were applied on a TLC plate, put into the chamber with the running buffer and incubated there till 95% of the TLC were saturated with buffer. The glycolipids visualized by using Hanessian's Stain (detection of hydrocarbons and phosphate-containing compounds) [184] and charred at 150°C on a heat plate. The staining with  $\alpha$ -naphtol buffer (detection of carbohydrates) was developed at 110°C.

Buffers for glycolipid extraction and isolation:	0.1 M sodium acetate buffer, pH 4.6
Running buffer for TLC:	65 ml CHCl <sub>3</sub> mixed slowly with 25 ml MeOH 4 ml H <sub>2</sub> O added dropwise
Hanessian's Stain:	471 ml H <sub>2</sub> O 29 ml H <sub>2</sub> SO <sub>4</sub> (98%) 0.5 g Ce(SO <sub>4</sub> ) × 4 H <sub>2</sub> O 25 g (NH <sub>4</sub> ) <sub>6</sub> Mo <sub>7</sub> O <sub>24</sub> × 4 H <sub>2</sub> O
$\alpha$ -Naphtol buffer:	50 ml MeOH 6 ml H <sub>2</sub> SO <sub>4</sub> (98%) added slowly under the hood on ice! 4 ml H <sub>2</sub> O added in drops 1.92 g $\alpha$ -naphtol

The isolated products were always resuspended in CHCl<sub>3</sub>/MeOH (8:2, by vol.) at a concentration of 4 mg/ml. Single glycolipids were isolated via silica gel chromatography or via scraping out from TLC. To remove the rests of silica gel from the eluted sample, the solution was transferred by filtration (0.2  $\mu$ m PTFE) to a new vial, dried under nitrogen (N<sub>2</sub>) and the mass of the isolated glycolipid was determined. Purity of the isolated glycolipids preparations was evaluated by TLC.

### 3.3.3 Isolation of the WTA

#### 3.3.3.1 WTA isolation using 5% TCA

For the WTA isolation the bacteria cells were disrupted applying a Vibrinogen mill (chapter 3.3.1), then washed with citric buffer, and separated from the glass beads by centrifugation. In order to separate the LTA from the mixture of cell envelope components, the combined supernatants were boiled in 4% SDS solution and centrifuged afterwards at 8,000 g, 4°C, 30 min (rotor JA 14, model Avanti J-26 XP, Beckman Coulter, USA).

Next, the pellet (WTA covalently bound to PGN) was incubated three times for 24 h with 5% TCA [185]. Each 5% TCA extract was centrifuged at 5,000 g, 4°C for 20 min and WTA preparations were dialyzed (3.5 ku cut off) against 50 mM ammonium acetate for 4-5 d. Further the WTA preparations were freeze-dried, dissolved in buffer A (15% propan-1-ol/ 0.1 M ammonium acetate) and filtered (0.45 µm). The sample was further purified applying anion-exchange chromatography on a HiTrep Q Sepharose column (25 × 16 mm) with a gradient from 0 to 1 M of NaCl of 36 columns volume (5 ml/column) as eluent with a flow rate of 3 ml/min. After the elution the column was washed, first with 20 columns volume of 1 M NaCl, then with 5 columns volume of 2 M NaCl. The Q Sepharose fractions 1–86 were combined to three samples according to their phosphate content [132]. The gel-permeation chromatography on a column (100 × 2.5 cm) of Sephadex G-10 eluted with a buffer containing 4 ml pyridine and 10 ml glacial acetic acid in 1 l water (pH 4.2) without a pump was used in order to remove the salt from the samples.

The Q Sepharose fractions were combined to three samples according to their phosphate content [182].

#### 3.3.3.2 WTA isolation via enzymatic treatment

The WTA (which is covalently linked to the PGN) was treated enzymatically to identify its linker as published by Bychowska *et al.* [186] with some modifications. In brief, the pellets of the broken cells were incubated in digestion buffer (pH 6.0) with lysozyme (0.1 mg/ml) at 37°C for 16 h, with DNase and RNase (0.1 mg/ml) at 37°C for 6 h and afterwards with proteinase K (0.1 mg/ml) at 56°C for 16 h. In order to avoid the hydrolysis of Ala the pH of the digestion buffer was adjusted to 6.0. However the conditions should not be too acidic because of the pH optima of the enzymes. Next, the samples were centrifuged and the supernatant was dialyzed (3.5 ku cut off) against water for 3 d and lyophilized. The sample was purified by high-performance liquid chromatography on octyl-sepharose, anion-exchange chromatography on

Q Sepharose and gel-permeation chromatography on Sephadex G10 using eluents as described in chapter 3.3.3.1.

### 3.3.4 Acetone precipitation of EPS

The bacteria were grown for 14 h in Brain-Heart-Infusion medium with 2% of casein hydrolysate at 37°C. The bacterial cells were harvested and washed three times with PBS, pH 7.2 by centrifugation at 8,000 g, 4°C, 30 min (rotor JLA 8.1000, model Avanti J-26 XP, Beckman Coulter, USA). The yielded nutrient medium and the supernatants were sterile filtrated and evaporated/lyophilized. One third of the yielded nutrient medium was dialyzed (3.5 ku cut off).

For the precipitation of EPS 300 ml acetone was added to every 100 ml of sterile medium/supernatant. Subsequently, the samples were incubated with stirring for 8 h at 4°C and stored afterwards at -20°C for 12 h.

The precipitates were centrifuged at 10,000 g, 4°C, 30 min and washed twice with acetone. The supernatants and the precipitates were evaporated, dissolved in water and freeze-dried. The dried supernatants were treated enzymatically as described in chapter 3.3.4.1 and dialyzed afterwards for 2 d against pyrogen-free water with 3-4 water changes a day. All samples were purified on Biogel P60 (100 × 2.5 cm) with a pump and eluted with a buffer containing 4 ml pyridine and 10 ml glacial acetic acid in 1 l. The positive fractions were combined and the isolated preparations were investigated by 1D and 2D NMR spectroscopy.

#### 3.3.4.1 Enzymatic treatment of the supernatants

Substances used for enzymatic treatment:

- RNase A from bovine pancreas (1 mg of enzyme/50 mg of substance)
- DNase I from bovine pancreas (0.5 mg of enzyme/50 mg of substance)
- Proteinase K recombinant PCR grade (0.5 mg of enzyme/50 mg of substance)

10 × digestion buffer (pH 7.5, adjusted with HCl):

- 1 M Tris/HCl
- 0.5 M NaCl
- 0.1 M MgCl<sub>2</sub>

Concentration of the substance:

- 5-10 mg/ml

RNase and DNase were added together to the samples and incubated at 37°C for 5 h in digestion buffer (1 ×), next proteinase K was directly used at 56°C for 1 h. The vials were shaken gently or just stirred from time to time in the process of enzymatic digestion.

### 3.3.5 Isolation of capsular polysaccharide

The isolation of the capsular polysaccharide was performed three times by using THB medium, BHI medium and BHI medium with 2% casein hydrolysate.

After the harvest and washing of the cells with PBS (pH 7.5) the biomass was incubated with stirring in 200 ml of 0.9% NaCl for 6 h at 22°C. Next, the cells were centrifuged (10,000 g, 4°C, 30 min, rotor JA 14, model J2-21, Beckman, USA). The supernatant was removed and dialyzed (3.5 ku cut off).

The pellet was incubated in 1% aqueous phenol solution for 48 h at 4°C with gentle stirring. The cells were centrifuged (10,000 g, 4°C, 30 min, rotor JA 14, model J2-21, Beckman, USA). The supernatant was taken up and dialyzed (3.5 ku cut off). All extracts were purified on the Biogel P60 (80 × 2.5 cm) and eluted with a buffer containing 4 ml pyridine and 10 ml glacial acetic acid in 1 l. The CPS containing fractions were combined, lyophilized and subjected for NMR. In case of *S. agalactiae* 0250 the extracts were purified on Biogel P60 (80 × 2.5 cm) and eluted with pyrogen free Millipore water to avoid acidic conditions, which can cleave the sialic acid, a typical component of GBS.

### 3.3.6 Isolation of rhamnan

The rhamnose-rich molecule of *S. agalactiae* 0250 was yielded in the phosphate-less fraction combined after Sephadex G10 WTA isolation process (chapter 3.3.3). Furthermore, the NaCl extract of CPS isolation from *S. agalactiae* 0250 and 1% phenol extract of CPS isolation from *S. dysgalactiae* 2023 revealed the presence of rhamnose-rich polymers (chapter 3.3.5). The rhamnan molecules were investigated by compositional analysis and subjected for 1D and 2D NMR spectroscopy.

## 3.4 Analytical methods

### 3.4.1 Chromatographic methods

Identification and analysis of neutral sugars, amino sugars, fatty acids and methylated products was performed applying gas liquid chromatography (GLC) and GLC/MS with GC ChemStation software.

To monitor and determine the components of the isolated molecules after methanolysis and acetylation, GLC-MS [Hewlett Packard HP 5890 (series II) gas chromatograph equipped with a fused-silica SPB-5 column (Supelco, 30 m  $\times$  0.25 mm  $\times$  0.25  $\mu$ m film thickness), FID and MS 5989A mass spectrometer with vacuum gauge controller 59827A] was used. The temperature program was 150°C for 3 min, then 5°C min<sup>-1</sup> to 330°C.

The components of neutral sugar analysis were detected as alditol acetates by GLC [HP 7890 A gas chromatograph with FID and a column of Phenyl MethylSiloxane HP-5 (Agilent Technologies, 30 m  $\times$  0.25 mm  $\times$  0.25  $\mu$ m film thickness)] with temperature program was 150°C for 3 min, then 3°C min<sup>-1</sup> to 250°C and afterwards 25°C min<sup>-1</sup> to 320°C.

The fatty acids were determined as methylated derivatives by GLC [HP 6890 N gas chromatograph with FID and a column of Phenyl MethylSiloxane HP-5 (Agilent Technologies, 30 m  $\times$  0.25 mm  $\times$  0.25  $\mu$ m film thickness)]. The temperature program was 120°C for 3 min, then 5°C min<sup>-1</sup> to 320°C.

### 3.4.2 Neutral sugar analysis

The neutral sugar analysis was performed like in [187] with some modifications. Briefly, for the quantitative determination of neutral sugars, doublets with 50 or 100  $\mu$ g of each sample were prepared. The hydrolysis was performed in 0.1 M hydrochloric acid (100°C, 48 h). Next, 30  $\mu$ l of a xylose solution (0.1 mg/ml) were added to each sample as the internal standard. The samples were dried under N<sub>2</sub> and rinsed 3 times with 10% ether/hexane solution (v/v) to remove fatty acids. After evaporation again under N<sub>2</sub>, 0.15 ml of water was added to each sample and pH 8 was adjusted with 1 M NaOH.

For reduction 3-4  $\times$  25  $\mu$ l of a NaBH<sub>4</sub> solution (3 mg/ml) were added to the samples, till the solution in the vial did not foam anymore. After incubation of the solutions in the dark for 16 h, 2 M HCl was added dropwise, and the reduction of the sugars was terminated. All samples were rinsed three times with 5% HAc/MeOH solution and afterwards rinsed three times with methanol. The samples were peracetylated by adding 50  $\mu$ l acetic anhydride (Ac<sub>2</sub>O) and 50  $\mu$ l distilled pyridine, incubated at 85°C for 10 min and evaporated under N<sub>2</sub>. Before injection in GLC (2  $\mu$ l of

20  $\mu\text{l}$ ), the samples were transferred salt-free with  $\text{CHCl}_3$  to new 1.5 ml vials. The concentration of neutral sugars was quantified relatively to the internal standard.

### 3.4.3 Amino sugar analysis

The amino sugar analysis was performed like in [187] with some modifications. First, 100  $\mu\text{g}$  of the investigated molecule were hydrolyzed in 200  $\mu\text{l}$  0.5 M hydrochloric acid at 100°C for 48 h. Afterwards, the sample was dried under  $\text{N}_2$  and rinsed three times with methanol. The sample was peracetylated as described above and washed again with methanol. Then, repeated reduction and peracetylation of the sample followed as described above (chapter 3.4.2). Two  $\mu\text{l}$  of 100  $\mu\text{l}$   $\text{CHCl}_3$  were injected in GLC. The amino sugars were analysed in GLC only qualitatively.

### 3.4.4 Fatty acids analysis

The fatty acid analysis was performed as described in [133] with some modifications. Briefly, 200  $\mu\text{g}$  of the investigated substance was taken for the quantification of fatty acids. The aliquot of 20  $\mu\text{l}$  of a 17:0 fatty acid solution (0.5 mg/ml) as internal standard was added to the sample and evaporated under  $\text{N}_2$ . Hydrolysis was performed in 1 ml of 0.5 M NaOH/MeOH (1:1, by vol.) at 85°C for 2 h. After the hydrolysis the samples were evaporated under  $\text{N}_2$ , diluted with 4 ml of water, and pH 3 of the sample was adjusted with 4 M HCl. Extraction of fatty acids was performed three times with 1 ml of  $\text{CHCl}_3$ . The samples were strongly shaken for 2 min, the extracted  $\text{CHCl}_3$  phases were combined and their volumes were reduced under  $\text{N}_2$ . Both phases were separated by short centrifugation at 2,000 g for 2 min. The obtained  $\text{CHCl}_3$  phases were combined in fresh 1.5 ml vials, and the volume was reduced by evaporation under  $\text{N}_2$ . Subsequently followed a twice treatment of the samples with diazomethane for 3 min. Diazomethane was evaporated under  $\text{N}_2$  until the yellow color was gone. The samples were subjected for GC (1  $\mu\text{l}$  of 100  $\mu\text{l}$ ). Fatty acids were quantified relatively to the standard.

### 3.4.5 Methanolysis

Weak methanolysis of each sample 200 mg proceeded with 200  $\mu\text{l}$  of 0.5 M HCl/MeOH at 85°C for 45 min, and strong methanolysis with 200  $\mu\text{l}$  2 M HCl/MeOH at 85°C for 45 min [187]. In both cases the samples were cooled, dried under  $\text{N}_2$  and 25  $\mu\text{l}$  of distilled pyridine and 25  $\mu\text{l}$  of  $\text{Ac}_2\text{O}$  were added for peracetylation at 85°C for 10 min. The samples were dried, rinsed once with methanol and dissolved in 50  $\mu\text{l}$   $\text{CHCl}_3$ . One  $\mu\text{l}$  of the sample was injected in GLC/MS.

### 3.4.6 Determination of the phosphate content

The determination of phosphate content was performed as described in [182] with some modifications. Briefly, for the determination of the inorganic phosphate content 5, 10 and 15  $\mu\text{l}$  of each sample (5 mg/ml) and pairs of 2, 4, 6, 8, 10  $\mu\text{l}$  of the standard solution were pipetted into glass tubes and 100  $\mu\text{l}$  of water was added to each tube. One blank was used for calibration. All samples were incubated with 900  $\mu\text{l}$  of the reagent at 37°C for 30 min. The extinction was measured at 820 nm. The following reagents were used for the measurement:

Standard: 5 mM  $\text{Na}_2\text{HPO}_4$   
Reagent: 700  $\mu\text{l}$  5 M  $\text{H}_2\text{SO}_4$   
4700  $\mu\text{l}$   $\text{H}_2\text{O}$   
600  $\mu\text{l}$  2.5% ammonium heptamolybdate  
3000  $\mu\text{l}$  10% ascorbic acid (freshly prepared)

In order to determine the total content of phosphate, 2, 4 and 8  $\mu\text{l}$  of each sample (5 mg/ml) and the doublets of 2, 4, 6, 8, 10  $\mu\text{l}$  of the standard were pipetted into glass tubes. After addition of 50  $\mu\text{l}$  water the tubes were placed in a vacuum desiccator for 18 h. One blank was used for calibration. Dried samples were incubated with 100  $\mu\text{l}$  releasing reagent at 100°C for 1 h and then at 165°C for 2 h. Next, the samples were cooled on ice and 1 ml of the color reagent was added to each tube. Later the solutions were incubated at 37°C for 90 min. The total phosphate measurement was performed at 820 nm.

The following reagents were used for the total phosphate measurement:

Standard: 5 mM  $\text{Na}_2\text{HPO}_4$   
Releasing reagent: 62.7 ml  $\text{H}_2\text{O}$   
30.6 ml concentrated  $\text{H}_2\text{SO}_4$   
6.7 ml 70%  $\text{HClO}_4$   
Colour reagent: 1 ml 1 M NaAc  
(freshly prepared in ice bath) 1 ml 2.5% ammonium heptamolybdate solution  
7 ml  $\text{H}_2\text{O}$   
1 ml 10% ascorbic acid (freshly prepared)

### 3.4.7 Methylation analysis

The methylation was performed as published in [188] with some modifications. The dried sample (not less than 500  $\mu\text{g}$ ) was dissolved in 1 ml DMSO and 300  $\mu\text{g}$  of powdered NaOH was added. Methylation proceeded with 500  $\mu\text{l}$   $\text{CH}_3\text{I}$  at 22°C for 1 h with stirring. Afterwards the sample was dried under  $\text{N}_2$ . The methylated product was extracted with  $\text{CHCl}_3/\text{H}_2\text{O}$  (2:7, by vol.). The chloroform extract was washed with water to remove DMSO and the rest of MeI, taken up in new vial, evaporated to dryness under  $\text{N}_2$  and methylated again. Hydrolysis was performed by incubation of the sample with 2 M trifluoroacetic acid (TFA) at 100°C for 2 h. Next, the sample was reduced with  $\text{NaBD}_4$  in  $\text{H}_2\text{O}/\text{MeOH}$  (1:1, by vol.) for 16 h at 22°C. Reduction was terminated by adding of 2 M HCl. Then the sample was dried under  $\text{N}_2$ , rinsed 3 times with 200  $\mu\text{l}$  of 5% AcOH/MeOH to remove boric acid and 3 times with MeOH, and evaporated each time. After the peracetylation (85°C, 8 min) the sample was analyzed by GLC/MS.

### 3.4.8 Determination of the absolute configuration

The determination of phosphate content was performed as already published in Rietschel *et. al* with some modifications [187]. To determine the absolute configuration of sugars and Ala, 250  $\mu\text{g}$  of sample was dissolved in 2 M HCl/MeOH and methanolysis was performed at 85°C for 16 h. Next the samples were dried under  $\text{N}_2$  and washed three times with methanol. Butanolysis was performed with 2 M HCl/R-BuOH and octanolysis with 2 M HCl/R-OctOH at 60°C for 16 h. The samples were then peracetylated (85°C, 10 min) and analyzed in GLC as described above. The respective D- and L-configured standards were used for the determination.

## 3.5 Preparative methods

### 3.5.1 Hydrofluoric acid treatment

LTA preparations of both streptococci treated with 48% aq. HF (50  $\mu\text{l}$  per 50 mg, 4°C, 48 h) which cleaved the glycerol phosphate backbone of the LTA. After repeated extraction with  $\text{H}_2\text{O}/\text{CHCl}_3/\text{MeOH}$  (3:3:1, by vol.), the lipid anchor was yielded in the organic phase. The combined organic phases were dried under  $\text{N}_2$ , resuspended in water, lyophilized, and subjected for NMR spectroscopy.

### 3.5.2 Hydrazinolysis

Mild hydrazine treatment removes ester-linked fatty acids (as in glycerol) and this was used to obtain the deacylated lipid anchor (recovered after HF treatment) as well as *O*-deacylated LTA. Hydrazinolysis was performed as described in [189]. First, 1 ml/20 mg abs. hydrazine was added to the dried LTA (9.2 mg, *S. agalactiae*; 9.2 mg, *S. dysgalactiae*) and lipid anchors (4.1 mg, *S. agalactiae*; 2.5 mg, *S. dysgalactiae*). The mixture was incubated at 37°C for 1 h. Hydrazine was destroyed by adding to the cooled sample 10 volumes of cold acetone. Sample was washed twice with acetone and the desired product was recovered from the water phase by chloroform – water extraction. *O*-Deacylated LTA but not the lipid anchor was dialyzed (3.5 ku cut off) against water in order to remove free Ala.

## 3.6 Structural analysis

### 3.6.1 NMR spectroscopy

The 1D [<sup>1</sup>H proton, <sup>13</sup>C carbon, <sup>31</sup>P phosphate] and 2D [correlation spectroscopy (<sup>1</sup>H, <sup>1</sup>H COSY), total correlation spectroscopy (TOCSY), rotating nuclear Overhauser effect spectroscopy (ROESY), <sup>1</sup>H, <sup>13</sup>C heteronuclear single quantum coherence with distortionless enhancement by polarization transfer (HSQC-DEPT), <sup>1</sup>H, <sup>13</sup>C heteronuclear multiple bond correlation (HMBC), <sup>1</sup>H, <sup>13</sup>C heteronuclear multiple quantum coherence (HMQC), HMBC without decoupling, <sup>1</sup>H, <sup>31</sup>P HMBC and <sup>1</sup>H, <sup>31</sup>P HMBC-TOCSY] NMR spectra were recorded with a Bruker DRX Avance 700 MHz spectrometer (operating frequencies 700.75 MHz for <sup>1</sup>H NMR, 176.2 MHz for <sup>13</sup>C NMR and 238.7 MHz for <sup>31</sup>P NMR). The resonances of hydrophilic samples were recorded on D<sub>2</sub>O solutions at 27°C relative to internal acetone ( $\delta_{\text{H}}$  2.225;  $\delta_{\text{C}}$  31.45) and to external 85% phosphoric acid ( $\delta_{\text{P}}$  0.00). The samples of the glycolipids were measured in MeOD/CDCl<sub>3</sub> solutions (1:2, by vol.) at 27°C relative to an internal standard of tetramethylsilan (TMS) ( $\delta_{\text{H}}$  0.00;  $\delta_{\text{C}}$  0.00). All NMR experiments were recorded and the spectra investigated applying standard Bruker software TopSpin 2.1.

The TOCSY experiments were measured in the phase sensitive mode with mixing times of 120 and 180 ms. The best resolution of the signals were obtained from measurements of TOCSY with mixing time of 180 ms. The <sup>1</sup>H, <sup>13</sup>C correlations were monitored in <sup>1</sup>H-detected mode via HSQC-DEPT with proton decoupling in the <sup>13</sup>C domain. HMBC spectra were adjusted to a *J* coupling constant value of 145 Hz and a long range proton carbon coupling constant of 10 Hz.

## 3.6.2 Mass spectrometry

### 3.6.2.1 ESI FT-ICR MS

A 7 Tesla Apex Qu-Instrument (Bruker Daltonics, Billerica, MA, USA) and a dual Apollo ion source were used for data generation of ESI FT-ICR MS analyses. The LTA preparations (~10 ng/ $\mu$ l) were dissolved for the negative ion mode in a water/2-propanol/triethylamine solution (50:50:0.001, by vol.) and sprayed at a flow rate of 2  $\mu$ l/min. The applied settings were 3.8 kV of capillary entrance voltage and 200°C of drying gas temperature. The mass spectra were charge deconvoluted, and mass numbers were expressed accordingly to the monoisotopic peaks of the neutral molecules.

### 3.6.2.2 MALDI FT-ICR MS

Structural investigations of the glycolipids were achieved applying MALDI FT ICR-MS. The experiments were performed on a Bruker Reflex II instrument (Bruker Franzen Analytik, Bremen, Germany) on APEX Qe-Instrument (Bruker Daltonics, Billerica, USA) equipped with a 7 Tesla actively shielded magnet and a dual Apollo ion source in positive ion mode. The methanol – water (1:1, v/v) solution was added to the samples (~1  $\mu$ g/ $\mu$ l). Matrix solution contained 2,5-dihydroxybenzoic acid (2,5-DHB) in 1% TFA at a concentration of 15  $\mu$ g/ $\mu$ l. Matrix solution and sample solution mixture (1:1, by vol.) were applied onto a stainless steel sample plate as 1.5  $\mu$ l droplets. The samples crystallized at 22°C. Laser irradiance was regulated in order to reduce the formation of DHB-adduct ions.

## 3.7 Immunological methods

Stimulation of the HEK293 cells *in vitro* by *S. agalactiae* 0250 and *S. dysgalactiae* 2023 bacterial cells were performed in cooperation with Prof. Dr. Hans-Martin Seyfert and Dr. Juliane Günther, Leibniz Institute for Farm Animal Biology, Dummerstorf, Germany.

### 3.7.1 Preparation of bacteria for stimulation of HEK293 cells

The *Streptococcus* bacteria were grown on Todd Hewitt Broth (37°C) to the logarithmic phase [optical density at 600 nm (OD<sub>600</sub>) of 0.5;  $1 \times 10^7$  cells/ml]. Dilution series were prepared and plated in order to calculate the cell counts accordingly to the OD. Subsequently, incubation of

*S. agalactiae* 0250 and *S. dysgalactiae* 2023 at 80°C for 1 h or *E. coli* 1303 at 60°C for 1 h killed the cells. Cell death was controlled by plating of the preparations. Finally, cells were centrifuged, the pellets were washed two times and resuspended in RPMI 1640 medium at a density of  $5 \times 10^8$  cells/ml. Aliquots of cell suspension were taken up and stored at -20°C. The HEK293 were stimulated with  $10^7$  cells/ml.

### **3.7.2 Transfection of HEK293 cells**

The assay of luciferase activity in HEK293 cells for evidence of the TLR signaling cascade were described [190]. All plasmid DNAs applied for transfection of HEK293 cells were prepared endotoxin-free. The eukaryotic cells were transiently transfected by plasmid DNAs using Lipofectamin 2000 (Invitrogen, Karlsruhe, Germany). An expression vector (100 ng) of the Renilla luciferase was used for the transfection. The vector is driven by an artificial promoter featuring five NF- $\kappa$ B attachment sites [ELAM-promoter; recloned from the pNiFty vector (Invitrogen)]. Additionally, HEK293 cells were transfected with bovine TLR2 (boTLR) gene cloned into pFLAG-CMV-1 expression vector [190]. Two different premixes were prepared, in order to transfect a single well of a six well plate:

Premix one: 3  $\mu$ g of DNA in 100  $\mu$ l of the salt base from the DMEM medium, no additives

Premix two: 6  $\mu$ l of Lipofectamin 2000 in 100  $\mu$ l of the salt base from the DMEM medium

After 5 min of incubation of each premix, both were combined and incubated again for 20 min. Double washings steps of the HEK293 cells (80% confluent) with PBS were performed in the meanwhile. Subsequently, the cells were covered with 800  $\mu$ l of DMEM salt base medium and 200  $\mu$ l of the premix were added. The cell were incubated for 3 h. Afterwards, 1 ml of DMEM medium, supplemented with twice the complement of all usual additives (including 20% foetal calf serum) was added. The cells were allowed to recover overnight. Immediately after the distribution of the cells in 24 well plates, the heat-inactivated *Streptococcus* or *E. coli* bacteria were added and incubated together with the HEK293 cells transfected 1) only with NF- $\kappa$ B and 2) with boTLR2 and NF- $\kappa$ B (boTLR2 + NF- $\kappa$ B) for the duration of the stimulation experiment.

### **3.7.3 Stimulation of HEK293 cells by cell envelope components**

Biological tests on human cells *in vitro* with cell envelope components as stimuli were conducted in cooperation with Prof. Dr. Holger Heine and under technical assistance of Ina Goroncy, Division of Innate Immunity, RCB. Briefly, HEK293 cells were transfected with the expression

plasmids as already described [191] and stimulated with appropriate cell wall components of *S. agalactiae* 0250 and *S. dysgalactiae* 2023 after 24 h of transfection. After 18 h of stimulation, supernatants were collected and the content of the interleukin CXCL-8 was quantified using a commercial ELISA (Biosource, Solingen, Germany). As positive controls the synthetic lipopeptide *N*-palmitoyl-*S*-[2,3-bis(palmitoyloxy)-(2*RS*)-propyl]-[*R*]-cysteiny-[*S*]-seryl-[*S*]-lysyl-[*S*]-lysyl-[*S*]-lysyl-[*S*]-lysine (Pam<sub>3</sub>C-SK<sub>4</sub>) for TLR2, lipopolysaccharide (LPS) from *S. enterica* sv. Friedenau (kind gift of Prof. Helmut Brade, RCB) for TLR4,  $\gamma$ -D-glutamyl-*meso*-diaminopimelic acid (iE-DAP) (courtesy of Prof. Koichi Fukase, Osaka, Japan) for NOD1, and *N*-acetylmuramyl-L-alanyl-D-isoglutamine (MDP) (provided by Prof. Shoichi Kusomoto, Osaka, Japan) for NOD2 were used.

### 3.7.3.1 Dealanylation of LTA samples

The native LTA preparations were incubated for 24 h in 0.1 M ammonium acetate buffer to cleave D-Ala from the hydrophilic backbone. Subsequently, the samples were dialyzed (3.5 ku cut off) against pyrogen-free water for 2-3 d with 3 water changes per day, lyophilized, subjected to <sup>1</sup>H NMR spectroscopy in order to prove whether the dealanylation was successful, and then used for biological investigations.

### 3.7.3.2 Hydrogen peroxide treatment of LTA samples

For the oxidation of putative lipopeptides present in the LTA preparations the samples were treated with H<sub>2</sub>O<sub>2</sub> by incubation for 1 h at 37°C as published in [192]. The H<sub>2</sub>O<sub>2</sub> was removed by drying of the samples under N<sub>2</sub>. The H<sub>2</sub>O<sub>2</sub>-treatment inactivates lipopeptides and -proteins, since the thioether group of the N-terminal cysteine will be oxidized to sulfoxide. Such lipoprotein is not capable to function as TLR2 ligand anymore [193]. The LTA preparations were examined by <sup>1</sup>H NMR spectroscopy prior to biological investigations to prove that the LTA has still the same structure compared to H<sub>2</sub>O<sub>2</sub>-untreated samples.

### 3.7.4 hMNC assay

Human mononuclear cells (hMNC) were separated from sodium citrate blood of healthy adult donors applying the Ficoll-Isopaque density gradient centrifugation [194]. The hMNC were washed with PBS and cultivated in RPMI 1640 medium supplemented with 10% autologous human serum, 100 U/ml penicillin and 100  $\mu$ g/ml streptomycin. The hMNC ( $1 \times 10^6$ /ml) were stimulated in duplicates of different concentrations of the indicated cell wall component from

*Streptococcus* species. LPS was used as a positive control. The IL-6 and TNF- $\alpha$  concentration of collected supernatants after 20 h of stimulation was quantified by ELISA.

### **3.7.5 Phagocytosis assay**

The experiment of phagocytosis capacity of bovine leukocytes in presence of the LTA was performed by Dr. Jamal Hussen in the group of Prof. Dr. Hans-Joachim Schuberth, Immunology Unit, University of Veterinary Medicine, Hannover, Germany.

#### **3.7.5.1 Separation of bovine leukocytes**

Blood was obtained from four healthy ruminants by venipuncture of the *vena jugularis externa* into heparinized vacutainer tubes (Becton Dickinson, Heidelberg, Germany), and was diluted with PBS (1:1, by vol.). The blood preparations were centrifuged at 4°C for 10 min at 1,000 g and the supernatant was removed. The hypotonic lysis of the erythrocytes was performed twice by adding distilled water (20 ml for 20 sec), the addition of 20 ml double concentrated PBS followed. At last, the bovine leukocytes were resuspended in RPMI medium (PAA, Pasching, Austria).

#### **3.7.5.2 Phagocytosis capacity assay**

Heat-killed *Staph. aureus* (Pansorbin, Calbiochem, Merck, Nottingham, UK) or *E. coli* (Institute of Veterinary Microbiology, Hannover, Germany) bacterial strains were used for the determination of the phagocytosis capacity. The bacteria were labeled with fluorescein isothiocyanate (FITC, Sigma-Aldrich, St. Louis, Missouri, USA) and centrifuged at 14,000 g for 5 min. The supernatant was removed, the pellet was resuspended in RPMI medium (PAA, Pasching, Austria) and dissolved to  $2 \times 10^8$  particles/ml. Peripheral blood leukocytes were added in 96 well plates ( $3 \times 10^5$  cells/well) and incubated with *Staph. aureus* or *E. coli* (adjusted ratio of 50 bacteria to one monocyte) for 60 min. at 37°C and 5% CO<sub>2</sub>. Samples without bacteria were used as negative controls. Three different concentrations (1, 10, 20  $\mu$ g/ml) of LTA from *S. agalactiae* 0250 or *S. dysgalactiae* 2023 were performed as parallel set ups in order to determine the effect of LTA on the phagocytosis capacity of monocytes and neutrophils. Subsequently, double washing steps of the cells with PBS followed. The cells were resuspended in 100  $\mu$ l PBS containing 2  $\mu$ g/ml propidium iodide to stain dead cells. Phagocytosis rates were determined flow cytometrically (Accuri C6, BD Biosciences) according to the characteristic forward and side scatter of neutrophils and monocytes and expressed in % of phagocytosing cells.

### 3.7.6 Stimulation of splenocytes by glycolipids

The *in vitro* assays of the glycolipids activity in iNKT cells were conducted and performed in cooperation with Dr. Gonzalez Roldan, Division of Immunobiology, RCB.

#### 3.7.6.1 Assay with murine spleen cells

The murine spleen cells were used in order to prove of the biological activity of the glycolipids of bovine mastitis isolates. The spleen cells from the WT mouse consists of an assembly of immunological active cells, i. e. dendritic cells, macrophages, neutrophils, T cells (including NKT cells), B cells and mature iNKT cells ( $\sim 10^6$ ) [195].

First, spleens were collected from freshly sacrificed mice and placed in 15-ml polypropylene tubes containing 5 ml ice-cold RPMI-1640/10% FBS. Next, erythrocyte-free single cell suspensions were obtained by pressing the spleens against a 100  $\mu\text{m}$ -mesh cell strainer followed by rinsing with 5 ml of phosphate buffer saline (PBS) solution. Cells contained in the suspension were centrifuged at 400  $g$  for 5 min and 4°C. For removal of erythrocytes, the cell pellet was resuspended in 2 ml of ice-cold ACK buffer and maintained on ice for 2 min. Next 10 ml of RPMI-1640/10% FBS were added to stop the cell lysis and the cell suspension was again centrifuged at 400  $g$  for 5 min and 4°C. The resulting cell pellet was resuspended in 5 ml of complete media and the cell number was determined by using a hemacytometer. Finally, the cell concentration was adjusted to  $10^6$  cells/ml in RPMI-1640/10% FBS and 100  $\mu\text{l}$  of the cell suspension were seeded into individual wells of a 96-well microtiter plate. Cells were kept in the incubator at 37°C and 5%  $\text{CO}_2$  while preparing the glycolipid antigens.

The synthetic glycolipid  $\alpha$ -galactosyl ceramide ( $\alpha\text{GalCer}$ ), which is the most potent iNKT ligand [196] was used as positive control. The glycolipid antigens to be tested were the G1, G2 and G3 isolated from *S. agalactiae* 0250 and *S. dysgalactiae* 2023. All antigens were resuspended in PBS (pH 7.0) containing 0.5% Tween-20 (as vehicle and as negative control) and added to the spleen cells at a final concentration of 20  $\mu\text{g}/\text{ml}$ .

The cells were incubated at 37°C and 5%  $\text{CO}_2$  with the indicated stimuli, and culture supernatants were collected after 72 h and analyzed for the presence of IFN- $\gamma$  and IL-4 by ELISA.



## 4 Results

### 4.1 Morphology and growth of the bacteria

#### 4.1.1 Growth of streptococci

First, the growth of *S. agalactiae* 0250 and *S. dysgalactiae* 2023 in THB medium as standing culture was monitored. Additionally screening of the growth of the bacteria with and without 5% CO<sub>2</sub> was performed (Figure 4.1).

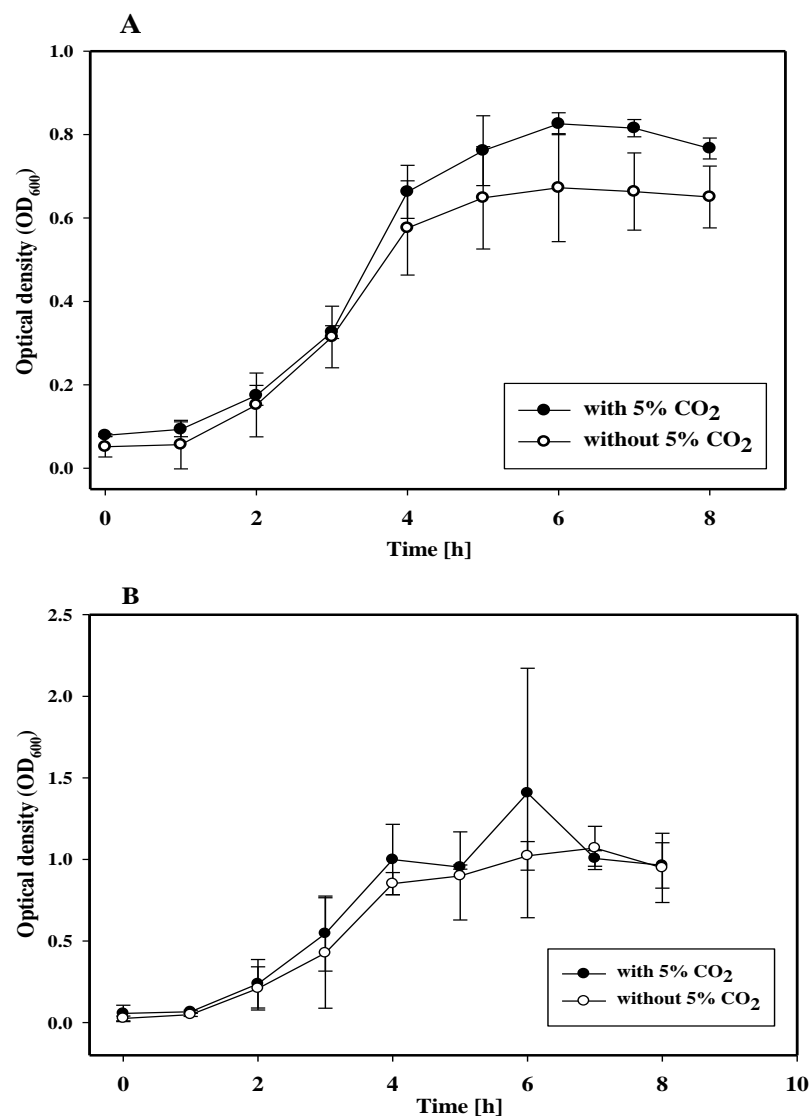


**Figure 4.1** Growth curves of *S. agalactiae* 0250 (A) and *S. dysgalactiae* 2023 (B).

The bacteria were incubated in THB medium and in THB medium with 5% CO<sub>2</sub> at 37°C for 8 h. The growth is demonstrated as mean  $\pm$  SD of 3 (*S. agalactiae* 0250) and of 2 (*S. dysgalactiae* 2023) measurements.

Both *Streptococcus* species entered after 2 h the log-phase and after 5-6 h of the exponential growth the stationary phase. The monitoring was stopped after 8 h of biomass cultivation in THB medium, because the bacteria entered the death phase. Both streptococci grew better under 5% CO<sub>2</sub> conditions. The mean value of maximum OD<sub>600</sub> of *S. agalactiae* 0250 measured by growing without CO<sub>2</sub> was 0.6 and with CO<sub>2</sub> 0.8, and the *S. dysgalactiae* maximum OD<sub>600</sub> was 1.0 without CO<sub>2</sub> and 1.4 with CO<sub>2</sub>. Especially, the maximum OD<sub>600</sub> of *S. dysgalactiae* showed considerable fluctuations.

The colonies of *S. agalactiae* 0250 and *S. dysgalactiae* 2023 looked smooth, round, light beige and glossy (Figure 4.2). After 24 h of growing on the agar plate *S. dysgalactiae* 2023 colonies became irregular with white-beige colonies, which appeared to grow on the already existent bacterial lawn (Figure 4.2). Presuming a contamination, both phenotypes were aimed to be separated by plating of unique colonies on a fresh THB agar plate, but the separation did not succeed. On fresh plates the strain grew again as irregularly shaped white colonies. Thus, it appeared clear that the culture was pure, and liquid media were inoculated with regular single colonies.

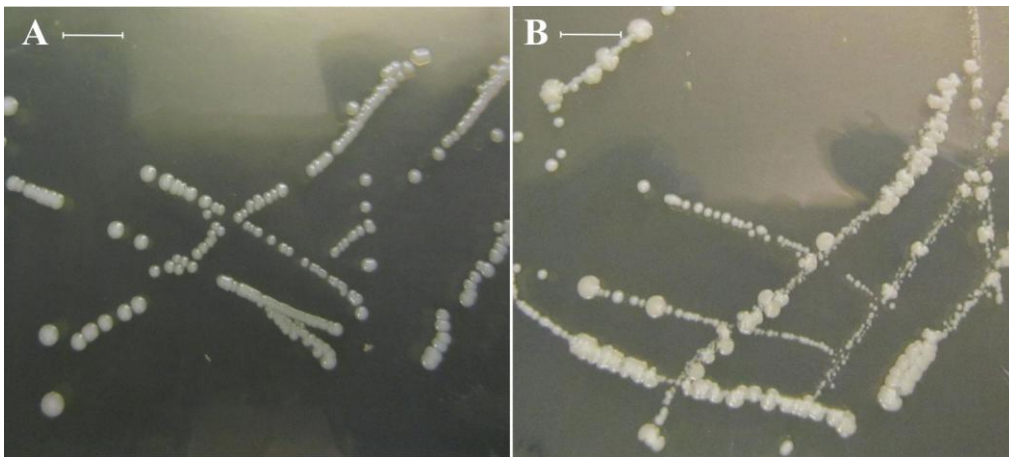


**Figure 4.2** Colonies of *S. agalactiae* 0250 (A) and *S. dysgalactiae* 2023 (B) grown on THB agar plate at 37°C for 48 h.

The bar corresponds to 0.5 mm.

#### 4.1.2 Transmission electron microscopy analyses

*S. agalactiae* 0250 and *S. dysgalactiae* 2023 were grown on different agar media: THB, BHI and BHI supplemented with 2% of casein hydrolysate, in order to prove if this can lead to some effects on cell surface representation or expression of different components in the cell envelope of the bacteria.

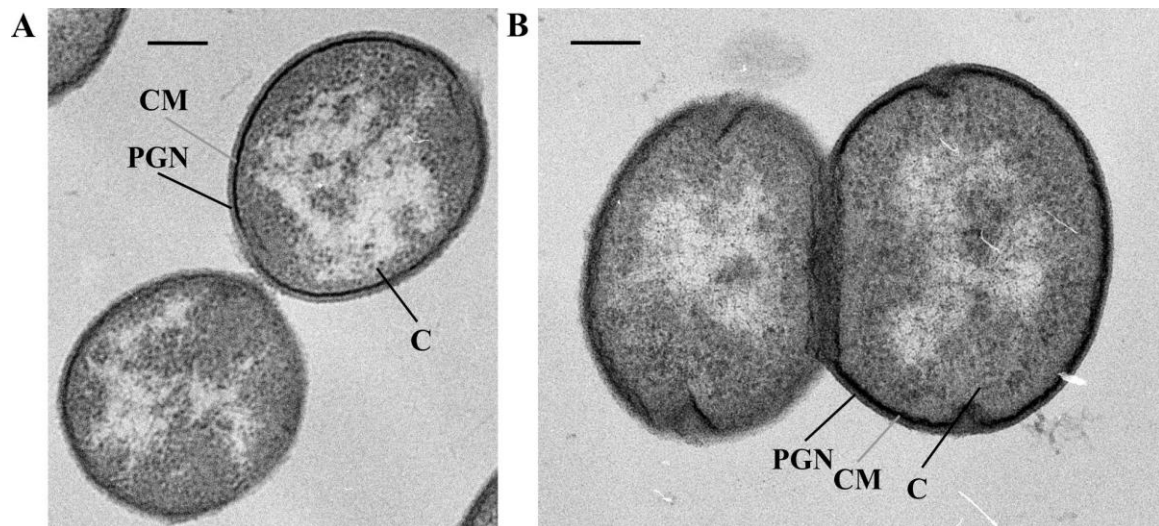


**Figure 4.3** Transmission electron micrograph of ultrathin sections of fixed *S. agalactiae* 0250 after 24 h of growing on THB medium (A) and BHI medium (B).

The bar corresponds to 0.15  $\mu\text{m}$ . C stands for cytoplasm, CM for cytoplasmic membrane, PGN for peptidoglycan.

In Figure 4.3 the cells of *S. agalactiae* 0250 are demonstrated possessing a thin, smooth cell envelope. The cytoplasm is surrounded by the cytoplasmic membrane and PGN. No encapsulation and no differences between the cells after growth on THB or BHI agar medium could be observed.

On the contrary, the Gram-positive cell envelope of *S. dysgalactiae* 2023 looked very thick on the TEM micrographs. Additionally to cytoplasmic membrane and PGN the cells appeared to produce CPS (Figure 4.4). The cells possessed the same thickness of the cell envelope independent from the growth on THB or BHI agar medium supplemented with 2% casein hydrolysate.

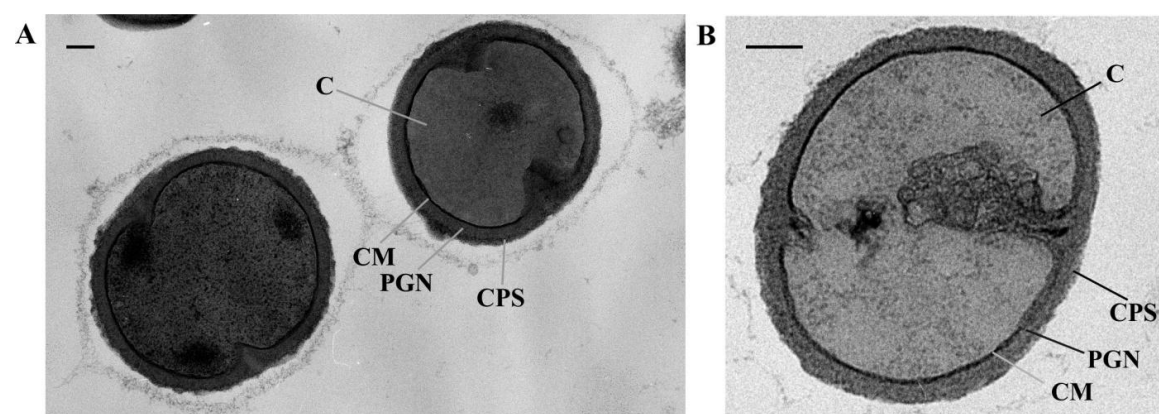


**Figure 4.4** Transmission electron micrograph of ultrathin sections of fixed *S. dysgalactiae* 2023 after 24 h of growing on THB medium (A) and BHI medium (B) supplemented with 2% of casein hydrolysate.

The bar corresponds to 0.15  $\mu\text{m}$ . C stands for cytoplasm, CM for cytoplasmic membrane.

## 4.2 Stimulation of HEK293 by *Streptococcus* cells

Both, heat-inactivated *S. agalactiae* 0250 and *S. dysgalactiae* 2023 cells were investigated whether they could activate HEK293 cells transiently transfected with boTLR2 and NF- $\kappa$ B *in vitro*. *E. coli* 1303 was used as a positive control and unstimulated cells as negative control.

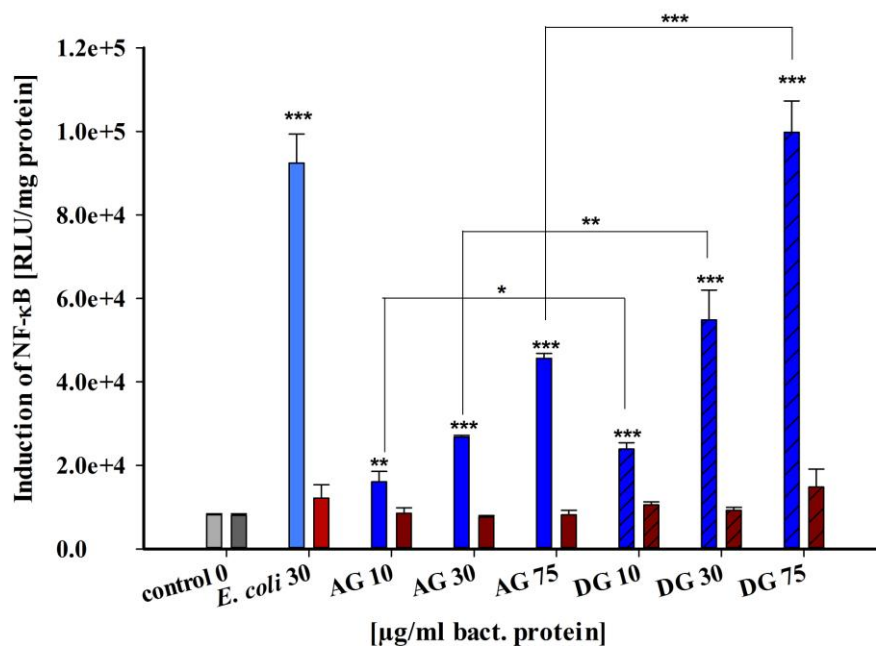


**Figure 4.5 Stimulation of HEK293 *in vitro* by whole cells of *S. agalactiae* 0250 (AG, unfilled) and *S. dysgalactiae* 2023 (DG, fasciated) and activation of HEK293 cells transfected with boTLR2 + NF- $\kappa$ B (blue) and with NF- $\kappa$ B (brown).**

For the stimulation of HEK293 cells transiently transfected with boTLR2+NF- $\kappa$ B and with NF- $\kappa$ B were applied 10, 30 and 75  $\mu$ g/ml of heat killed *S. dysgalactiae* 2023 (AG10, AG30, AG75) and *S. agalactiae* 0250 (DG10, DG30, DG75) and 30  $\mu$ g/ml of *E. coli* 1303 ( $10^7$  heat killed cells/ml). The unstimulated cells served as a negative control. The induction of NF- $\kappa$ B was measured in relative light units (RLU) per mg protein produced by luciferase reporter gene. The calculations of total RNA are expressed as bold mean  $\pm$  SD of 3 measurements. Significance of the data above the bars is expressed in \*  $p < 0.05$ , \*\*  $p < 0.01$ , \*\*\*  $p < 0.001$  compared to the control by application of the unpaired t-test. Obtained results in case of equal bacterial concentrations were compared to each other using unpaired t-test.

The HEK293 cells were stimulated for 3 h, 6 h and 24 h with heat-killed *E. coli* and *Streptococcus* cells. *E. coli* was used as a positive control and demonstrated high activation of HEK293 via boTLR2. The *Streptococcus* cells activated HEK293 NF- $\kappa$ B pathway via boTLR2 (Figure 4.5). The results for activation of boTLR2 were in case of both streptococci at each bacterial concentration and in case of *E. coli* statistically significant compared to the control (\*\*  $p < 0.01$ , \*\*\*  $p < 0.001$ ). The activation of HEK293 cells via boTLR2 by *S. dysgalactiae* 2023 was nearly two times more than the activation HEK293 cells via boTLR2 by *S. agalactiae* 0250 and the obtained activations in case of equal bacterial concentrations were statistically significant compared to each other (\*  $p < 0.05$ , \*\*  $p < 0.01$ , \*\*\*  $p < 0.001$ ).

## 4.3 Structural analysis of LTA

### 4.3.1 Isolation and compositional analysis of LTA

The first molecule investigated of both streptococci was the LTA. Successfully recovered after *n*-butanol/water extraction [64], followed by hydrophobic interaction chromatography (HIC), native LTA were yielded 0.5 mg/g of the *S. agalactiae* 0250 wet mass (mean of 4 isolations) and 0.6 mg/g of the *S. dysgalactiae* wet mass (mean of 3 isolations). First, LTA were analyzed by weak and strong methanolysis. The weak methanolysis of the isolated native LTA of *S. agalactiae* 0250 revealed in a bigger amount of Gro, Gro-P, Gro-Ala, 6-deoxyhexose (6d Hex), Gal, glucose (Glc), 18:0, 18:1, Gro-Hex, Gro-16:0 and Gro-18:0. The same compounds with additional 16:1, 18:0-ol acetate, Gro-Ala-P, but lacking Gal, were detected by weak methanolysis of native LTA of *S. dysgalactiae* 2023.

**Table 4.1** Calculated approx. molecular ratios of the FA from the LTA of *S. agalactiae* 0250 and *S. dysgalactiae* 2023.

Fatty acid	<i>S. agalactiae</i> 0250	<i>S. dysgalactiae</i> 2023
12:0	1	1
14:0	2.8	3
16:1	2.8	2.6
16:1	3.3	5.3
16:0	17.8	18.2
18:2	3.5	1.4
18:1	22.3	18
18:1	21.3	15.4
18:0	19.3	11

The two values of 16:1 fatty acid and 18:1 fatty acid corresponded to different localizations of the double bounds.

Neutral sugar analysis of LTA from *S. agalactiae* 0250 identified Glc, rhamnose (Rha), and Gal (in an approx. molecular ratio 8:1:0.2), and Glc and Rha (calculated in particular approx. molecular ratio of 5:1) in the LTA from *S. dysgalactiae* 2023. The fatty acid analysis revealed the presence of 16:1, 16:0, 18:1, and 18:0 [approx. molecular ratios: 1:2.9:7.1:3.2 (*S. agalactiae*), 1:2.3:4.2:1.4 (*S. dysgalactiae*)] (detailed calculation of approx. molecular ratios is demonstrated in Table 4.1).

The determination of the phosphate content of the LTA molecule revealed 3.3  $\mu\text{mol P/mg LTA}$  in case of *S. agalactiae* 0250 and 3.7  $\mu\text{mol P/mg LTA}$  in case of *S. dysgalactiae* 2023. The amino acid Ala was identified in both LTA preparations (185 nmol/mg LTA *S. agalactiae* 0250, 144 nmol/mg LTA *S. dysgalactiae* 2023). The obtained molecular ratios of FA/Ala/P are 2.7/1/17.8 for *S. agalactiae* LTA and 4/1/25.7 for *S. dysgalactiae* LTA.

No signals of Rha and Gal were detected on NMR spectra during further investigations, thus those hexoses were considered as contamination. The absolute configurations of Ala and Glc were determined as D.

### 4.3.2 NMR investigation of the LTA

The native LTA of both *Streptococcus* species were investigated by 1D and 2D NMR experiments.  $^1\text{H}$  NMR spectra revealed no significant differences between both LTA preparations (Figure 4.6). The data discussed below refer to the LTA isolated from *S. dysgalactiae* 2023. The 1D  $^1\text{H}$  NMR spectrum showed characteristic signals for Gro substituted by Ala at O-2 (H-2,  $\delta$  5.39), Ala (H-2,  $\delta$  4.29; H-3,  $\delta$  1.63), H-3 of free Ala ( $\delta$  1.50), other signals of Gro ( $\delta$  4.11 – 3.65), and of fatty acids ( $\delta$  2.33 – 0.86). In addition, two less intense anomeric signals belonging to two Glcp residues (at  $\delta$  5.17 and  $\delta$  5.10) were observed.

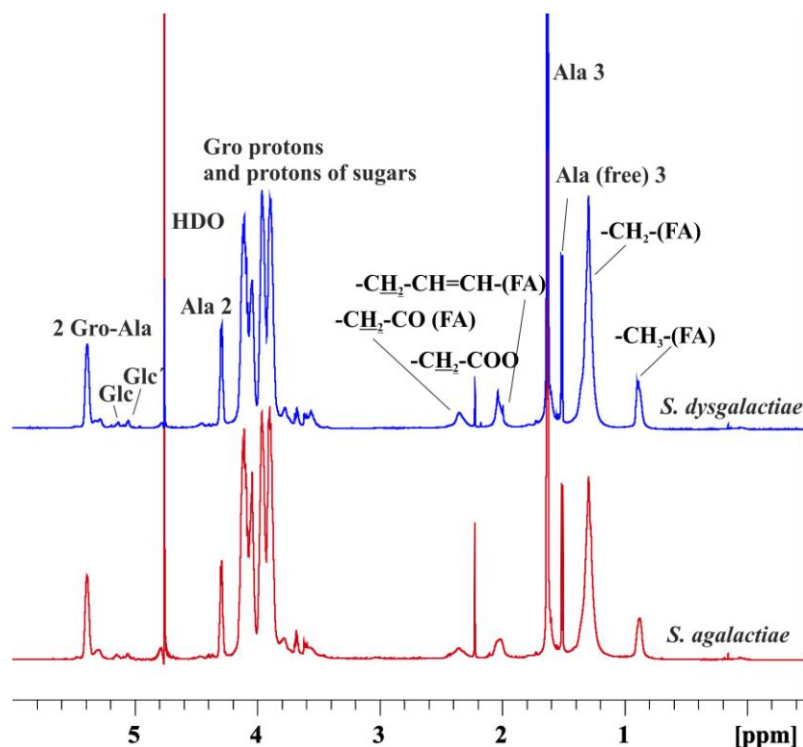


**Figure 4.6**  $^1\text{H}$  NMR spectra of the native LTA from *S. agalactiae* 0250 and *S. dysgalactiae* 2023. The spectra were recorded at 27°C and 700 MHz relative to external acetone ( $\delta_{\text{H}}$  2.225;  $\delta_{\text{C}}$  31.45).

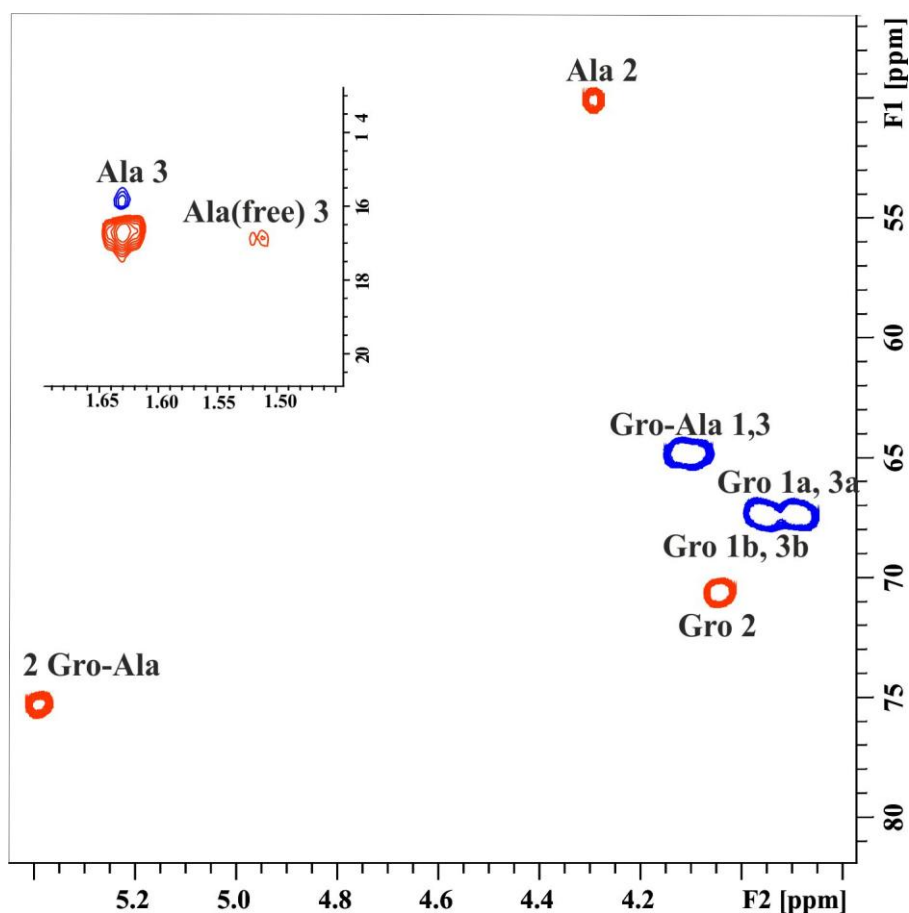


**Figure 4.7** Excerpt of  $^1\text{H}$ ,  $^{13}\text{C}$  HSQC-DEPT spectrum of the native LTA of *S. dysgalactiae* 2023. The spectra were recorded at 27°C and 700 MHz relative to external acetone ( $\delta_{\text{H}}$  2.225;  $\delta_{\text{C}}$  31.45). The chemical shifts of protons and carbons of the native LTA of *S. agalactiae* 0250 were very similar.

**Table 4.2**  $^1\text{H}$  and  $^{13}\text{C}$  chemical shift data (in ppm) of the native LTA isolated from *S. dysgalactiae* 2023

Residue		1(a)	1b	2	3(a)	3b
P-Gro-P	$^1\text{H}$	3.90	3.96	4.04	3.90	3.96
	$^{13}\text{C}$	67.47		70.67-	67.47	
P-Gro(-P)-Ala	$^1\text{H}$	4.11	4.11	5.39	4.11	4.11
	$^{13}\text{C}$	64.89		<b><u>75.44</u></b>	64.89	
Ala-(P-)Gro-P	$^1\text{H}$	-	-	4.29	1.63	
	$^{13}\text{C}$	171.23		50.11	16.5	
Ala free	$^1\text{H}$	-		3.92	1.50	
	$^{13}\text{C}$	175.72		51.01	16.92	

1D and 2D NMR spectra were recorded in  $\text{D}_2\text{O}$  at 700 MHz and 27°C relative to external acetone ( $\delta_{\text{H}}$  2.225;  $\delta_{\text{C}}$  31.45). Underlined and bold chemical shifts indicate substituted positions. The chemical shifts of protons and carbons of the native LTA of *S. agalactiae* 0250 were very similar.

All identified chemical shifts of the 2D NMR spectra such as  $^1\text{H}$ ,  $^1\text{H}$  COSY, TOCSY, ROESY, and  $^1\text{H}$ ,  $^{13}\text{C}$  HSQC and HMBC experiments could be assigned (Table 4.2). In a  $^{31}\text{P}$  NMR spectrum a phosphodiester group ( $\delta$  0.39) was observed, and in a  $^1\text{H}$ ,  $^{31}\text{P}$  HMBC the correlation of H-1b,3a and H-3a,1b of Gro with phosphodiester groups. A phosphodiester group ( $\delta$  0.39) was observed in  $^{31}\text{P}$  NMR spectrum and the linkage of H-1a,3b and H-3a,1b of P-Gro-P in  $^1\text{H}$ ,  $^{31}\text{P}$  HMBC with phosphodiester group. Additionally, the cross peak Gro H-2/Ala C-1 in the HMBC spectrum revealed the substitution of Gro by D-Ala at O-2.

### 4.3.3 ESI/MS investigation of the LTA

The native LTA of both *Streptococcus* species were investigated by ESI FT-ICR MS. The measurement of the native LTA from *S. dysgalactiae* 2023 (Figure 4.8) identified the prominent molecular mass at 918.632 u, which corresponded to the lipid anchor composed of 2 hexoses, 1 Gro, 1 16:1, and 1 18:0 (calculated mass 918.628 u; Table 4.3). Additionally, ESI FT-ICR MS experiments revealed heterogeneous acylation patterns of the Gro residue in the lipid anchor i.e. 16:1 + 16:0, 16:1 + 18:1, 16:1 + 18:0, 18:0 + 18:1, as well as the length of the poly(phospho-Gro) chain ( $\Delta m = 154$  u). The longest chain of the hydrophilic backbone from LTA of *S. dysgalactiae* 2023 as observed by ESI FT-ICR MS contained 27 GroP units substituted with 11 D-Ala molecules and attached to the lipid anchor (Table 4.3). The measurements of two different LTA preparations of *S. agalactiae* 0250 did not succeed in identifying the mass composition.

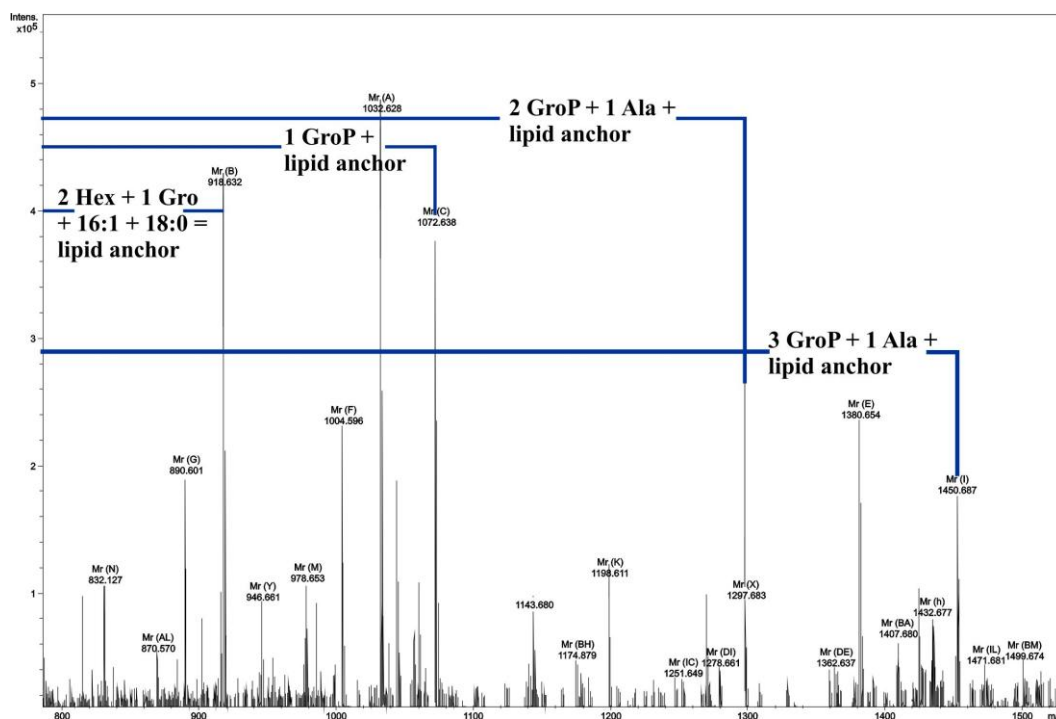


**Figure 4.8** Part of the ESI FT-ICR mass spectrum from the native LTA of *S. dysgalactiae* 2023. The measurements were performed in the negative mode at 5 V.

**Table 4.3 The assigned and calculated mass peaks from the LTA of *S. dysgalactiae* 2023.**

For calculations average mass units of 71.037 for Ala, 74.036 for Gro, 162.052 for Hex, 79.966 for P, 210.198 for 16:0, 236.214 for 16:1, 264.245 for 18:1 and 278.261 were used. The ESI-MS analysis of the LTA from *S. dysgalactiae* 2023 revealed up to 27 GroP units of the hydrophilic backbone.

Detected u	Components	Calculated u	Repeating units
890.601	16:1, 16:0, 2 Hex, 1 Gro	890.596	
918.632	16:1, 18:0, 2 Hex, 1 Gro	918.628	
946.661	18:1, 18:0, 2 Hex, 1 Gro	946.659	
1072.638	16:1, 18:0, 2 Hex, 2 Gro, 1 P	1072.631	1
1143.680	16:1, 18:0, 2 Hex, 2 Gro, 1 P, 1 Ala	1143.668	1
1297.683	16:1, 18:0, 2 Hex, 3 Gro, 2 P, 1 Ala	1297.671	2
1380.654	16:1, 18:0, 2 Hex, 4 Gro, 3 P	1380.637	3
1534.656	16:1, 18:0, 2 Hex, 5 Gro, 4 P	1534.640	4
1767.749	16:1, 18:0, 2 Hex, 5 Gro, 4 P, 2 Ala	1767.715	4
1759.703	16:1, 18:0, 2 Hex, 6 Gro, 5 P, 1 Ala	1759.681	5
1830.725	16:1, 18:0, 2 Hex, 6 Gro, 5 P, 2 Ala	1830.718	5
1984.734	16:1, 18:0, 2 Hex, 7 Gro, 6 P, 2 Ala	1984.721	6
2055.767	16:1, 18:0, 2 Hex, 7 Gro, 6 P, 3 Ala	2055.758	6
2138.744	16:1, 18:0, 2 Hex, 8 Gro, 7 P, 2 Ala	2138.724	7
2181.745	16:1, 16:0, 2 Hex, 8 Gro, 7 P, 3 Ala	2181.730	7
2207.770	16:1, 18:1, 2 Hex, 8 Gro, 7 P, 3 Ala	2207.745	7
2434.857	16:1, 18:1, 2 Hex, 9 Gro, 8 P, 4 Ala	2434.801	8
3346.919	16:1, 18:0, 2 Hex, 14 Gro, 13 P, 6 Ala	3346.891	13
3808.937	16:1, 18:0, 2 Hex, 16 Gro, 15 P, 6 Ala	3808.900	15
3879.993	16:1, 18:0, 2 Hex, 16 Gro, 15 P, 7 Ala	3879.938	15
4638.095	16:1, 18:0, 2 Hex, 21 Gro, 20 P, 9 Ala	4638.024	20
5858.151	16:1, 18:0, 2 Hex, 28 Gro, 27 P, 11 Ala	5858.120	27

ESI FT-ICR mass spectrum of *S. dysgalactiae* 2023 LTA was performed in the negative mode at 5 V.

#### 4.3.4 Isolation and NMR investigation of the lipid anchor of the LTA

Weak signals belonging to two Glcp residues in the NMR spectra of the native LTA were assumed to originate from the lipid anchor. The isolation and identification of its backbone structure was performed by depolymerization using 48% aq. HF. After the treatment of 16.8 mg

LTA of *S. agalactiae* 0250 and 10.1 mg LTA of *S. dysgalactiae* 2023 with 48% aq. HF the glycerol phosphate backbone was cleaved from the LTA. Successful  $\text{CHCl}_3/\text{MeOH}/\text{H}_2\text{O}$  extraction recovered the lipid anchor in the organic phase [4.1 mg (24.4%), *S. agalactiae* 0250; 2.5 mg (24.7%), *S. dysgalactiae* 2023], which was subjected to NMR spectroscopy. Further, this lipid was deacylated with abs. hydrazine. The yields of the isolated LTA lipid backbone were 1.7 mg (10.1%) for *S. agalactiae* 0250 and 1.4 mg (13.9%) for *S. dysgalactiae* 2023. These preparations were subjected to NMR spectroscopy.

$^1\text{H}$  NMR spectrum revealed both H-1 of Glc ( $\delta_{\text{H}}$  5.17) and Glc' ( $\delta_{\text{H}}$  5.10) (Table 4.4). COSY and TOCSY experiments were applied for assignment of the proton chemical shifts of the two hexoses and one Gro, which comprised the linker backbone of the LTA. The corresponding carbon chemical shifts were determined by a  $^1\text{H},^{13}\text{C}$  HSQC-DEPT NMR experiment (Figure 4.9). In a ROESY NMR experiment, the presence of *intra*-residual nOe contacts of the Glc residues between H-1 and H-2 and  $J_{1,2}$  values of 3.52 Hz (Glc) and  $J_{1,2}$  3.96 Hz (Glc') identified both as  $\alpha$ -pyranoses. The *gluco* configuration was determined by an *intra*-residual H-2/H-4 nOe connectivity. NOe contacts observed between Glc' H-1/Glc H-2 and Glc H-1/Gro H-3 identified the structure of the linker backbone as  $\alpha$ -D-Glcp-(1 $\rightarrow$ 2)- $\alpha$ -D-Glcp-(1 $\rightarrow$ 3)-Gro, which was confirmed by the products of methylation analysis, i.e. 1,5-di-*O*-acetyl-2,3,4-tri-*O*-methyl-[1- $^2\text{H}$ ]glucitol and 1,2,5-tri-*O*-acetyl-3,4-di-*O*-methyl-[1- $^2\text{H}$ ]glucitol.

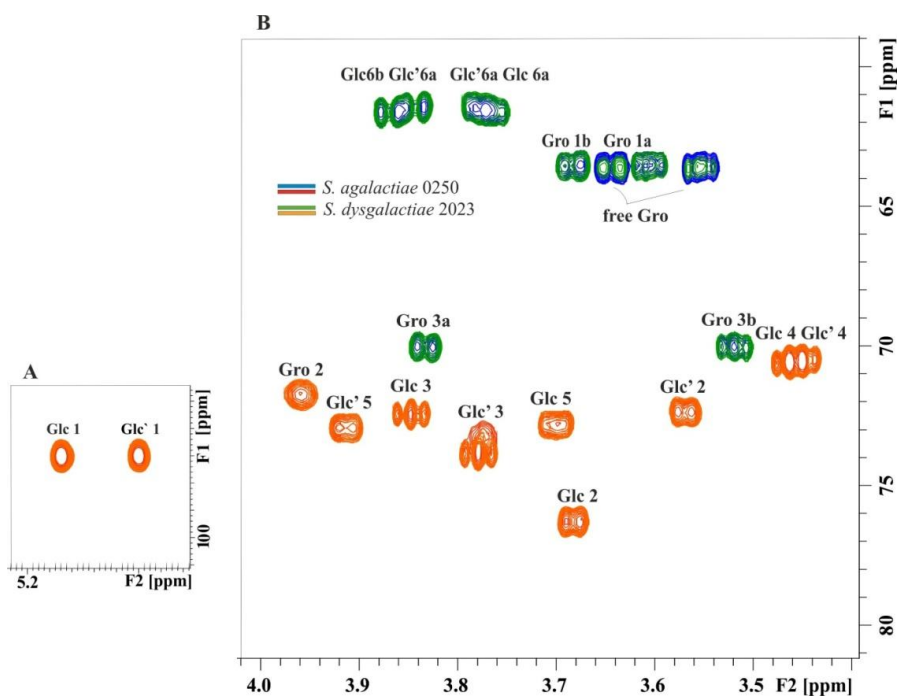


**Figure 4.9** Exerpts of the overlaid  $^1\text{H},^{13}\text{C}$  HSQC-DEPT spectra of *O*-deacylated lipid anchors of both *Streptococcus* species.

The exerpts of  $^1\text{H},^{13}\text{C}$  HSQC-DEPT spectra were taken from the anomeric region (A), ring proton and glycerol regions (B). The spectra were measured in  $\text{D}_2\text{O}$  at  $27^\circ\text{C}$  relative to external acetone ( $\delta_{\text{H}}$  2.225;  $\delta_{\text{C}}$  31.45).

**Table 4.4**  $^1\text{H}$  and  $^{13}\text{C}$  chemical shift data (in ppm) of the *O*-deacylated lipid anchor isolated from LTA of *S. dysgalactiae* 2023

Residue		1(a)	1b	2	3(a)	3b	4	5	6a	6b
$\alpha$ -D-Glcp	$^1\text{H}$	5.17	3.68	3.85	3.46	3.70	3.77	3.86		
	$^{13}\text{C}$	97.03	<b><u>76.34</u></b>	72.48	70.66	72.87	61.61			
$\alpha$ -D-Glcp'	$^1\text{H}$	5.10	3.57	3.77	3.45	3.91	3.78	3.83		
	$^{13}\text{C}$	97.03	72.39	73.89	70.53	72.95	61.52			
Gro	$^1\text{H}$	3.60	3.68	3.96	3.89	3.52				
	$^{13}\text{C}$	63.68	71.75	<b><u>70.11</u></b>						

1D and 2D NMR spectra were recorded in  $\text{D}_2\text{O}$  at 700 MHz and 27°C relative to external acetone ( $\delta_{\text{H}} 2.225$ ;  $\delta_{\text{C}} 31.45$ ). Underlined and bold chemical shifts indicate substituted positions. The chemical shifts of protons and carbons of the native LTA of *S. agalactiae* 0250 were very similar.

**Table 4.5**  $^1\text{H}$  and  $^{13}\text{C}$  chemical shift data (in ppm) of the aqueous phase components obtained after HF treatment of LTA isolated from *S. dysgalactiae* 2023

Residue		1(a)	1b	2	3(a)	3b
Gro	$^1\text{H}$	3.55	3.66	3.78	3.57	3.65
	$^{13}\text{C}$	63.72	73.29	63.72		
Gro-Ala (Ala in pos. 2)	$^1\text{H}$	3.77	3.81	5.13	3.77	3.81
	$^{13}\text{C}$	61.19	<b><u>78.69</u></b>	61.19		
Gro'-Ala (Ala in pos. 1)	$^1\text{H}$	4.28	4.37	4.02	3.64	3.67
	$^{13}\text{C}$	<b><u>68.16</u></b>	70.43	63.23		
Ala-Gro	$^1\text{H}$	-	-	4.26		
	$^{13}\text{C}$	170.21	50.04	16.32		
Ala free	$^1\text{H}$	-	-	4.02		
	$^{13}\text{C}$	n.d.	50.04	16.74		

1D and 2D NMR spectra were recorded in  $\text{D}_2\text{O}$  at 700 MHz and 27°C relative to external acetone ( $\delta_{\text{H}} 2.225$ ;  $\delta_{\text{C}} 31.45$ ). Underlined and bold chemical shifts indicate substituted positions. n.d. stands for not determined. The chemical shifts of protons and carbons of the native LTA of *S. agalactiae* 0250 were very similar.

The analysis of the aqueous phase obtained after HF treatment of the native LTA confirmed D-Ala as the only substituent of Gro at *O*-2 (H-1a,3a  $\delta$  3.77; H-1b,3b,  $\delta$  3.81; H-2,  $\delta$  5.13, Table 4.5). Due to the migration of Ala to *O*-1 of Gro after cleavage of the phosphodiester bonds prominent signals belonging to a Gro'-Ala residue were observed (H-1a,  $\delta$  4.28; H-1b,  $\delta$  4.37; H-2,  $\delta$  4.02;

H-3a,  $\delta$  3.64; H-3b,  $\delta$  3.67). Additionally, signals corresponding to unsubstituted Gro, bound and free D-Ala were assigned (Table 4.5).

In order to prove the linkage of the poly(phospho-Gro) chain to Glc<sup>3</sup> of the lipid anchor, the LTA (9.2 mg, *S. agalactiae*; 9.2 mg *S. dysgalactiae*) was *O*-deacylated with abs. hydrazine. The <sup>1</sup>H NMR spectrum of the product (6.5 mg, 70%, *S. agalactiae*; 5.9 mg, 64%, *S. dysgalactiae*) as compared to native LTA lacked signals of fatty acids, Gro-Ala, and Ala. Signals corresponding to Glc and Glc<sup>3</sup> were more pronounced, and the correlation Gro C-1/Glc<sup>3</sup> H-6 was observed on the HMBC spectrum (not shown), identifying the linkage of the hydrophilic backbone of LTA to *O*-6 of Glc<sup>3</sup>.

The degree of LTA substitution by D-Ala was quantified as 37% (*S. dysgalactiae*), and 33% (*S. agalactiae*) by the integral ratio of total Gro signals ( $\delta$  4.11 – 3.62 and  $\delta$  5.35) and the signal at  $\delta$  1.64 corresponding to the CH<sub>3</sub> group of bound D-Ala. The integral ratio of the anomeric proton of Glc ( $\delta$  5.17 ppm) in the <sup>1</sup>H NMR spectrum of deacylated LTA and region of Gro signals ( $\delta$  4.05 – 3.87 ppm) identified the average chain length of 29 GroP units for *S. dysgalactiae* 2023, and 35 GroP units for *S. agalactiae* 0250. This average chain length of LTA from *S. dysgalactiae* was concordant with the 27 GroP units detected in ESI FT-ICR MS analysis.

In summary, the isolated LTAs from both *Streptococcus* species possessed the lipid anchor structure  $\alpha$ -D-Glcp-(1 $\rightarrow$ 2)- $\alpha$ -D-Glcp-(1 $\rightarrow$ 3)-1,2-diacyl-*sn*-Gro linked to the hydrophilic backbone consisting of poly(*sn*-glycerol-1-phosphate), randomly substituted at *O*-2 of glycerol by D-Ala (Figure 4.10).

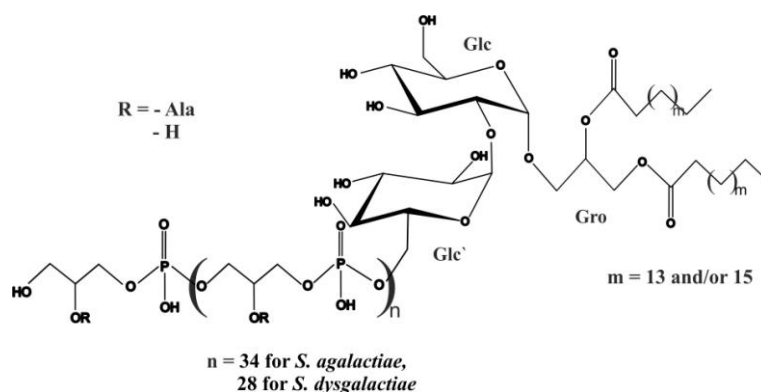


**Figure 4.10** The structure of the LTA from *S. agalactiae* 0250 and *S. dysgalactiae* 2023.

The lipid anchor structure of both *Streptococcus* species was  $\alpha$ -D-Glcp-(1 $\rightarrow$ 2)- $\alpha$ -D-Glcp-(1 $\rightarrow$ 3)-1,2-diacyl-*sn*-Gro. The hydrophilic backbone of the LTAs comprised poly(*sn*-glycerol 1-phosphate) randomly substituted at *O*-2 of glycerol by D-Ala.

## 4.4 Biological activity of the LTA

### 4.4.1 HEK293 assay with native LTA

LTA of Gram-positive bacteria has been controversially described in the past to be TLR2 or TLR4 active. In presented study the native and H<sub>2</sub>O<sub>2</sub>-treated LTA preparations of both *S. agalactiae* 0250 and *S. dysgalactiae* 2023 species were investigated with regard to their biological activity in HEK293 cells transiently transfected with NOD1, NOD2, TLR2 and TLR4.

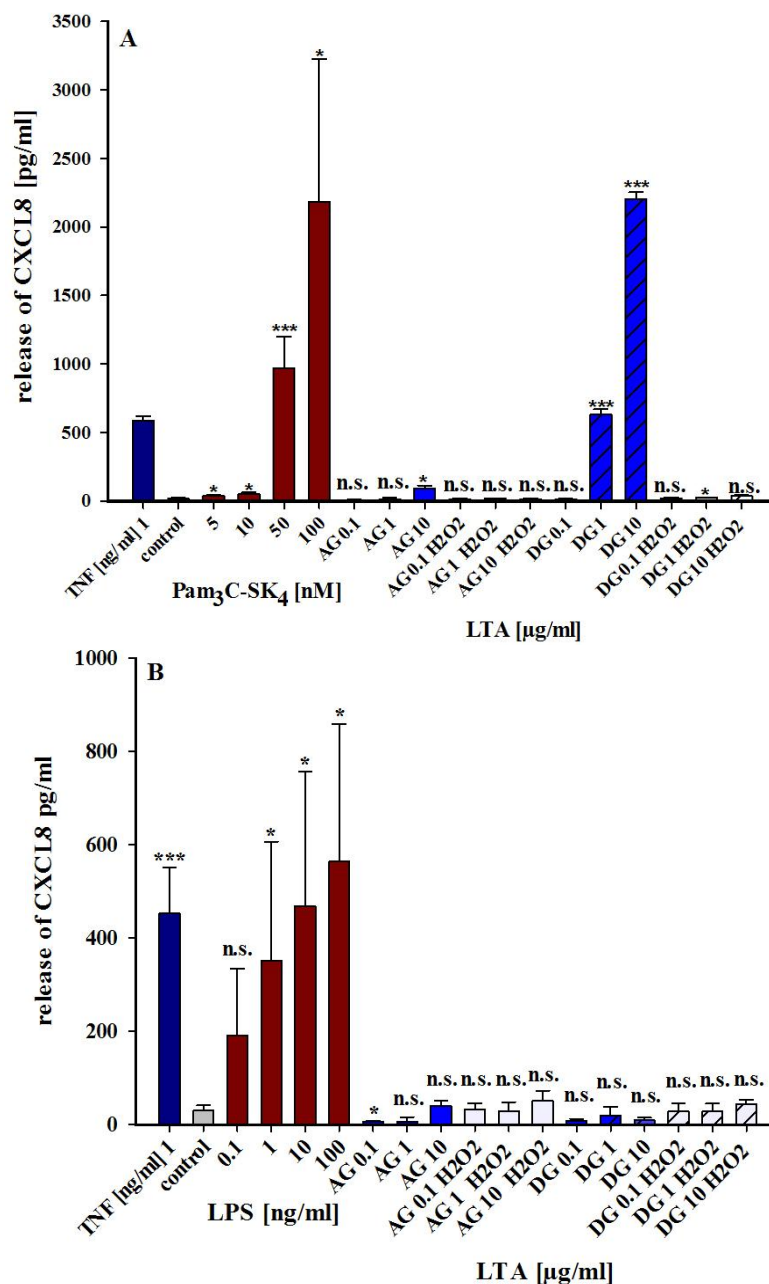


**Figure 4.11** Activation either of TLR2- (A) or TLR4- (B) transfected HEK293 cells by LTA of *S. agalactiae* 0250 (AG, not filled) and *S. dysgalactiae* 2023 (DG, fasciated).

The activation was measured as CXCL8 release in pg/ml. The LTA preparations in blue were not treated by H<sub>2</sub>O<sub>2</sub> and can contain putative lipoproteins, the preparations in white were H<sub>2</sub>O<sub>2</sub>-treated. The applied LTA concentrations were 0.1, 1 and 10 µg/ml. As positive controls Pam<sub>3</sub>C-SK<sub>4</sub> [nM] and TNF-α [ng/ml] were used in case of TLR2-, and LPS [ng/ml] and TNF-α [ng/ml] in case of TLR4-transfected cells. Results are expressed as mean ± SD of three measurements. Significance of the data above the bars is expressed in \*  $p < 0.05$ , \*\*  $p < 0.01$ , \*\*\*  $p < 0.001$  compared to the control applying unpaired t-test.

The activation of transiently transfected HEK293 cells by streptococci LTA showed clearly the importance of the H<sub>2</sub>O<sub>2</sub>-treatment (Figure 4.11). Especially the native LTA preparations of *S. dysgalactiae* resulted in high CLXL8 release. In case of activation of TLR2 by native *S. dysgalactiae* LTA the activation was even statistically significant. The TLR4 transfected cells demonstrated a slight activation by the LTA, the values were however under the smallest concentration (0.1 ng/ml) of LPS used as a positive control. The LTA preparations of *S. agalactiae* 0250 and *S. dysgalactiae* 2023 could neither activate the HEK293 cells via TLR2 nor via TLR4. The preparations were also NOD1- and NOD2- inactive, demonstrating the lack of PGN and the purity of the samples (data not shown).

#### 4.4.2 Stimulation of hMNC by LTA

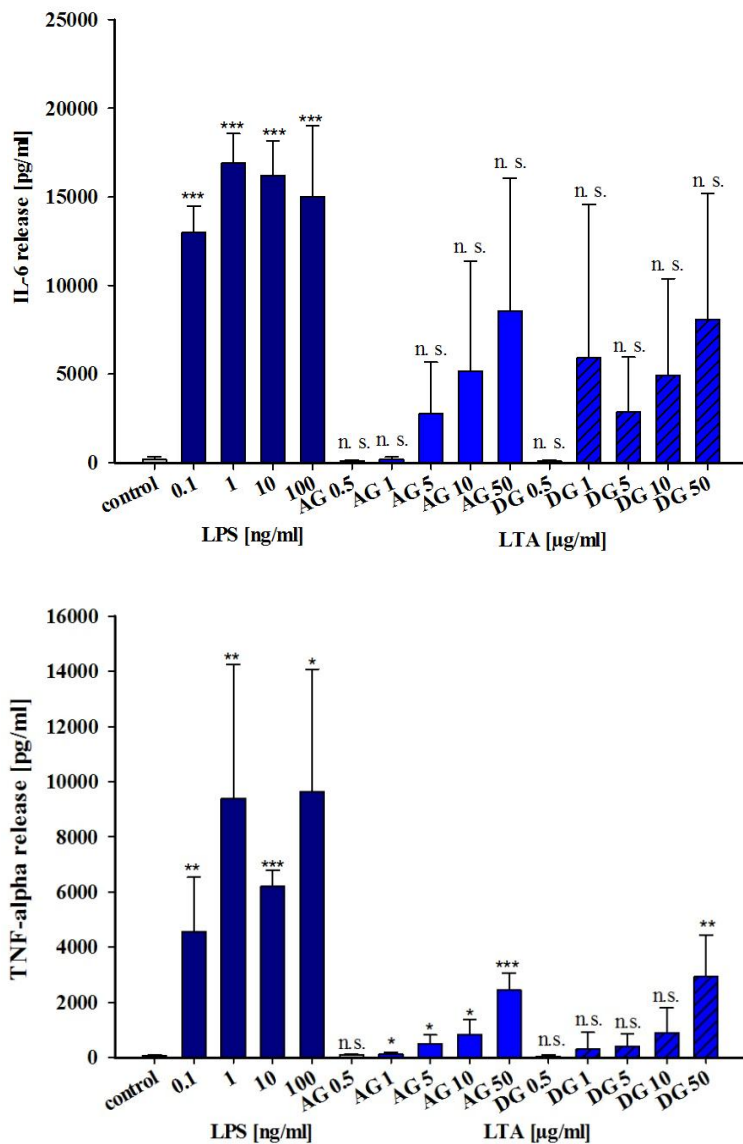


**Figure 4.12 Stimulation of hMNC by H<sub>2</sub>O<sub>2</sub>-treated LTAs of *S. agalactiae* 0250 (AG, blue, not filled) and *S. dysgalactiae* 2023 (DG, blue, fasciated).**

The activation of hMNC was measured as IL-6 release or TNF- $\alpha$  release in pg/ml. The applied LTA concentrations were 0.5, 1, 10 and 50  $\mu$ g/ml. The LTA preparations are H<sub>2</sub>O<sub>2</sub>-treated. As positive control LPS [ng/ml] was used. Results are expressed as mean  $\pm$  SD of 3 measurements. Significance of the data above the bars is expressed in \*  $p < 0.05$ , \*\*  $p < 0.01$ , \*\*\*  $p < 0.001$  compared to the control, applying unpaired t-test.

Additionally, the H<sub>2</sub>O<sub>2</sub>-treated LTA preparations of *S. agalactiae* 0250 and *S. dysgalactiae* 2023 were investigated concerning activation of hMNC (Figure 4.12). The cells were incubated for 20 h with different concentrations of LTA (0.5, 1, 10 and 50 µg/ml), and IL-6 and TNF-α production was measured. LPS of *E. coli* (0.1, 1, 10 and 100 ng/ml) was used as a positive control. The LTA of both streptococci slightly activated the hMNC. To obtain results in the same range the stimulation dosis of LTA needs to be 1000 times higher than that of LPS. The increase of TNF-α was statistically significant in case of LTA of *S. agalactiae* 0250 as compared to the negative control. LTA of *S. dysgalactiae* 2023 only at 50 µg/ml concentration provoked statistically significant increase of TNF-α. The trend of increased IL-6 release after stimulation with LTA of both streptococci was observed, however determined results were not statistically significant.

#### 4.4.3 Effect of Ala on biological activity of LTA in HEK293 cells

The significance of D-Ala substitution for biological activity of LTA has been discussed in the past. The alanylated and dealanylated native LTA preparations were tested for TLR2 and TLR4 (data not shown) activity in the HEK293 transfection system (Figure 4.13).

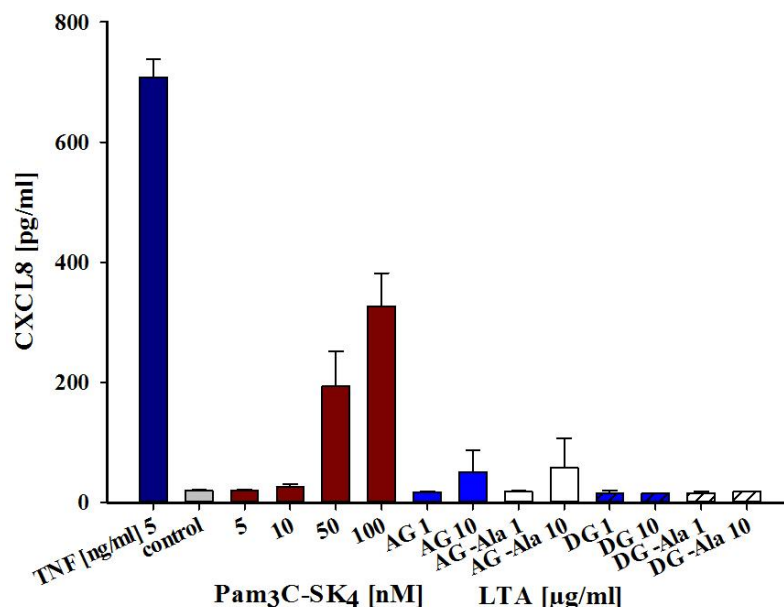


**Figure 4.13** Activation of TLR2-transfected HEK293 cells by native LTA of *S. agalactiae* 0250 (AG, not filled) and *S. dysgalactiae* 2023 (DG, fasciated).

As the activation CXCL8 release in pg/ml was measured. The LTA preparations in blue are alanylated, the preparations in white are dealanylated. The applied LTA concentrations were 1 and 10 µg/ml. As positive controls Pam<sub>3</sub>C-SK<sub>4</sub> [nM] and TNF-α [ng/ml] were used. Results of one assay (N=1) with three measurements are expressed mean ± SD.

The measurements of CXCL8 after the stimulation of HEK293 by both *Streptococcus* strains demonstrated no differences between the alanylated and dealanylated LTA. Slight activity of the LTA preparation from *S. agalactiae* 0250 could originate from lipoprotein or lipoprotein-like components, since the samples were not H<sub>2</sub>O<sub>2</sub>-treated.

#### 4.4.4 Phagocytosis capacity of the leukocytes in the presence of LTA

The effects of the presence of H<sub>2</sub>O<sub>2</sub>-treated native LTA from both *Streptococcus* species on phagocytosis capacity of bovine neutrophils and monocytes were examined. Leukocyte phagocytosis of *E. coli* or *Staph. aureus* cells in the presence or absence of streptococci LTA was investigated. LTA of *S. agalactiae* 0250 and *S. dysgalactiae* 2023 had a negative effect on phagocytosis capacity, especially *Staph. aureus* cells were less phagocytosed by neutrophils and monocytes (Figure 4.14, A and Figure 4.15, A) compared to the negative control. The data were statistically significant (\*  $p < 0.05$ ).

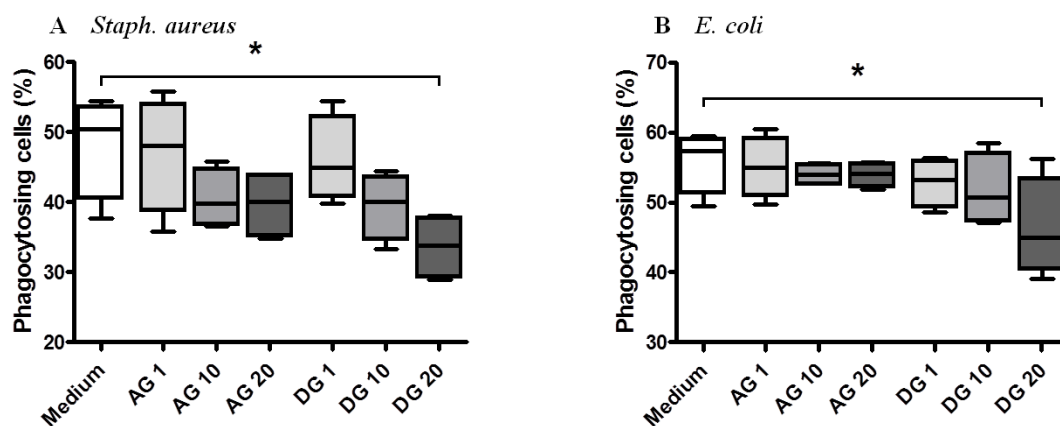


**Figure 4.14 Influence of LTA from *S. agalactiae* 0250 and *S. dysgalactiae* 2023 on the phagocytosis capacity of neutrophils.**

Bovine leukocytes ( $n = 4$  cows) were incubated with *Staph. aureus* (A) or *E. coli* (B) in the presence or absence (medium) of LTA from *S. agalactiae* 0250 (AG) or *S. dysgalactiae* 2023 (DG). LTA was used at 1, 10 or 20  $\mu\text{g/ml}$ . Results are expressed as percent of viable neutrophils with ingested bacteria. (\*  $p < 0.05$ , ANOVA one way test).

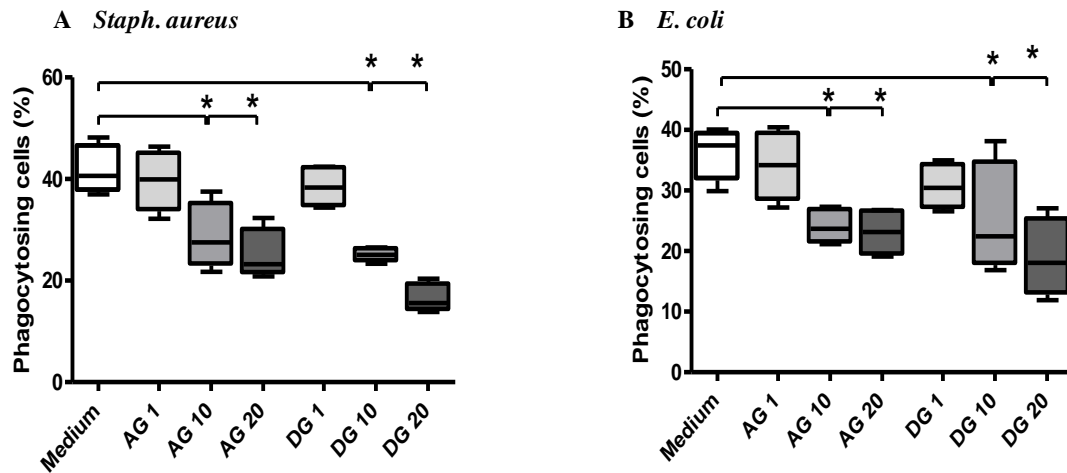


**Figure 4.15 Influence of LTA from *S. agalactiae* 0250 and *S. dysgalactiae* 2023 on the phagocytosis capacity of monocytes.**

Bovine leukocytes ( $n = 4$  cows) were incubated with *Staph. aureus* (A) or *E. coli* (B) in the presence or absence (medium) of LTA from *S. agalactiae* 0250 (AG) or *S. dysgalactiae* 2023 (DG). LTA was used at 1, 10 or 20  $\mu\text{g/ml}$ . Results are expressed as percent of viable monocytes with ingested bacteria. (\*  $p < 0.05$ , ANOVA one way test).

In the presence of LTA (20  $\mu\text{g/ml}$ ) from *S. agalactiae* 0250 the phagocytosis capacity of the neutrophils in presence of *Staph. aureus* was decreased from 50% (without LTA) to 41% and that of monocytes from 40 to 24%. The reduction effect on phagocytosis capacity of *Staph. aureus* was even bigger in the presence of LTA from *S. dysgalactiae* (neutrophils: 0, 1, 10, 20  $\mu\text{g/ml}$  LTA - 50%, 45%, 40%, 35%; monocytes: 0, 1, 10, 20  $\mu\text{g/ml}$  LTA - 41%, 38%, 24%, 19%) than in case of the presence of *S. agalactiae* 0250 LTA.

The native LTA of both *Streptococcus* species reduced also the phagocytosis capacity of monocytes in case of *E. coli* (0, 1, 10, 20  $\mu\text{g/ml}$  LTA from *S. agalactiae* 0250 - 38%, 36%, 24%, 23%; 0, 1, 10, 20  $\mu\text{g/ml}$  LTA from *S. dysgalactiae* 2023 - 38%, 31%, 24%, 20%; Figure 4.14, B). On contrary, the LTA from *S. agalactiae* 0250 had nearly no effect on the phagocytosis of *E. coli* by bovine neutrophils (0, 1, 10, 20  $\mu\text{g/ml}$  LTA - 58%, 55%, 54%, 54%), and the presence of the LTA from *S. dysgalactiae* reduced slightly the phagocytosis capacity from 58% (without LTA) to 47% (20  $\mu\text{g/ml}$  LTA) (Figure 4.14, B).

## 4.5 Investigation of the glycolipids of *Streptococcus* species

### 4.5.1 Isolation of the glycolipids

The glycolipids of *S. agalactiae* 0250 and *S. dysgalactiae* 2023 were successfully achieved from butanol phase of disrupted wet cells via Bligh and Dyer extraction. The crude extract of lipids and glycolipids of both *Streptococcus* species was separated by column chromatography (silica gel)

with an increased gradient of MeOH in CHCl<sub>3</sub> (3% - 50%). The analysis of each eluted fraction showed that *S. agalactiae* 0250 produced 4 different glycolipids (G1-G4) and *S. dysgalactiae* 2023 6 (G1-G6) (Figure 4.16).

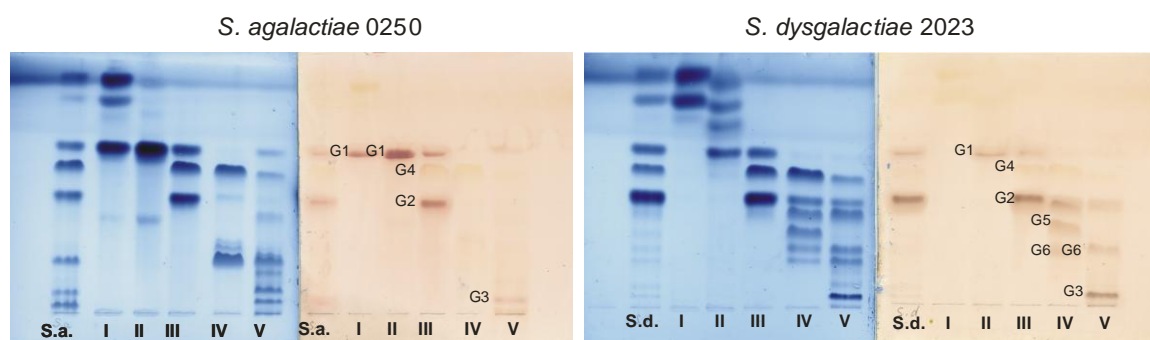


**Figure 4.16** TLC with overview of recovered lipids and glycolipids of *S. agalactiae* 0250 and *S. dysgalactiae* 2023.

Lipids and glycolipids were stained with Hanessian's stain (blue) and glycolipids were stained by  $\alpha$ -naphthol/sulfuric acid (pink). The lipids and glycolipids were eluted on silica gel column (7 × 1 cm) with CHCl<sub>3</sub>/MeOH fractions: I 97:3; II 95:5; III 90:10; IV 85:15; V 50:50. TLC was developed with CHCl<sub>3</sub>/MeOH/H<sub>2</sub>O (65/25/4, by vol.).

The glycolipids G4, G5 and G6 were present in very small amount and, thus, were difficult to purify for structural investigation. G1, G2 and G3 of both *Streptococcus* species were structurally elucidated applying 1D and 2D NMR spectroscopy, ESI FT ICR MS and MALDI FT ICR MS.

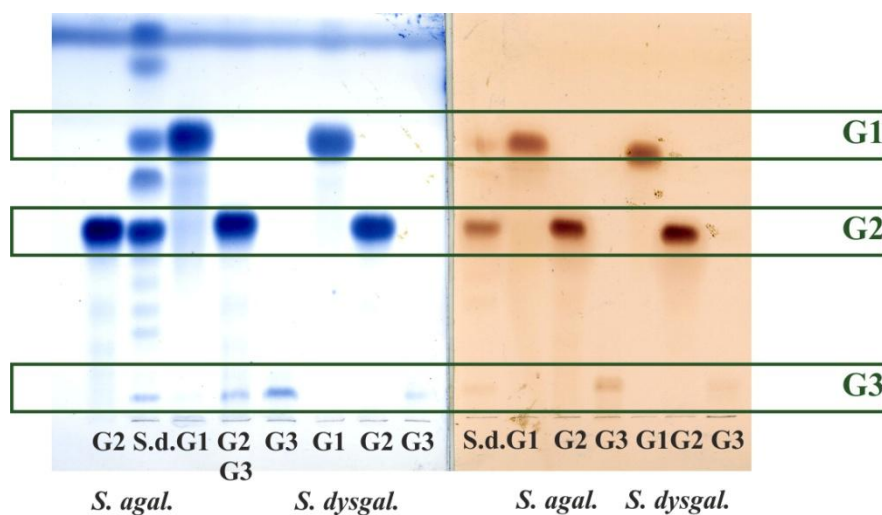


**Figure 4.17** Purified glycolipids G1, G2, G3 of *S. agalactiae* 0250 and *S. dysgalactiae* 2023. TLC was developed with CHCl<sub>3</sub>/MeOH/H<sub>2</sub>O (65/25/4, by vol.).

Both *Streptococcus* species produced three isolated glycolipids in bigger amounts. The yield of the revealed glycolipids was achieved in the ratio of G1/G2/G3 5/8/1.

### 4.5.2 ESI FT-ICR MS and MALDI FT-ICR MS analysis of the glycolipids

Applying ESI FT ICR MS and MALDI FT ICR MS experiments the fatty acids composition of the glycolipids G2 and G3 of both *Streptococcus* species could be elucidated. The obtained different fatty acids substitution pattern in the glycolipids is depicted in the Table 4.6.

**Table 4.6 Summary of fatty acid composition of the glycolipids from *S. agalactiae* 0250 and *S. dysgalactiae* 2023.**

The data were generated applying ESI FT-ICR MS and MALDI FT-ICR MS experiments. The used calculation average mass units were 200.18 for 12:0, 228.21 for 14:0, 256.24 for 16:0, 254.22 for 16:1, 284,27 for 18:0, 282.26 for 18:1 and 280.24 for 18:2. N. d. stands for not determined.

	G1	G2	G3
<i>S. agalactiae</i> 0250	n.d.	16:0 + 18:1; 16:0 + 16:1; 18:0 + 16:1; 18:1 + 18:1	16:0+16:1; 18:0+16:1; 18:1+18:1; 18:1+18:2
<i>S. dysgalactiae</i> 2023	n.d.	12:0+14:0; 14:0+14:0; 18:0+16:1; 18:0+18:1; 18:0+18:2	12:0+14:0; 14:0+14:0; 16:0+14:0; 16:0+16:1; 18:0+16:1; 18:1+18:1; 18:1+18:2

### 4.5.3 NMR spectroscopy of the glycolipids

The isolated glycolipids of *S. agalactiae* 0250 and *S. dysgalactiae* 2023 were subjected to 1D and 2D NMR spectroscopy. <sup>1</sup>H NMR spectra of the glycolipids revealed the chemical shifts of **Gro** substituted by **FA** at *O*-2 (H-2,  $\delta$  5.26) and of one **Glc** ( $\delta$  4.83, G1) or two **Glc** ( $\delta$  5.00 and  $\delta$  4.96, G2;  $\delta$  4.98 and  $\delta$  4.92, G3) in the anomeric regions. Further characteristic fatty acids signals of all glycolipids were identified in the region  $\delta$  2.34 - 0.89 (Figure 4.18).

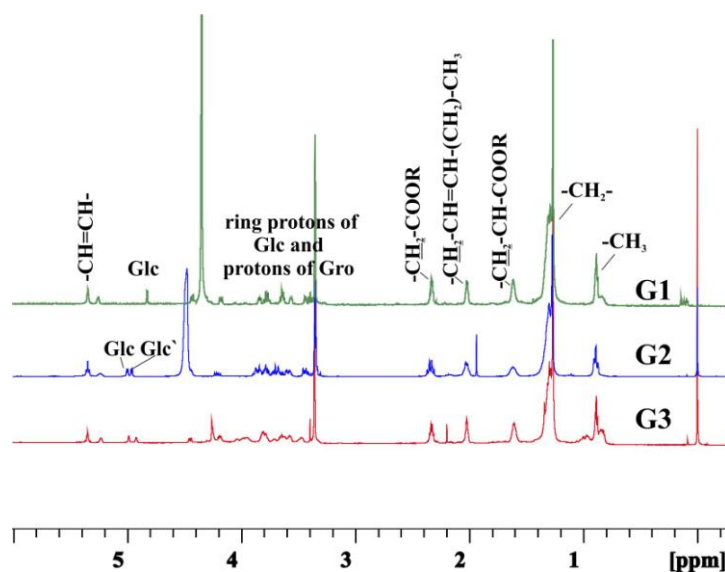


**Figure 4.18** The  $^1\text{H}$  NMR proton spectra of the glycolipids from *S. agalactiae* 0250.

The  $^1\text{H}$  NMR spectra were recorded in  $\text{CDCl}_3/\text{MeOD}$  (2:1, by vol.) at 700 MHz and at 27°C relative to the internal standard TMS ( $\delta_{\text{H}}$  0.00;  $\delta_{\text{C}}$  0.00).

**Table 4.7**  $^1\text{H}$  and  $^{13}\text{C}$  chemical shift data (in ppm) of glycolipid G1 of *S. dysgalactiae* 2023

Residue		1(a)	1b	2	3(a)	3b	4	5	6a	6b
$\alpha\text{-D-Glc}$	$^1\text{H}$	4.83	3.43	3.64	3.39	3.56	3.79	3.77		
	$^{13}\text{C}$	99.63	72.55	74.09	70.49	72.45	61.80			
<b>Gro</b>	$^1\text{H}$	4.18	4.43	5.26	3.83	3.63				
	$^{13}\text{C}$	62.95	70.40	<b><u>66.44</u></b>						

1D and 2D spectra were recorded in  $\text{CDCl}_3/\text{MeOD}$  (2:1, by vol.) at 700 MHz and at 27°C relative to the internal standard of TMS ( $\delta_{\text{H}}$  0.00;  $\delta_{\text{C}}$  0.00). Underlined and bold chemical shifts indicate substituted positions. The chemical shifts of protons and carbons of G1 of *S. agalactiae* 0250 were very similar.

The COSY and TOCSY 2D NMR experiments enabled identification of all proton chemical shifts data of tested glycolipids, and  $^1\text{H}, ^{13}\text{C}$  HSQC-DEPT experiment revealed the corresponding carbon chemical shifts of the molecules (Tables 4.7; 4.8; 4.9).

The *inter-residual* nOe contact **Glc** 1/**Gro** 3a,b in the ROESY experiment and the cross peak **Glc**, H-1/**Gro**, C-3 in the  $^1\text{H}, ^{13}\text{C}$  HMBC experiment G1 glycolipids of *S. agalactiae* 0250 and *S. dysgalactiae* 2023 revealed the substitution of **Glc** by **Gro**. The linkages of G2 from both *Streptococcus* species were determined by ROESY as **Glc**<sup>1</sup>/**Glc** 2 and **Glc** 1/**Gro** 3a,b and HMBC revealed cross peaks **Glc**<sup>1</sup>, H-1/**Glc**, C-2.

In G3 of both species *inter-residual* nOe contacts were observed in ROESY as **Glc**<sup>1</sup>/**Glc** 2 and **Glc** 1/**Gro** 3a,b and HMBC revealed cross peaks **Glc**<sup>1</sup>, H-1/**Glc**, C-2. The  $^1\text{H}, ^{13}\text{C}$  HSQC-DEPT

spectrum showed clearly the presence of Gro-P in G3. The linkages between Gro-P and Gro-Glc-Glc of G3, could not be identified from  $^{31}\text{P}$  and  $^1\text{H}, ^{31}\text{P}$  HMBC spectra.

**Table 4.8  $^1\text{H}$  and  $^{13}\text{C}$  chemical shift data (in ppm) of G2 of *S. dysgalactiae* 2023**

Residue		1(a)	1b	2	3(a)	3b	4	5	6a	6b
$\alpha\text{-D-Glcp}$	$^1\text{H}$	5.00		3.59		3.78	3.43	3.58	3.68	3.78
	$^{13}\text{C}$	97.07		<u>77.27</u>		72.39	69.90	72.39	61.61	
$\alpha\text{-D-Glcp}'$	$^1\text{H}$	4.96		3.44		3.69	3.32	3.87	3.78	3.83
	$^{13}\text{C}$	97.24		72.39		74.15	70.83	72.75	61.74	
Gro	$^1\text{H}$	4.20	4.42	5.23	3.84	3.65				
	$^{13}\text{C}$	63.20		70.49	<u>66.24</u>					

1D and 2D spectra were recorded in  $\text{CDCl}_3/\text{MeOD}$  (2:1, by vol.) at 700 MHz and at 27°C relative to the internal standard of TMS ( $\delta_{\text{H}}$  0.00;  $\delta_{\text{C}}$  0.00). Underlined and bold chemical shifts indicate substituted positions. The chemical shifts of protons and carbons of *S. agalactiae* 0250 were very similar.

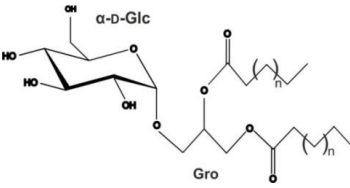
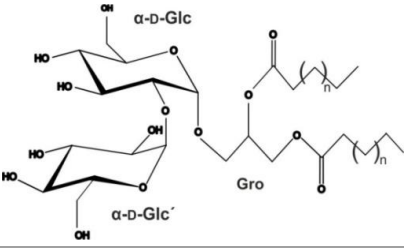
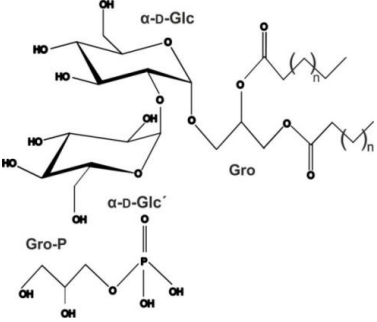
**Table 4.9  $^1\text{H}$  and  $^{13}\text{C}$  chemical shift data (in ppm) of G3 of *S. dysgalactiae* 2023**

Residue		1(a)	1b	2	3(a)	3b	4	5	6a	6b
$\alpha\text{-D-Glcp}$	$^1\text{H}$	4.99		3.57		3.77	3.47	3.56	3.78	3.80
	$^{13}\text{C}$	96.98		<u>78.27</u>		72.10	69.78	72.17	61.32	
$\alpha\text{-D-Glcp}'$	$^1\text{H}$	4.95		3.45		3.71	3.32	4.03	3.98	4.18
	$^{13}\text{C}$	97.20		72.17		73.56	70.35	71.82	<u>65.43</u>	
Gro	$^1\text{H}$	4.18	4.44	5.26	3.65	3.81				
	$^{13}\text{C}$	62.92		70.52	<u>66.40</u>					
Gro-P	$^1\text{H}$	3.94	3.93	3.80	3.62	3.60				
	$^{13}\text{C}$	<u>66.78</u>		71.27	62.49					

1D and 2D spectra were recorded in  $\text{CDCl}_3/\text{MeOD}$  (2:1, by vol.) at 700 MHz and at 27°C relative to the internal standard of TMS ( $\delta_{\text{H}}$  0.00;  $\delta_{\text{C}}$  0.00). Underlined and bold chemical shifts indicate substituted positions. The chemical shifts of protons and carbons of *S. agalactiae* 0250 were very similar.

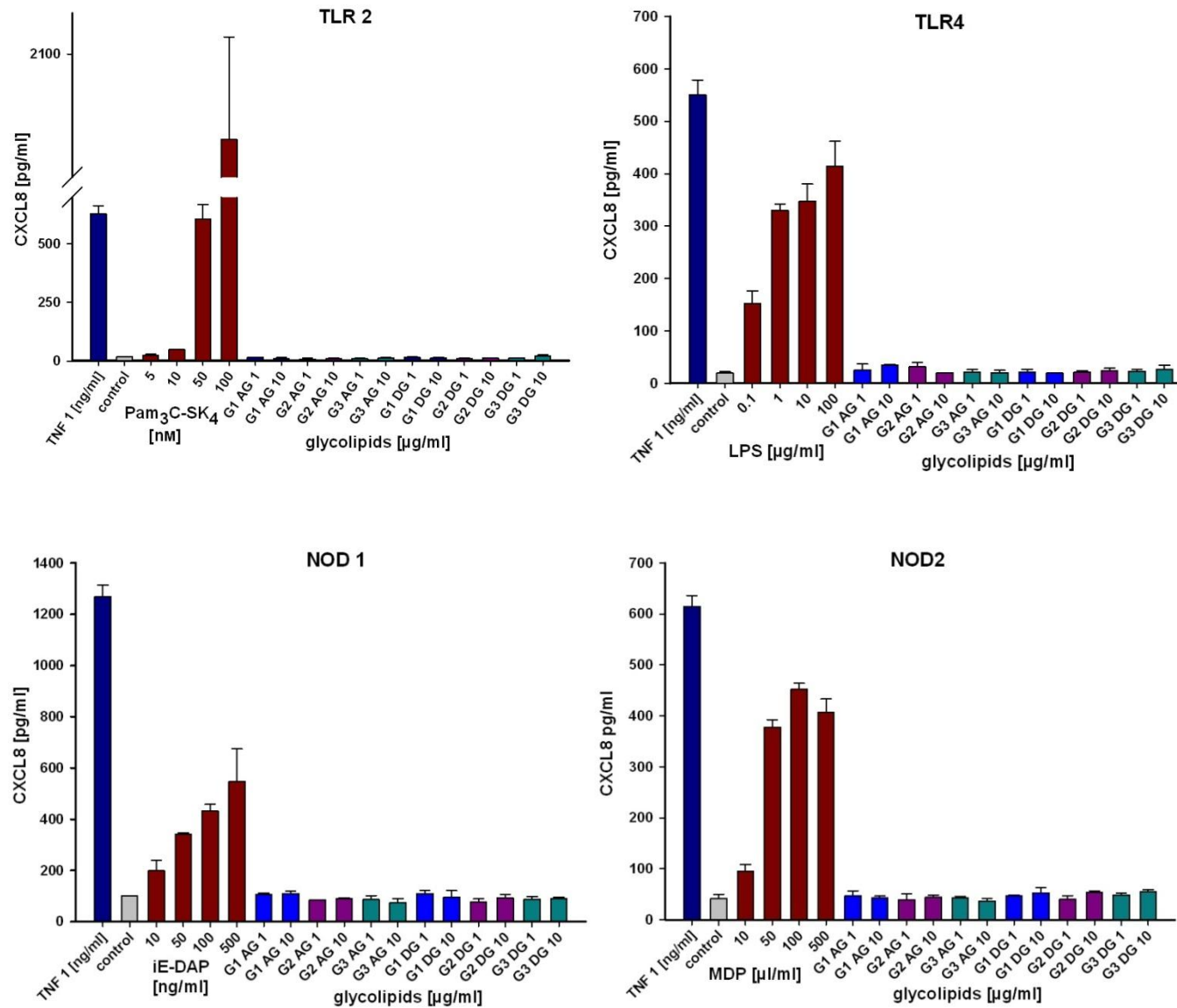
Taken together, the cytoplasmic membrane of both *Streptococcus* species contained three glycolipids in bigger amounts: G1,  $\alpha\text{-D-Glcp-(1}\rightarrow\text{3)-1,2-diacyl-sn-Gro}$  (monoglucosyl diacylglycerol), G2,  $\alpha\text{-D-Glcp-(1}\rightarrow\text{2)-}\alpha\text{-D-Glcp-(1}\rightarrow\text{3)-1,2-diacyl-sn-Gro}$  (diglucosyl diacylglycerol), and G3, glyceryl-3-phospho- $\alpha\text{-D-Glcp-(1}\rightarrow\text{2)-}\alpha\text{-D-Glcp-(1}\rightarrow\text{3)-1,2-diacyl-sn-Gro}$  (glycerophosphoryl diglucosyl diacylglycerol (Table 4.10).

Table 4.10 Glycolipid structures

Glycolipid	Structure
G1 monoglucosyl diacylglycerol (MGlcDAG)	
G2 diglucosyl diacylglycerol (DGlcDAG)	
G3 glycerophosphoryl diglucosyl diacylglycerol (GroP-DGlcDAG)	 The linkage of Gro-P and Glc' could not be identified.

#### 4.5.4 Immunological activity of the glycolipids in HEK293 cells

The isolated glycolipids G1, G2 and G3 of *S. agalactiae* 0250 and *S. dysgalactiae* 2023 were subjected to activate of TLR1, TLR2, NOD1 and NOD2 in transiently transfected HEK293 cells (Figure 4.19). The HEK293 cells were stimulated with appropriate glycolipids of *S. agalactiae* 0250 and *S. dysgalactiae* 2023 after 24 h of transfection. As positive controls were used TNF- $\alpha$  and iE-DAP for NOD1 transfected cells, TNF- $\alpha$  and MDP for NOD2 transfected cells, Pam<sub>3</sub>C-SK<sub>4</sub> and TNF- $\alpha$  in case of TLR2 and LPS and TNF- $\alpha$  in case of TLR4 transfected cells. The glycolipids G1, G2 and G3 (applied at 1 or 10  $\mu$ g/ml) could not activate such transfected HEK293 cells via TLR4, TLR2, NOD1 or NOD2. These assays showed that the tested glycolipids were free of LPS, lipopeptides and PGN contamination.



**Figure 4.19 Activation of HEK293 cells transfected with NOD1, NOD2, TLR2 or TLR4 by G1 (blue), G2 (dark pink) and G3 (dark cyan) from *S. agalactiae* 0250 (AG, not filled) and *S. dysgalactiae* 2023 (DG, fasciated).**

The glycolipids were applied at 1 or 10 μg/ml. As positive controls were used TNF-α [ng/ml] and iE-DAP [ng/ml] for NOD1-transfected cells, TNF-α [ng/ml] and MDP [ng/ml] for NOD2-transfected cells, Pam<sub>3</sub>C-SK<sub>4</sub> [nM] and TNF-α [μg/ml] in case of TLR2- and LPS [μg/ml] and TNF-α [μg/ml] in case of TLR4-transfected cells. Results are expressed as mean ± SD of one assay (N=1) with two measurements.

#### 4.5.5 Stimulation of splenocytes by glycolipids

The obtained glycolipids G1, G2 and G3 of *S. agalactiae* 0250 and *S. dysgalactiae* 2023 were investigated with regard to the induction of cytokine production by murine spleen cells. Especially iNKT cells were shown to produce cytokines after presentation of glycolipids by APCs [197]. The biological activity of G1, G2 and G3 was first investigated by their incubation with the splenocytes for 72 h. The amounts of IL-4 and IFN- $\gamma$  were measured by ELISA.

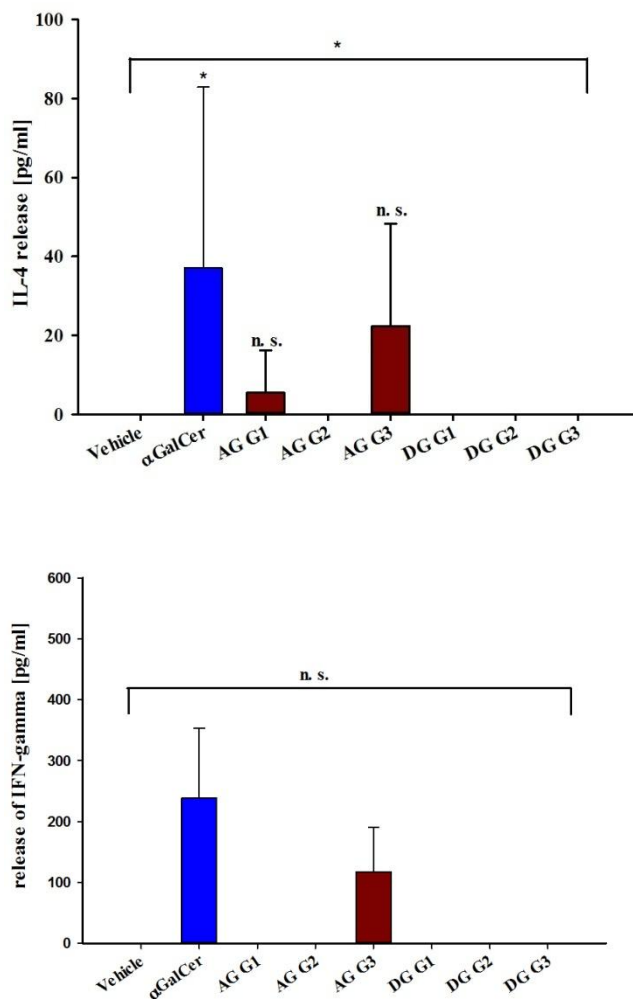


**Figure 4.20** Release of IL-4 and IFN- $\gamma$  by murine splenocytes after incubation with 20  $\mu$ g/ml of G1, G2 and G3 of *S. agalactiae* 0250 (AG) and *S. dysgalactiae* 2023 (DG) for 72 h.

As positive control was used  $\alpha$ GalCer (20  $\mu$ g/ml) and vehicle (0.5% Tween-20) was applied as negative control. The results were expressed as mean  $\pm$  SD of three different measurements. Significance of the data above the bars is expressed in \*  $p < 0.05$ , applying ANOVA one way test. In the case statistically significant data were achieved applying ANOVA one way test, Dunnett's method (comparison of the data versus control) was applied afterwards.

Despite the fact that glycolipids G1 and G3 of *S. agalactiae* 0250 and *S. dysgalactiae* 2023 display the same structures, only G1 and G3 of *S. agalactiae* 0250 induced slight IL-4 production and additionally only the glycolipid G3 of *S. agalactiae* 0250 induced IFN- $\gamma$  production by murine spleen cells. The range of all measurements of IL-4 release by spleen cells was statistically significant (\*  $p < 0.05$ ). Statistically significant IL-4 release was achieved applying  $\alpha$ GalCer, but not in case of stimulation by glycolipids. The range of all measurements of IFN- $\gamma$  release by murine spleen cells was not statistically significant (\*  $p < 0.05$ ).

## 4.6 WTA

### 4.6.1 Isolation and investigation of the WTA from streptococci

The WTA preparation of *S. agalactiae* 0250 and *S. dysgalactiae* 2023 obtained by cleavage with TCA was purified first by HIC and separated further on Q Sepharose. Subsequently, the phosphate content of the obtained fractions was determined, which revealed three fractions i. e. phosphate-less fraction P1, low-grade phosphate fraction P2 and high-grade phosphate fraction P3 (Figure 4.21).

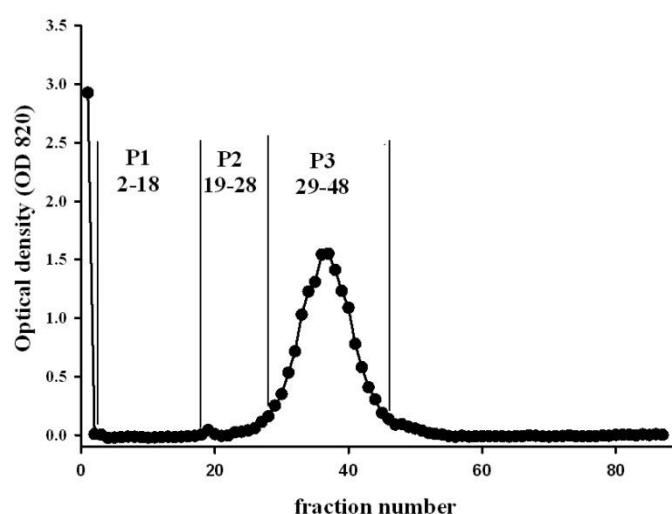


**Figure 4.21 Phosphate content of the Q Sepharose fractions.**

The measurement was performed photometrically at 820 nm. The 87 fractions were recovered applying Q Sepharose column of the WTA preparation from *S. dysgalactiae* 2023. The diagram of the phosphate measurements of the WTA preparation from *S. agalactiae* 0250 was very similar.

Three fractions P1, P2 and P3 were investigated by weak methanolysis, neutral sugar analysis, and subjected for  $^1\text{H}$  NMR spectroscopy. The results of these investigations demonstrated the differences of the fractions not only concerning their phosphate content. P1 of both species was rich of Rha, but in P1 of *S. dysgalactiae* also mannose (Man), Glc, GlcN and galactosamine

(GalN) were detectable. The  $^1\text{H}$  NMR spectrum of P1 of both *Streptococcus* species contained many signals in the anomeric region, characteristic signals of  $\text{CH}_3$  of Rha and NAc groups. The compositional analysis of P3 revealed high amounts of Rha and some Glc (Rha/Glc 13/1) (Table 4.11). In the  $^1\text{H}$  NMR spectrum of P3 of both *Streptococcus* species  $\text{CH}_3$  shifts of bound and free Ala,  $\text{CH}$  shift of Gro substituted by Ala and two signals of anomeric protons were present (Figure 4.22). The P3 fraction was considered the WTA preparation (chapter 4.6.2). The fraction P2 had characteristics of both P1 and P3 and appeared to be a mixture of P1 and P3.

**Table 4.11** Calculated molecular ratios of the neutral sugar analysis of the WTA preparations: fractions P1, P2 and P3.

Substance	Fractions of AG WTA preparation molecular ratio			Fractions of DG WTA preparation molecular ratio		
	P1	P2	P3	P1	P2	P3
Rha	2.7	3.6	12.7	39	9	2.5
Man	2.3	0.1		1.5	2.3	-
Glc	1	1	1	1	1	1
Gal	0.6	0.4	-	0.2	0.4	-
GlcN	-	1	-	0.9	-	-
GalN	-	-	-	1.4	1	-

AG stands for *S. agalactiae* 0250, DG stands for *S. dysgalactiae* 2023, Man for mannose.

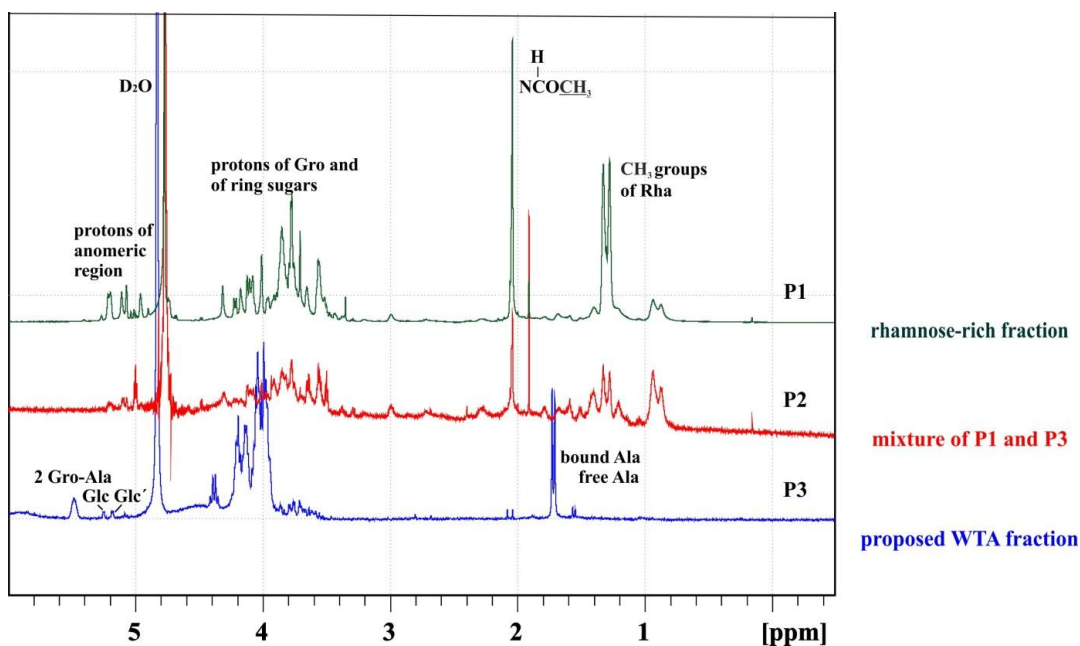


**Figure 4.22**  $^1\text{H}$  NMR spectra of P1, P2 and P3 isolated from *S. dysgalactiae* 2023.

The fractions were recovered in process of the WTA preparation. The spectra were recorded at  $27^\circ\text{C}$  and 700 MHz relative to external acetone ( $\delta_{\text{H}}$  2.225;  $\delta_{\text{C}}$  31.45). The revealed  $^1\text{H}$  NMR spectra of *S. agalactiae* 0250 were likewise.

## 4.6.2 NMR spectroscopy of WTA

$^1\text{H}$  NMR spectra revealed no significant differences between both WTA (P3 fractions). The data discussed below refer to the WTA preparation isolated from *S. dysgalactiae* 2023. The 1D and 2D NMR analysis of the WTA of *Streptococcus* species revealed three different Glc residues: Glcp (**A**), which was covalently bound to the Glcp (**B**), but is not substituted at position C-6, or which was covalently bound to Glcp (**B'**), substituted by phosphate at C-6 (Figure 4.23). Subsequently, five different Gro were observed in the sample: P-Gro-P (**D**) – unsubstituted Gro of the GroP-chain, P-Gro(-P)-Ala (**E**) – Gro of the GroP-chain substituted by Ala, Gro-Glc (**F**) – Gro substituted by Glc at C-3, P-Gro (**G**) – Gro with the phosphate group bound only at C-1 but not at C-3, and free Gro (**H**).

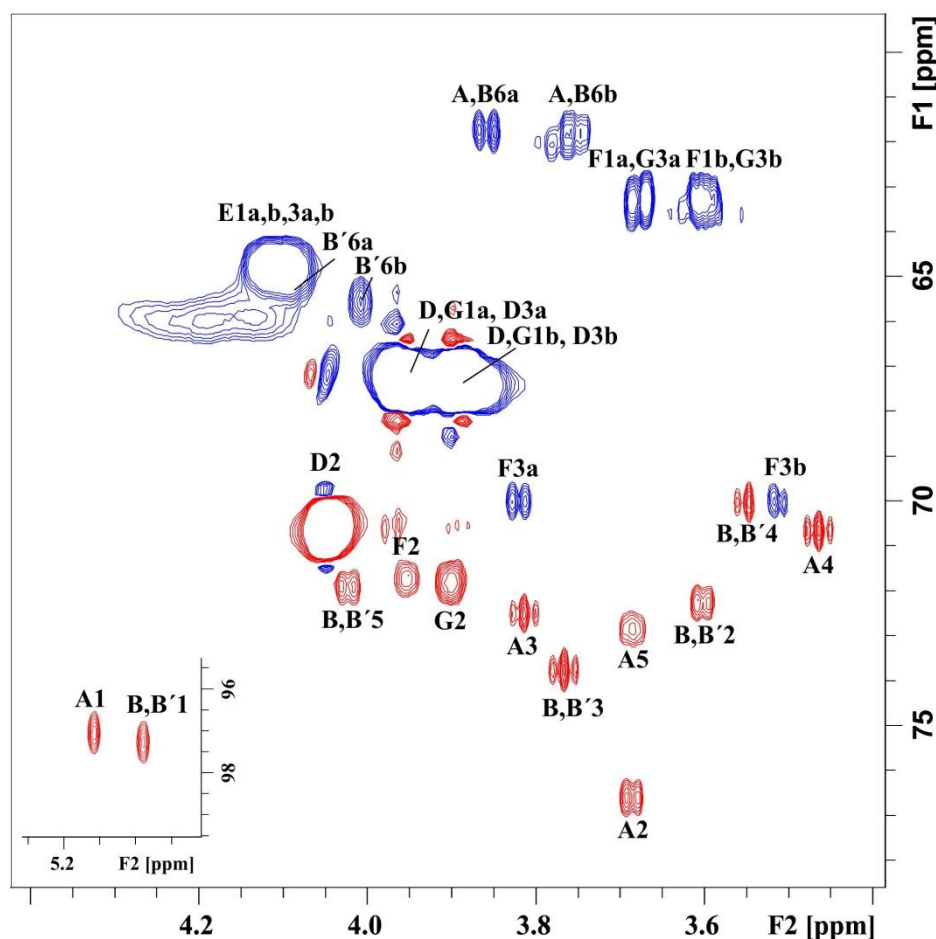


**Figure 4.23** Excerpt of the  $^1\text{H}$ ,  $^{13}\text{C}$  HSQC-DEPT spectrum of the WTA from *S. dysgalactiae* 2023. The spectrum was measured in  $\text{D}_2\text{O}$  at  $27^\circ\text{C}$  relative to external acetone ( $\delta_{\text{H}}$  2.225;  $\delta_{\text{C}}$  31.45). The capital letters refer to the molecules defined in Table 4.12. The chemical shifts of protons and carbons of *S. agalactiae* 0250 were very similar.

Table 4.12  $^1\text{H}$  and  $^{13}\text{C}$  chemical shift data (in ppm) of the WTA preparation of *S. dysgalactiae* 2023

Residue		1a	1b	2	3a	3b	4	5	6a	6b
$\alpha$ -D-Glcp A	$^1\text{H}$	5.16		3.69		3.82	3.47	3.69	3.85	3.77
	$^{13}\text{C}$	97.06		<b><u>76.79</u></b>		72.61	70.70	72.86	63.25	
$\alpha$ -D-Glcp B/ B'	$^1\text{H}$	5.09		3.60		3.77	3.54	4.02	3.86/ 4.02	3.74/ 4.09
	$^{13}\text{C}$	97.25		72.26		73.70	70.0	71.90	61.97/ <b><u>65.63</u></b>	
P-Gro-P D	$^1\text{H}$	3.96	3.89	4.05	3.96	3.89				
	$^{13}\text{C}$	67.28		70.56	67.28					
P-Gro(- P)-Ala E	$^1\text{H}$	4.10	4.10	5.39	4.10	4.10				
	$^{13}\text{C}$	64.58		<b><u>75.29</u></b>	64.58					
Gro-Glc F	$^1\text{H}$	3.69	3.60	3.83	3.81	3.51				
	$^{13}\text{C}$	63.25		71.98	<b><u>70.60</u></b>					
P-Gro G	$^1\text{H}$	3.96	3.89	3.94	3.63	3.52				
	$^{13}\text{C}$	<b><u>67.28</u></b>		73.22	63.83					
Gro free H	$^1\text{H}$	3.61	3.55	3.77	3.63	3.52				
	$^{13}\text{C}$	63.83		73.22	63.83					
Gro Ala- (P-Gro-P)	$^1\text{H}$	-		4.30	1.63					
	$^{13}\text{C}$	171.20		50.20	16.50					
Ala free	$^1\text{H}$	-		3.77	1.45					
	$^{13}\text{C}$	176.30		51.37	17.15					

1D and 2D NMR spectra were recorded in  $\text{D}_2\text{O}$  at 700 MHz and 27°C relative to external acetone ( $\delta_{\text{H}}$  2.225;  $\delta_{\text{C}}$  31.45). Underlined and bold chemical shifts indicate substituted positions. The chemical shifts of protons and carbons of *S. agalactiae* 0250 were very similar.

The Glc residues of the WTA of both *Streptococcus* species were identified as  $\alpha$ -pyranoses [Glc (**A**)  $^3J_{1,2} = 3.56$  Hz (Glc<sub>p</sub>), Glc (**B**, **B'**)  $^3J_{1,2} = 3.89$  Hz (Glc<sub>p</sub>) *S. agalactiae*; Glc (**A**)  $^3J_{1,2} = 2.98$  Hz (Glc<sub>p</sub>), Glc (**B**, **B'**)  $^3J_{1,2} = 3.13$  Hz (Glc<sub>p</sub>) *S. dysgalactiae*]. The integral ratio of the anomeric proton of Glc ( $\delta$  5.17 ppm) in the  $^1\text{H}$  NMR spectrum of WTA and the Gro signals ( $\delta$  4.04 – 3.89 ppm) identified an average chain length of 48 for *S. agalactiae* 0250, and 20 for *S. dysgalactiae* 2023. Due to the impurification of the WTA preparation of *S. agalactiae* the results indicating the chain length are imprecise.

The linkage between Glc<sub>p</sub> (**B**) or (**B'**) and Glc<sub>p</sub> (**A**) was identified by a ROESY experiment (cross peak at  $\delta$  5.09/3.51), and the *inter-residual* nOe contact between **A** H-1/**F** H-3b revealed the linkage between Glc<sub>p</sub> (**A**) and the Gro (**F**). The correlation P/Glc **B'** H-6 could be obtained on  $^1\text{H}$ ,  $^{31}\text{P}$  HMBC spectrum, identifying the linkage of hydrophilic backbone of WTA to *O*-6 of Glc<sub>p</sub> (**B'**). In the  $^1\text{H}$ ,  $^{31}\text{P}$  HMBC spectrum crosspeaks from phosphodiester groups at  $\delta$  1.43 to Gro **D** 1a,3a ( $\delta$  3.96) and 1b,3b ( $\delta$  3.89) and Gro **G** 1a ( $\delta$  3.96) and 1b ( $\delta$  3.89), and at  $\delta$  1.11 to Gro **E** 1a,b, 3a,b ( $\delta$  4.10) were identified. A cross peak P-Gro(-P)-Ala (**E**), H-2/Gro-Ala, C-1 was observed in the  $^1\text{H}$ ,  $^{13}\text{C}$  HMBC spectrum which confirmed the substitution of Gro by Ala at *O*-2.

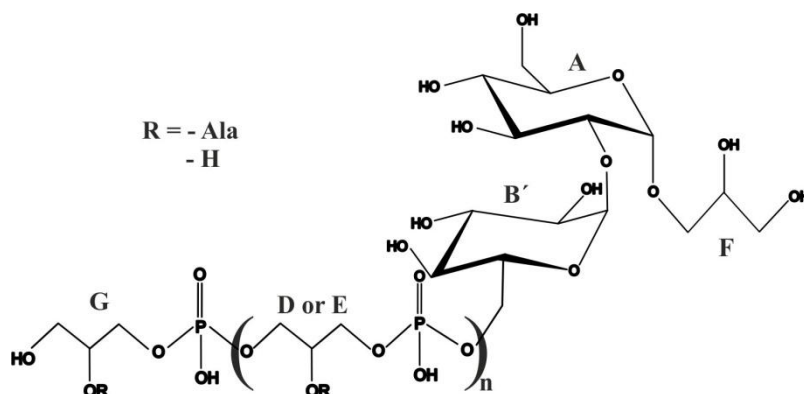


**Figure 4.24** The proposed structure of the WTA from *S. agalactiae* 0250 and *S. dysgalactiae* 2023.

The anchor structure of both *Streptococcus* species was identified as  $\alpha$ -D-Glc<sub>p</sub>-(1 $\rightarrow$ 2)- $\alpha$ -D-Glc<sub>p</sub>-(1 $\rightarrow$ 3)-1,2-diacyl-*sn*-Gro and the hydrophilic backbone of the WTA was shown to contain poly(*sn*-glycerol-1-phosphate) randomly substituted at *O*-2 of glycerol by D-Ala. The capital letters refer to the molecules defined in Table 4.12.

The WTA from the two *Streptococcus* species showed the presence of the linker structure  $\alpha$ -D-Glc<sub>p</sub>-(1 $\rightarrow$ 2)- $\alpha$ -D-Glc<sub>p</sub>-(1 $\rightarrow$ 3)-*sn*-Gro bound to the hydrophilic backbone, which consisted of poly(*sn*-Gro 1-phosphate) and was randomly substituted at *O*-2 of Gro by D-Ala (Figure 4.24). Additionally, the sample contained non-substituted linker with distal glucose depicted as Glc **B**.

### 4.6.3 WTA isolation by enzymatic treatment

Per definition WTA is covalently linked to PGN. The linkage units of WTA to PGN of Gram-positive bacteria are different. It was aimed to identify the linkage units of the WTA of both *S. agalactiae* 0250 and *S. dysgalactiae* 2023. Therefore, enzymatic treatment of the PGN after cell disruption was performed in order to isolate the WTA bound to a fragment of PGN.

The extract obtained after the treatment by lysozyme, RNase, DNase and proteinase K and dialysis, was purified by the same procedure described above (chapter 4.6.1), samples were purified by HIC from the LTA and Q Sepharose. The diagram of the FPLC and obtained graph of the phosphate content were a bit different compared to the graphs after WTA isolation applying TCA. Three fractions were obtained after anion-exchange chromatography, namely P1, P2 and P3. The chemical composition of the fractions corresponded to the chemical composition of the P1-P3 fraction after TCA isolation (4.6.2). The P3 fraction was subjected to NMR spectroscopy.

Unfortunately, 1D and 2D NMR spectra of the WTA preparation (P3) after enzymatic treatment revealed high level of contamination present in the sample. Thus, the sample was not further examined and structure elucidation was not possible.

## 4.7 Rhamnose-rich polysaccharides

### 4.7.1 Determination of the rhamnan structure of *S. agalactiae* 0250

The rhamnose-rich molecule from *S. agalactiae* 0250 was isolated either applying a CPS isolation protocol or during WTA isolation (P1 fraction, chapter 4.6.1). In neutral sugar analysis Rha/Man/Glc/Gal in the approx. molecular ratios of 2.7/2.3/1/0.6 were detected. The absolute configuration of Rha was determined as L.

Fourteen *CH* shifts of anomeric protons ( $\delta$  5.57 – 4.89), a crowded region of the ring protons and the strong 6-deoxy-Hex *CH*<sub>3</sub> signals of Rha ( $\delta$  1.27 – 1.30) were observed in <sup>1</sup>H NMR spectrum of the *S. agalactiae* 0250 rhamnan. Furthermore the *CH*<sub>3</sub> shifts of *N*-acetyl group ( $\delta$  2.10) and of lactic acid ( $\delta$  1.36) were detected.

Four terminal Rha, one Rha substituted at C-2 and C-4, and three Rha substituted at C-2 were detected by 2D NMR experiments (Table 4.14) and methylation analysis (Table 4.13). Furthermore, three Gal and one GlcNAc, both substituted on position C-3 were identified. Further detected components were *N*-acetylmuramic acid (MurNAc) and Gro.

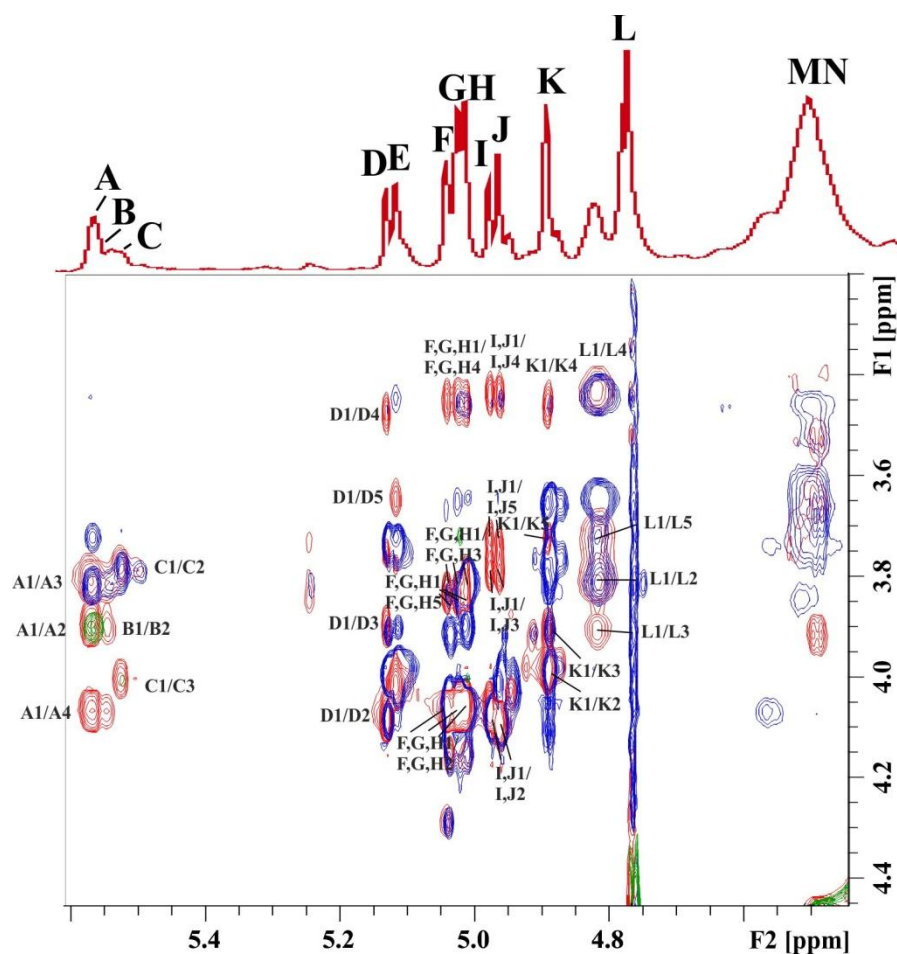


**Figure 4.25** Excerpt of  $^1\text{H}$  and overlaid  $^1\text{H},^1\text{H}$  TOCSY and  $^1\text{H},^1\text{H}$  ROESY NMR spectra of the rhamnose-rich polysaccharide preparation from *S. agalactiae* 0250.

The spectra were recorded in  $\text{D}_2\text{O}$  at  $27^\circ\text{C}$  and 700 MHz relative to external acetone ( $\delta_{\text{H}} 2.225$ ;  $\delta_{\text{C}} 31.45$ ).

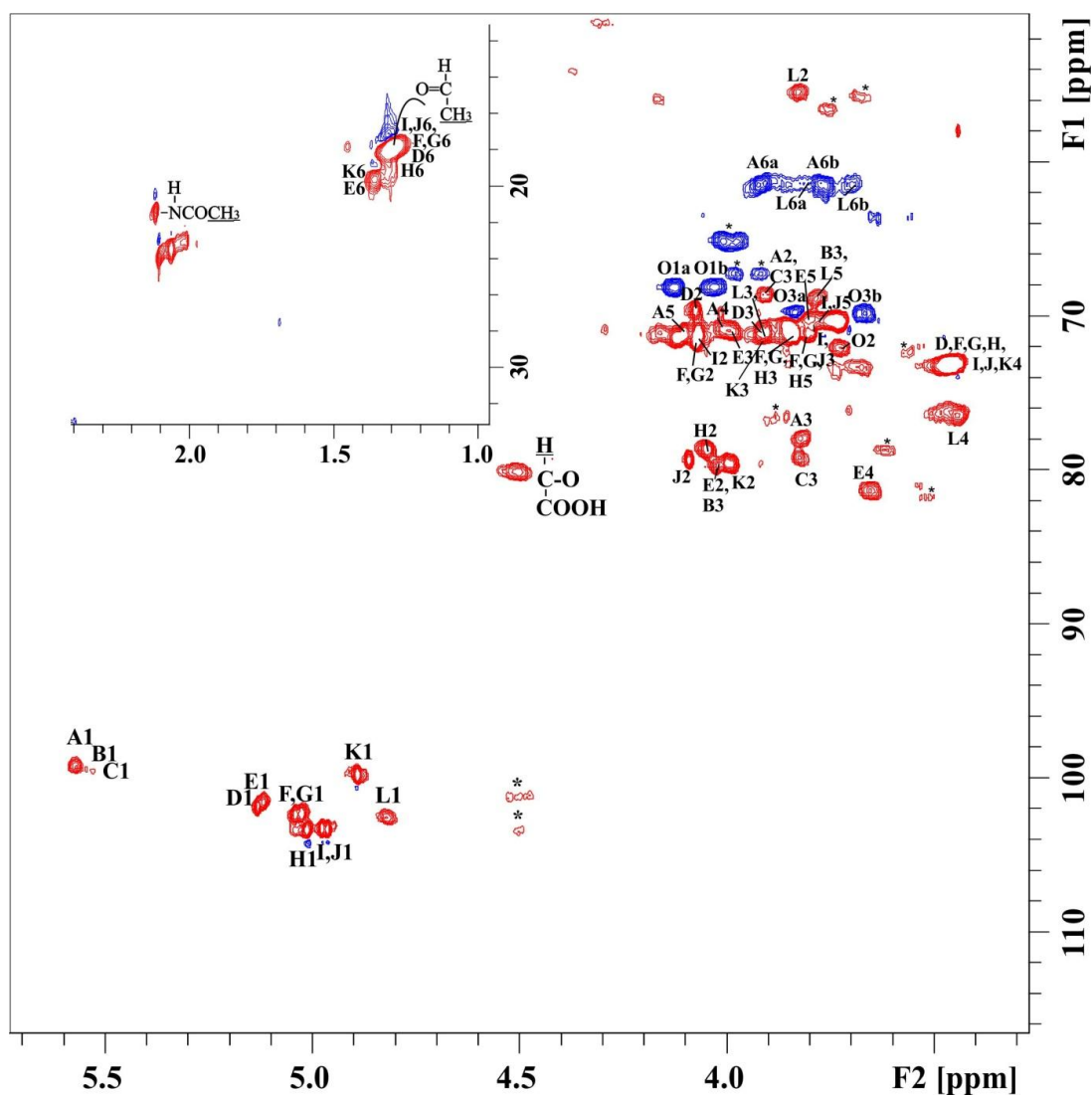
$^1\text{H}$  NMR spectrum revealed additionally two spin systems named **M** and **N** with anomeric protons located close to each other ( $\delta_{\text{H}} 4.53$ ;  $\delta_{\text{H}} 4.49$ ). 2D NMR helped with finding other characteristic signals belonging to those spin systems, such as C-2 of carbon atom bearing an acetamido function ( $\delta_{\text{H}} 3.77$ ;  $\delta_{\text{C}} 55.82$ /  $\delta_{\text{H}} 3.66$ ;  $\delta_{\text{C}} 56.55$ ),  $\text{CH}_3$  group ( $\delta_{\text{H}} 1.36$ ;  $\delta_{\text{C}} 18.63$ ) of lactic acid, and C=O from *N*-acetyl groups ( $\delta_{\text{C}} 181.90/175.84$ ). Due to the fact that methylation analysis (Table 4.13) showed components of PGN in the rhamnan preparation, it was assumed that **M** stands for 4- $\beta$ -GlcNAc and **N** for  $\beta$ -MurNAc. Characteristic PGN components were present in smaller amounts compared to the rhamnose-containing chains, as demonstrated on overlaid  $^1\text{H},^1\text{H}$  TOCSY and  $^1\text{H},^1\text{H}$  ROESY NMR spectra (Figure 4.25). However, after methylation the ratio of **M/N** to the rhamnan components was the other way round, i. e. PGN components were the major ones. Probably huge rhamnan polymer could not be well dissolved during methylation compared to PGN, thus was not accessible. PGN presence in the rhamnan preparation was considered as contamination.

Table 4.13 Methylation analysis data of the rhamnose-rich polysaccharide of *S. agalactiae* 0250.

Partially <i>O</i> -methylated alditol acetates	Substitution at	Approx. mol. ratio
	<b>Rhamnose</b>	
1,5-di- <i>O</i> -acetyl-6-deoxy-2,3,4-tri- <i>O</i> -methyl-[1- <sup>2</sup> H]mannitol	terminal	16.2
1,2,5-tri- <i>O</i> -acetyl-6-deoxy-3,4-di- <i>O</i> -methyl-[1- <sup>2</sup> H]mannitol	2-substituted	11.5
1,2,4,5-tetra- <i>O</i> -acetyl-6-deoxy-3- <i>O</i> -methyl-[1- <sup>2</sup> H]mannitol	2,4-substituted	5.7
	<b>Hexose</b>	
1,5-di- <i>O</i> -acetyl 2,3,4,6- tetra- <i>O</i> -methyl-[1- <sup>2</sup> H]glucitol	terminal	3.4
1,3,5-tri- <i>O</i> -acetyl-2,4,6-tri- <i>O</i> -methyl-[1- <sup>2</sup> H]glucitol	3-substituted	3.0
1,4,5-tri- <i>O</i> -acetyl-2,3,6-tri- <i>O</i> -methyl-[1- <sup>2</sup> H]glucitol	4-substituted	3.0
1,2,3,5-tetra- <i>O</i> -acetyl-4,6-di- <i>O</i> -methyl-[1- <sup>2</sup> H]glucitol	2,3-substituted	3.0
1,3,5,6-tetra- <i>O</i> -acetyl-2,4-di- <i>O</i> -methyl-[1- <sup>2</sup> H]glucitol	3,6-substituted	3.0
	<b><i>N</i>-HexNAc</b>	
2-acetamido-1,4,5-tri- <i>O</i> -acetyl-2-deoxy-3,6-di- <i>O</i> -methyl-[1- <sup>2</sup> H]glucitol	4-substituted	20.6
	<b><i>N</i>-MurNAc</b>	
2-acetamido-3-carboxyethyl-1,5-di- <i>O</i> -acetyl-2,3-di-deoxy-4,6-di- <i>O</i> -methyl-[1- <sup>2</sup> H]glucitol	nonsubstituted	30.4

Additionally, GroP was present (<sup>1</sup>H, <sup>31</sup>P HMBC NMR revealed cross peaks at  $\delta_{\text{H}}$  4.13/ $\delta_{\text{P}}$  1.43 and  $\delta_{\text{H}}$  4.03/ $\delta_{\text{P}}$  1.43) which was neither linked to Rha-containing chains nor to PGN.

The *manno* configuration of rhamnoses was determined by <sup>3</sup>*J*<sub>1,2</sub> values of ~ 1 Hz of anomeric protons and the *gluco* configuration of GlcpNAc was confirmed by detection of H-4/H-2 nOe connectivity in the NOESY NMR spectrum. The anomeric configurations of rhamnoses were determined applying a coupled <sup>1</sup>H, <sup>13</sup>C HSQC spectrum, namely **A** as  $\alpha$ -Gal (*J*<sub>C1, H1</sub> = 178 Hz), **D** as  $\alpha$ -Rha (*J*<sub>C1, H1</sub> = 174 Hz), **E**, **H**, **J** as  $\alpha$ -Rha (*J*<sub>C1, H1</sub> = 173 Hz), **F**, **G** as  $\alpha$ -Rha (*J*<sub>C1, H1</sub> = 170 Hz), **I** as  $\alpha$ -Rha (*J*<sub>C1, H1</sub> = 171 Hz) and **K** as  $\alpha$ -Rha (*J*<sub>C1, H1</sub> = 172 Hz).



**Figure 4.26** Excerpt of the  $^1\text{H},^{13}\text{C}$  HSQC-DEPT spectrum of the rhamnose-rich polysaccharide of *S. agalactiae* 0250

The spectra were recorded in  $\text{D}_2\text{O}$  at  $27^\circ\text{C}$  and 700 MHz relative to external acetone ( $\delta_{\text{H}}$  2.225;  $\delta_{\text{C}}$  31.45). The capital letters refer to the residues defined in the Table 4.14. \* stands for not identified chemical signals.

Table 4.14  $^1\text{H}$  and  $^{13}\text{C}$  chemical shift data (in ppm) of the rhamnan of *S. agalactiae* 0250

Residue		1a	1b	2	3a	3b	4	5	6a	6b
3- $\alpha$ -D-Galp <b>A</b>	$^1\text{H}$	5.57		3.90		3.82	4.01	4.09	3.90	3.78
	$^{13}\text{C}$	99.20		68.66		<u>77.96</u>	70.87	71.33	61.36	
3- $\alpha$ -D-Galp <b>B</b>	$^1\text{H}$	5.53		3.78		4.01	n.d.	n.d.	n.d.	
	$^{13}\text{C}$	99.55		68.9		<u>79.61</u>	n.d.	n.d.	n.d.	
3- $\alpha$ -D-Galp <b>C</b>	$^1\text{H}$	5.54		3.89		3.81	n.d.	n.d.	n.d.	
	$^{13}\text{C}$	99.46		68.66		<u>79.18</u>	n.d.	n.d.	n.d.	
t- $\alpha$ -Rha <b>D</b>	$^1\text{H}$	5.13		4.08		3.90	3.47	3.75	1.29	
	$^{13}\text{C}$	101.92		69.71		71.10	73.19	71.41	17.83	
2,4- $\alpha$ -Rha <b>E</b>	$^1\text{H}$	5.12		4.02		3.98	3.65	3.79	1.34	
	$^{13}\text{C}$	101.58		<u>79.71</u>		71.01	<u>81.44</u>	70.24	19.67	
t- $\alpha$ -Rha <b>F</b>	$^1\text{H}$	5.04		4.07		3.84	3.45	3.83	1.29	
	$^{13}\text{C}$	102.52		71.30		71.10	73.09	71.19	17.83	
t- $\alpha$ -Rha <b>G</b>	$^1\text{H}$	5.03		4.06		3.83	3.45	3.80	1.29	
	$^{13}\text{C}$	103.41		71.30		71.10	73.09	71.12	17.83	
2- $\alpha$ -Rha <b>H</b>	$^1\text{H}$	5.02		4.05		3.82	3.45	3.80	1.28	
	$^{13}\text{C}$	102.52		<u>78.76</u>		71.10	73.09	71.12	17.89	
t- $\alpha$ -Rha <b>I</b>	$^1\text{H}$	4.98		4.06		3.79	3.43	3.73	1.26	
	$^{13}\text{C}$	103.88		71.36		71.10	73.22	70.35	17.73	
2- $\alpha$ -Rha <b>J</b>	$^1\text{H}$	4.96		4.09		3.79	3.44	3.73	1.26	
	$^{13}\text{C}$	103.88		<u>79.37</u>		71.10	73.22	70.35	17.73	
2- $\alpha$ -Rha <b>K</b>	$^1\text{H}$	4.89		3.99		3.90	3.46	3.72	1.32	
	$^{13}\text{C}$	99.85		<u>79.57</u>		71.12	73.22	70.35	18.31	
Gro <b>O</b>	$^1\text{H}$	4.13	4.03	3.73	3.83	3.67	-	-	-	
	$^{13}\text{C}$	<u>68.21</u>		72.06	<u>69.77</u>		-	-	-	
	$^{31}\text{P}$	1.43		-		-	-	-	-	

1D and 2D spectra were recorded in  $\text{D}_2\text{O}$  at 700 MHz and 27°C relative to external acetone ( $\delta_{\text{H}}$  2.225;  $\delta_{\text{C}}$  31.45). Underlined chemical shifts indicate substituted positions. n.d. stands for not determined.



#### 4.7.2 Determination of the rhamnan structure of *S. dysgalactiae* 2023

The rhamnan molecule of *S. dysgalactiae* was obtained during WTA isolation method. Additionally, the same molecule was recovered from the 1% phenol extract.

The molecular ratio of sugars of the rhamnose-rich fraction of *S. dysgalactiae* was identified as Rha/Man/Glc/Gal/GalN/GlcN = 39/1.5/1/0.2/1.4/0.9. The absolute configuration of Rha was determined as L.

The <sup>1</sup>H NMR spectrum of this molecule revealed 9 chemical shifts of anomeric protons ( $\delta$  5.57 – 4.89), a crowded region of ring protons, the CH<sub>3</sub> group of a *N*-acetyl ( $\delta$  2.03) and the strong 6-deoxy CH<sub>3</sub> signals ( $\delta$  1.26 – 1.30) of rhamnoses.

The investigation of the 1D and 2D NMR spectra and the methylation analyses (Table 4.16) revealed two Rha substituted at C-2 and C-3, one 3-substituted Rha and one 2-substituted Rha. Also, one terminal *N*-acetylgalactosamine (GalNAc), one 3-substituted GalNAc, one 4-substituted GalNAc and a (1→3)-linked *N*-acetylhexosamine disaccharide were identified. ROESY and HMBC NMR spectra elucidated the linkages between the identified sugars and aminosugars.

**Table 4.16 Methylation analysis data of the rhamnose-rich polysaccharide of *S. dysgalactiae* 2023.**

Partially <i>O</i> -methylated alditol acetates	Substitution at	Ratio
	<b>Rhamnose</b>	
1,5-di- <i>O</i> -acetyl-6-deoxy-2,3,4-tri- <i>O</i> -methyl-[1- <sup>2</sup> H]mannitol	terminal	0.4
1,2,5-tri- <i>O</i> -acetyl-6-deoxy-3,4-di- <i>O</i> -methyl-[1- <sup>2</sup> H]mannitol	2-substituted	20.5
1,3,5-tri- <i>O</i> -acetyl-6-deoxy-2,4-di- <i>O</i> -methyl-[1- <sup>2</sup> H]mannitol	3-substituted	35.2
1,2,3,5-tetra- <i>O</i> -acetyl-6-deoxy-4-mono- <i>O</i> -methyl-[1- <sup>2</sup> H]mannitol	2,3-substituted	22.1
	<b>Hexose</b>	
1,4,5-tri- <i>O</i> -acetyl-2,3,6-tri- <i>O</i> -methyl-[1- <sup>2</sup> H]glucitol	4-substituted	5.5
	<b>HexNAc</b>	
2-acetamido-1,5-di- <i>O</i> -acetyl-2-deoxy-3,4,6-tri- <i>O</i> -methyl-[1- <sup>2</sup> H]glucitol	terminal	6.1
2-acetamido-1,3,5-tri- <i>O</i> -acetyl-2-deoxy-4,6-di- <i>O</i> -methyl-[1- <sup>2</sup> H]glucitol	3-substituted	6.0
2-acetamido-1,4,5-tri- <i>O</i> -acetyl-2-deoxy-3,6-di- <i>O</i> -methyl-[1- <sup>2</sup> H]glucitol	4-substituted	1.2
	<b>HexNAc disaccharide</b>	
2-acetamido-1,3,5-tri- <i>O</i> -acetyl-2-deoxy-4,6-di- <i>O</i> -methyl-[1- <sup>2</sup> H]glucitol - 2-acetamido 1,5-di- <i>O</i> -acetyl-2-deoxy-3,4,6-tri- <i>O</i> -methyl-[1- <sup>2</sup> H]glucitol	3-substituted	3.0

The assignment of 11 spin systems (A-K) of rhamnose-rich polysaccharides was performed applying  $^1\text{H}$ ,  $^1\text{H}$  COSY, TOCSY, ROESY, and  $^1\text{H}$ ,  $^{13}\text{C}$  HSQC and HMBC (Table 4.17, Figure 4.28, Figure 4.29). Furthermore, the nOe contacts to **I'** and to **X** were identified and included to proposed structures. In the spin system of **I'** H-1 could be identified at  $\delta$  4.89 and H-6 at  $\delta$  1.30, which confirmed it as Rha, but the full spin system of **I'** was absent in the  $^1\text{H}$ ,  $^1\text{H}$  TOCSY NMR spectrum. **X** stands for an unknown molecule, the spin system of which was covered by the spins system of **J**. The full spin systems of the molecules present in small amounts were not detectable. Their importance and their belonging to the rhamnan of *S. dysgalactiae* could be elucidated applying further purification or degradation experiments of the molecule.

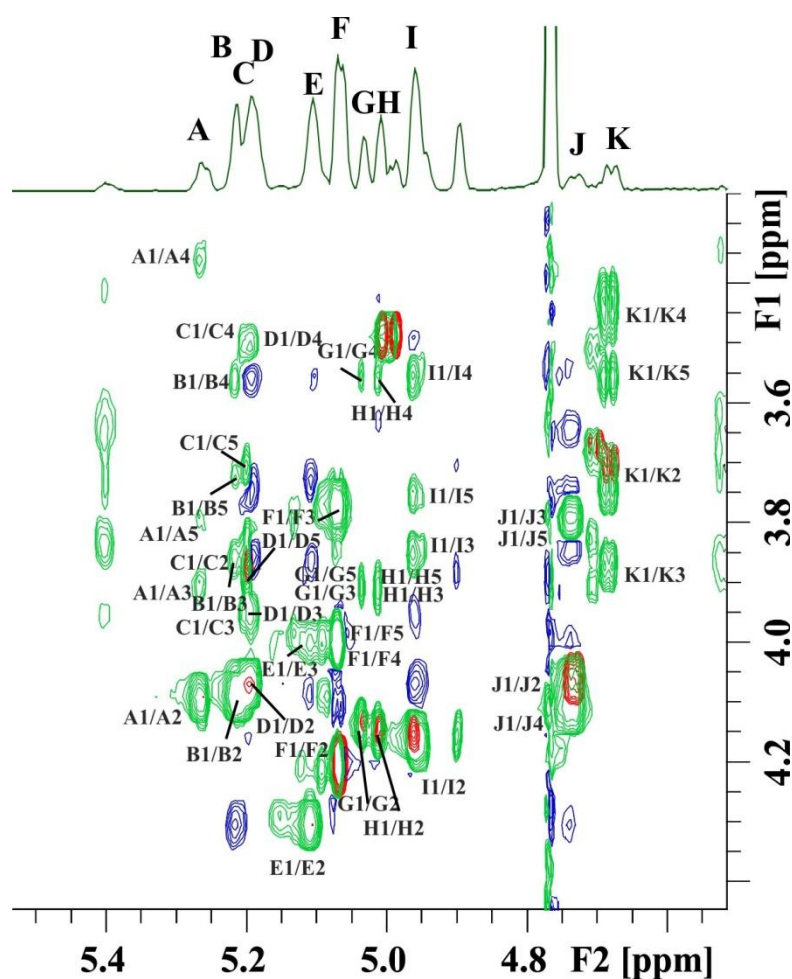


**Figure 4.28** Excerpt of overlaid  $^1\text{H}$  and overlaid  $^1\text{H}$ ,  $^1\text{H}$  COSY and  $^1\text{H}$ ,  $^1\text{H}$  TOCSY NMR spectra demonstrate the chemical shifts of the rhamnose-rich polysaccharide of *S. dysgalactiae* 2023.

The spectra were recorded in  $\text{D}_2\text{O}$  at  $27^\circ\text{C}$  and 700 MHz relative to external acetone ( $\delta_{\text{H}}$  2.225;  $\delta_{\text{C}}$  31.45). The capital letters refer to the residues defined in the Table 4.17. E1/E4 and E1/E5 are not seen on the figure and are not declared.

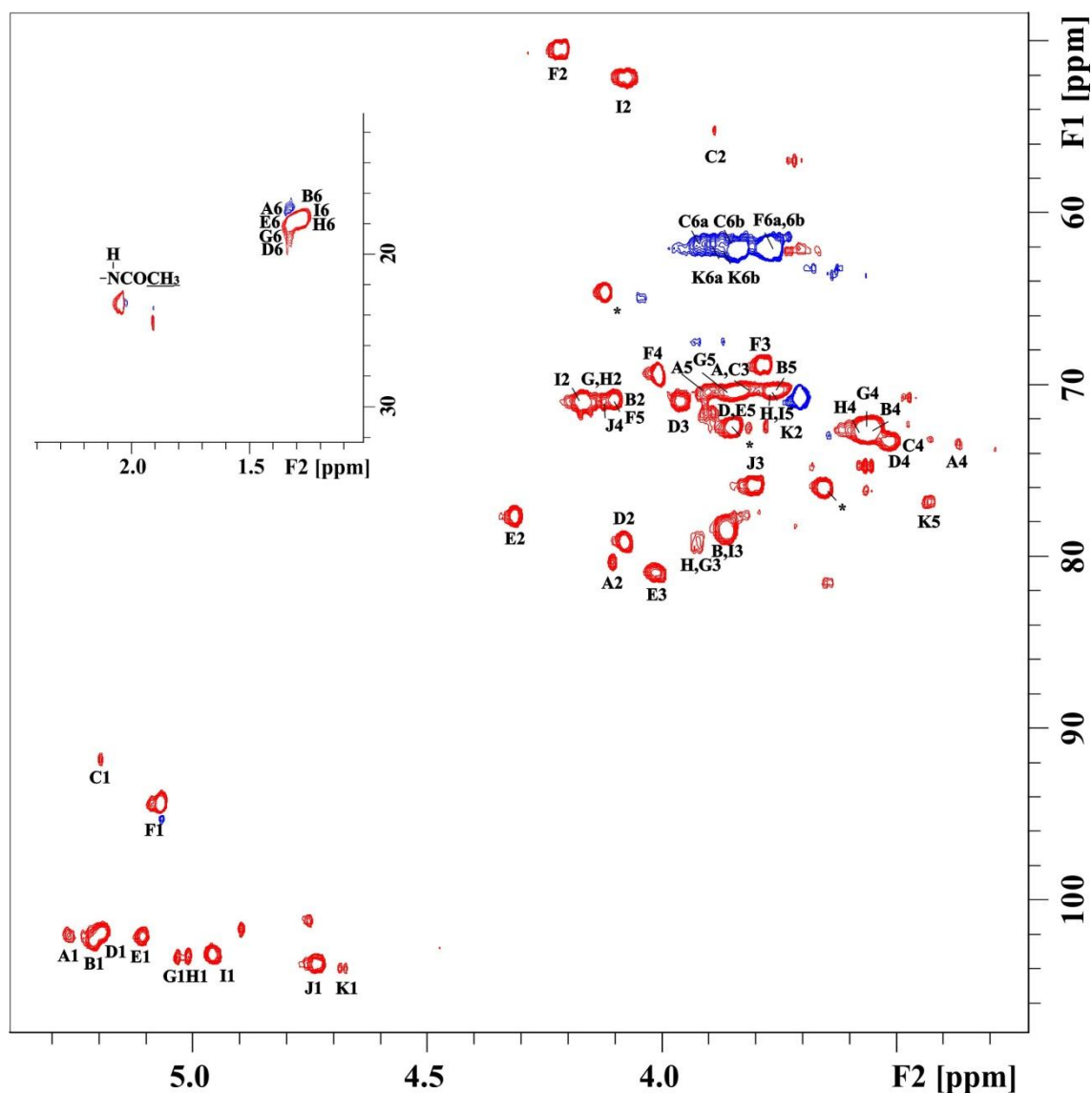


**Figure 4.29** Excerpt of  $^1\text{H}$ ,  $^{13}\text{C}$  HSQC-DEPT spectrum of rhamnan of *S. dysgalactiae* 2023. The spectra were recorded in  $\text{D}_2\text{O}$  at  $27^\circ\text{C}$  and 700 MHz relative to external acetone ( $\delta_{\text{H}} 2.225$ ;  $\delta_{\text{C}} 31.45$ ). The capital letters refer to the residues defined in the Table 4.17. \* stands for not identified molecule.

The *manno* configuration of rhamnoses was determined by  $J_{1,2}$  values of  $\sim 1$  Hz of anomeric protons. The *gluco* configuration of GlcpNAc was obtained by detection of the nOe contact H-4/H-2 in the NOESY NMR spectrum, and the *galacto* configuration of t- $\alpha$ -GalNAc and 3- $\beta$ -GalNAc by detection of *intra*-residual H-3/H-4 and H-3/H-5 nOe connectivities.

The anomeric configurations of the sugars were determined applying a  $^1\text{H}$ ,  $^{13}\text{C}$  HSQC NMR experiment. This analysis revealed **A** as  $\alpha$ -Rha ( $J_{\text{C}_1, \text{H}_1} = 178$  Hz), **B**, **D**, **E**, **G**, **H** as  $\alpha$ -Rha ( $J_{\text{C}_1, \text{H}_1} = 177$  Hz), **C** as  $\alpha$ -GlcNAc ( $J_{\text{C}_1, \text{H}_1} = 172$  Hz), **F** as  $\alpha$ -GalNAc ( $J_{\text{C}_1, \text{H}_1} = 175$  Hz), **I** as  $\alpha$ -Rha ( $J_{\text{C}_1, \text{H}_1} = 176$  Hz) and **J**, **K** as  $\beta$ -GalNAc ( $J_{\text{C}_1, \text{H}_1} = 162$  Hz).

Table 4.17  $^1\text{H}$  and  $^{13}\text{C}$  chemical shift data (in ppm) of the rhamnan of *S. dysgalactiae* 2023

Residue		1	2	3	4	5	6a	6b	NAc
2- $\alpha$ -Rhap <b>A</b>	$^1\text{H}$	5.26	4.10	3.79	3.36	3.91	1.30		
	$^{13}\text{C}$	102.06	<b><u>80.28</u></b>	70.43	73.44	70.44	17.86		
2,3- $\alpha$ -Rhap <b>B</b>	$^1\text{H}$	5.21	4.09	3.86	3.56	3.73	1.26		
	$^{13}\text{C}$	102.39	<b><u>79.14</u></b>	<b><u>78.13</u></b>	72.67	70.10	17.80		
t- $\alpha$ - Glc $p$ NAc <b>C</b>	$^1\text{H}$	5.20	3.88	3.81	3.51	3.70	3.89	3.91	n.d.
	$^{13}\text{C}$	91.83	55.00	70.39	73.21	73.94	61.84		n.d.
2- $\alpha$ -Rhap <b>D</b>	$^1\text{H}$	5.19	4.07	3.95	3.52	3.83	1.32		
	$^{13}\text{C}$	101.87	<b><u>79.20</u></b>	71.10	73.30	70.34	18.03		
2,3- $\alpha$ -Rhap <b>E</b>	$^1\text{H}$	5.10	4.30	4.00	3.54	3.85	1.32		
	$^{13}\text{C}$	102.14	<b><u>77.69</u></b>	<b><u>80.98</u></b>	72.93	70.43	17.94		
t- $\alpha$ - Gal $p$ NAc <b>F</b>	$^1\text{H}$	5.07	4.20	3.78	4.00	4.10	3.77	3.77	2.04
	$^{13}\text{C}$	94.58	50.50	68.83	69.57	70.89	62.34		175.69
3- $\alpha$ -Rhap <b>G</b>	$^1\text{H}$	5.03	4.14	3.91	3.55	3.88	1.30		
	$^{13}\text{C}$	103.37	71.04	<b><u>79.48</u></b>	72.41	70.41	17.85		
3- $\alpha$ -Rha <b>H</b>	$^1\text{H}$	5.01	4.15	3.91	3.56	3.79	1.28		
	$^{13}\text{C}$	103.29	71.02	<b><u>79.48</u></b>	72.47	70.36	17.81		
3- $\alpha$ -Rhap <b>I</b>	$^1\text{H}$	4.96	4.17	3.85	3.55	3.76	1.27		
	$^{13}\text{C}$	103.44	70.98	<b><u>78.49</u></b>	74.66	70.39	17.80		
3- $\beta$ - Gal $p$ NAc <b>J</b>	$^1\text{H}$	4.74	4.08	3.79	4.11	3.83	3.83	3.85	2.03
	$^{13}\text{C}$	103.88	52.09	<b><u>75.86</u></b>	70.77	75.89	62.13		175.29
4- $\beta$ -Glc $p$ <b>K</b>	$^1\text{H}$	4.69	3.74	3.55	3.45	3.43	3.75	3.87	
	$^{13}\text{C}$	104.02	70.29	74.69	<b><u>73.22</u></b>	76.82	62.19		

1D and 2D spectra were recorded in  $\text{D}_2\text{O}$  at  $27^\circ\text{C}$  relative to external acetone ( $\delta_{\text{H}}$  2.225;  $\delta_{\text{C}}$  31.45). Underlined and bold chemical shifts indicate substituted positions. n.d. stands for not determined.

The following linkages between the residues were determined applying a HMBC experiment: **A**, H-1/B, C-3; **B**, H-1/E, C-2; **D**, H-1/B, C-3, **I**, H-1/D, **B** C-2 and **K**, H-1/A, C-2, **E**, H-1/B, C-3, **E**, H-1/D, C-3, **J**, H-1/E, C-3 and **F**, H-1/J, C-3. The ROESY experiments confirmed the HBMC data revealing the *inter*-residual nOe contacts between **A**-1/**B**-3, **B**-1/**E**-2, **D**-1/**B**-3, **I**-1/**D**, **B**-3, **K**-1/**A**-2, **E**-1/**B**-3, **E**-1/**D**-3, **J**-1/**E**-3 and **F**-1/**J**-3. The very strong ROESY signal **J**-1/**E**-3 between



from *S. agalactiae* 0250 and *S. dysgalactiae* 2023 (Figure 4.31). Additionally, the precipitate of *S. dysgalactiae* possessed a strong  $\text{CH}_3$  signal ( $\delta$  0.80 – 1.20) of Rha, and that of *S. agalactiae* 0250 possessed signals of a *N*-acetyl group and acetic acid. Since anomeric regions of all three samples were identical it was concluded that they all contained only mannose-rich polysaccharide. No EPS polymer produced by *S. agalactiae* 0250 and *S. dysgalactiae* 2023 was found. The precipitates consisted only of polysaccharide(s) present in the growth medium.

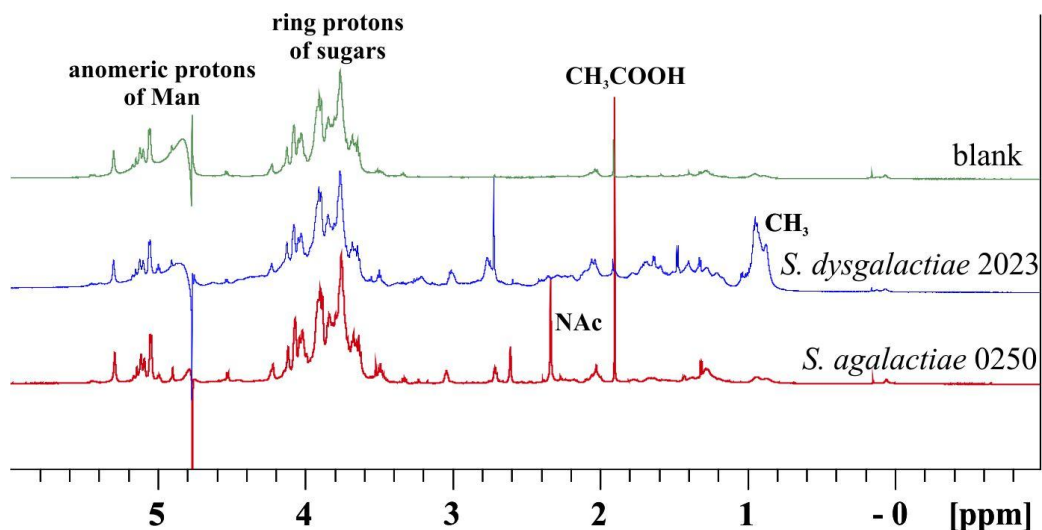


**Figure 4.31**  $^1\text{H}$  NMR spectra of the supernatant preparations after growth of *S. agalactiae* 0250 and *S. dysgalactiae* 2023 and without growth of bacteria (blank).

The cells were grown in BHI supplemented with 2% casein hydrolysate. The spectra were recorded in  $\text{D}_2\text{O}$  at  $27^\circ\text{C}$  and 700 MHz relative to external acetone ( $\delta_{\text{H}}$  2.225;  $\delta_{\text{C}}$  31.45).



## 5 Discussion

The structural composition of the cell wall components from bovine mastitis pathogens is quite poorly investigated. In the present work, the cell envelope components from the two bovine mastitis bacteria *S. agalactiae* 0250 and *S. dysgalactiae* 2023, isolated from clinical mastitis cases in the UK, were analyzed. Their cell envelope components can serve as representatives for other *S. agalactiae* and *S. dysgalactiae* species, which are still present in the dairy cattle [21, 44]. LTA, WTA, glycolipids, CPS and EPS structures were shown to be immunologically relevant. These components (except EPS) and the rhamnose-rich polysaccharide from both *Streptococcus* species were isolated and structurally investigated. The biological properties and activities of the LTA and the glycolipids were elucidated.

First, the whole cells of the *S. agalactiae* 0250 and *S. dysgalactiae* 2023 were investigated for boTLR2 and NF- $\kappa$ B stimulating activity in HEK293 cells. The results showed that these cells are capable of induce activity NF- $\kappa$ B on HEK293 cells that is mediated through boTLR2. Analogical assays with bovine *S. agalactiae* could not demonstrate this [136]. However, the TLR2 receptor was shown to be important in the defense against *S. agalactiae* as meningitis pathogen, since human isolates of WT GBS were virulent for TLR2<sup>-/-</sup> mice [198].

### 5.1 Structural investigation and biological characterization of the LTA

Both LTA polymers of the *Streptococcus* species as investigated in this study and the bovine mastitis isolate *Streptococcus uberis* 233 had a similar LTA structure of type I, with differences in the poly(phospho-Gro) chain length and the level of D-Ala substitution [64]. As shown by previous studies of the LTA from two human isolates of *S. agalactiae*, the LTA of *S. agalactiae* DS2242-77 contained D-Ala, D-Glc, glycerol, phosphate and 10 different major fatty acids, as well as  $22 \pm 1.8$  GroP units in the hydrophilic backbone and was anchored in the cytoplasmic membrane via glycerophosphoryldiglycosyl diglyceride [199]. The LTA structure of *S. agalactiae* COH1 was similar to that of the present study, except for a shorter hydrophilic backbone of 19 GroP units [95].

The lipid anchor of the herein investigated LTA polymers contained kojibiose. Kojibiose-containing anchor structures have been identified earlier in the LTA of *Lactococcus* spp.,

*Streptococcus* spp., *Enterococcus faecalis* and *Lactococcus lactis* [200, 201]. The hydrophilic backbone of streptococci LTA has been shown to be linked to a lipid anchor containing gentiobiose [91]. LTA molecules containing a poly(phospho-Gro) chain substituted nonstoichiometrically by Ala and sugar residues have also been identified in *Staph. aureus* [180], *E. faecalis* [202, 203], *L. lactis* [200], *B. subtilis* [204, 205]. The type I structure of LTA with a lipid anchor containing a conserved kojibiose seems to be very common in *Streptococcus*, *Lactococcus* and *Enterococcus* species. All of these bacteria belong now to families *Streptococcaceae* (genera *Streptococcus*, *Lactococcus*) and *Enterococcaceae* (genus *Enterococcus*), and were classified previously in the same genus *Streptococcus* until rRNA analysis showed that the bacteria can be divided in three different clusters [30, 206]. Although LTA was shown to be dispensable for viability of the bacterial cells, it plays an important role in cell division, resistance to environmental stress, antimicrobial peptides, fatty acids, cationic antibiotics and lytic enzymes produced by the host [207, 208]. As a conserved and characteristic component of Gram-positive bacteria with clearly defined functions, being recognized by innate immunity, it fulfills the characteristics, which confirmed the LTA as a PAMP [118].

LTA polymers of GBS containing long poly-GroP chains (30-35 GroP units) have been discussed to be characteristic for invasive GBS diseases, whereas GBS with a short LTA polymers of 10-15 GroP units seemed to be asymptomatic [209]. The LTA from bovine *S. agalactiae* 0250 of this work possessed a long poly-GroP chain of 34 GroP units, and that of *S. dysgalactiae* 2023 of 28 GroP units, which could be the reason for the difficulties to resolve the masses in ESI FT-ICR MS.

The LTA was reported to be recognized by TLR2 and TLR4 [95, 131]. However, this was disproved by the identification of lipopeptide contaminations in LTA preparations [132]. Crystallography studies showed that TLR2/TLR6 dimer is not responsible for LTA recognition as well. The heterodimer TLR2/TLR6 recognizes diacylated lipopeptides, where the fatty acids accommodate in the pocket of TLR2 and the head-group of the lipopeptides in the pocket of TLR6 [127]. The LTA polymer possesses diacylated lipid anchor, but not the peptides head-group. The receptor for LTA has not been found yet. LTA is considered to activate the C-type lectin pathway of complement [210, 211].

The LTA preparations of bovine streptococci were examined for their biological activity by using *in vitro* HEK293 cells assays. The tests showed that H<sub>2</sub>O<sub>2</sub>-treated LTA preparations were TLR2-, TLR4-, NOD1- and NOD2-inactive. These results indicated that the samples were free of lipopeptides, LPS or PGN contaminations, suggesting that the signaling pathway of LTA is not directed through TLR2 and TLR4.

Nevertheless, the H<sub>2</sub>O<sub>2</sub>-treated LTA of *S. agalactiae* 0250 and *S. dysgalactiae* 2023 were capable to induce IL-6 and TNF- $\alpha$  release by hMNC. IL-6 and TNF- $\alpha$  are known as inflammatory cytokines inducing NF- $\kappa$ B signaling pathway [212, 213]. The amount of LTA, which was added upon stimulation of hMNC, was 1000 times higher than the amount of LPS used as a positive control. Thus, the question remains how relevant is this amount for triggering the immune response in the cow's udder. Even if the LTA of *S. agalactiae* 0250 and *S. dysgalactiae* 2023 would induce the inflammation, it would be only a minor one. Furthermore, it would be interesting to find out which other cytokines can be released upon hMNC or pbMEC stimulation with LTA of these streptococci. Especially the activation of pbMEC is of interest in the context of the immune response processes in the cows' udder.

## 5.2 Influence of LTA on phagocytosis

The phagocytosis assay using monocytes and neutrophils in the presence of native D-alanylated and H<sub>2</sub>O<sub>2</sub>-treated LTA of both *Streptococcus* species revealed diminished phagocytosis capacity of *E. coli* and *Staph. aureus* by bovine monocytes and neutrophils. Interestingly, it means that LTA of *S. agalactiae* and *S. dysgalactiae* exhibited protective role for both Gram-positive and Gram-negative bacteria. Treatment of *S. dysgalactiae* cells with 0.9% NaCl for 6 h allowed obtaining deacylated LTA (dLTA) molecule. However, the molecules which can be released by such mild treatment must be located on the surface of the cell [214]. It is attractive to speculate that the bacteria release a certain amount of LTA into the environment or, more precise, to the infected host and retard thereby the recognition of the pathogen and their phagocytosis.

Several effects of PAMPs and antigens have been determined, providing the host-adaptation of the bacterial species and/or protection against host immune response mechanisms, in particular survival in the phagosomes or resistance the phagocytosis. For example, the two-component system CovS/CovR of different human *S. agalactiae* isolates of meningitis is responsible for production of the acidic environment in the phagosome and survival in the host macrophages [215]. Biofilm production of *S. pneumoniae* was shown to help to resist the neutrophil phagocytosis [216].

The *AdltA* GAS cells with dealanylated LTA were shown to be more susceptible to antimicrobial peptides and lysozyme than wild-type (WT) cells. They were more rapidly killed by neutrophils and were less adherent and invasive in pharyngeal epithelial cells [217]. Bovine bacterial species were described to resist phagocytosis. The  $\alpha_2$ -macroglobulin-trypsin of *S. dysgalactiae* binds to own proteins, which was shown to protect the cells from phagocytosis by PMNs [218]. The indirect influence of different CpG motifs changed the kinetic of bovine PMN cell apoptosis. The

additive negative effect on PMN vitality was achieved in presence of CpG motifs in combination with LTA of *Staph. aureus* or LPS of *E. coli* [219]. Calvinho *et al.* reported that bovine *S. dysgalactiae* of hydrophilic character are more resistant to phagocytosis than hydrophobic cells, however, the hydrophobic cells could better adhere to MECs [220].

### 5.3 Structural investigation and biological characterization of the glycolipids

The isolated and purified glycolipids G1 (MGlcDAG), G2 (DGlcDAG) and G3 (GroP-DGlcDAG) were characterized for both *Streptococcus* species. The MGlcDAG and DGlcDAG glycolipids and GroP-DGlcDAG have been described previously for *S. agalactiae* and *S. dysgalactiae* and various other streptococci such as *S. pyogenes*, *S. suis* and *E. faecalis* [197, 221]. A glycosylbisphosphatidyl glycolipid and triglycosyl diacylglycerol have been identified in GBS as well, which were not detected in the present work. *S. pneumoniae* has also MGlcDAG in its glycolipids repertoire, and the second glycolipid in large amounts is  $\alpha$ -D-Galp-(1→2)- $\alpha$ -D-Glcp-(1→3)-1,2-diacyl-*sn*-Gro [197].

The DGlcDAG has the same structure as the LTA lipid anchor of both investigated *Streptococcus* species. The DGlcDAG was proposed to anchor the LTA. In detail, *S. agalactiae* COH1  $\Delta$ iaaA mutant was shown to produce only MGlcDAG, resulting in the inability to anchor LTA. The mutant was less virulent in a murine model of meningitis and was shown to be faster eliminated by the immune system of the mouse [98]. In contrast to *S. agalactiae*, mutant strain of *E. faecalis* without capability to produce DGlcDAG, was shown to anchor more and longer LTA polymers compared to the WT cells via MGlcDAG. Additionally, the absence of DGlcDAG was also described to play an important role in biofilm formation, especially in its last stage – in the accumulation of the bacteria in the growing biofilm of *E. faecalis* [115]. A recent published PhD work proved the inability of a bovine mastitis pathogen *S. uberis* O140J::ISS1P' (sub0538 & sub0539) mutant to form biofilm, due to lower amounts of MGlcDAG and DGlcDAG [222]. The biofilm formation of bovine mastitis species is considered to lead to recurrent infections in cows' udder, to protect the bacteria against the action of antimicrobial agents and thus enable them to persist in the invaded tissue [163, 223].

The aim of the current work was to investigate the immunological relevance of the glycolipids. The purity of the preparations was checked in HEK293 cells transfection system. The glycolipids of *S. agalactiae* 0250 and *S. dysgalactiae* 2023 could not activate the HEK293 cells via TLR2, TLR4, NOD1 or NOD2, which suggested that the samples did not contain contaminants such as LPS, PGN, lipopeptide or lipopeptide-like components.

It is known that bacterial and self glycolipids are immunomodulatory active and recognized by NKT cells restricted to CD1d receptor [224]. The responses of iNKT cells to glycosphinglipids (GSL) or  $\alpha$ GalGer are known. As strong stimuli,  $\alpha$ GalGer and GSL are therefore often taken as positive controls in stimulation experiments of the cells with glycolipids [225]. Galactosyldiacylglycerol (GalDAG) was already demonstrated to activate the NKT cells and to accommodate the A' and F' pockets of mCD1d [226].

In the present work, the glycolipids MGlcDAG, DGlcDAG and GroP-DGlcDAG of *S. agalactiae* 0250 and *S. dysgalactiae* 2023 stimulated murine splenocytes for 72 h. The ELISA measurements revealed that MGlcDAG (G1) and GroP-DGlcDAG (G3) of *S. agalactiae* 0250 could activate the NKT cells leading to release of IL-4, however GroP-DGlcDAG showed higher activity than MGlcDAG. MGlcDAG and DGlcDAG of human pathogen GBS and MGlcDAG of *S. pneumoniae* were shown to initiate cytokine responses by V $\alpha$ 14 iNKT cells *in vivo*. In this case, decreased responses to disaccharide glycolipids compared to MGlcDAGs were proven [197]. The glycolipids G1, G2 and G3 of *S. dysgalactiae* 2023 could not activate the murine splenocytes despite the fact to possess the same chemical structure compared to *S. agalactiae* 0250. Furthermore, in case of the glycolipids was shown that the saturation of the fatty acids as well as the length [138]. It is necessary to perform further experiments, for example proliferation experiments of the splenocytes, in order to obtain plausible results. Stimulation of bone marrow-derived NKT cells with the glycolipids would be another possibility to show the activity against NKT cells and the relevance of the glycolipids of bovine streptococci in inflammatory responses.

## 5.4 Structural investigation of the WTA

The isolation of the WTA was first performed with TCA, which had already been applied earlier [185, 186]. The revealed WTA preparations of *S. agalactiae* 0250 and *S. dysgalactiae* 2023 possessed the same structure like the dLTA. dLTA of these *Streptococcus* species comprises the linkage unit of kojibiose attached to glycerol and the poly(phospho-Gro) chains substituted by D-alanine. The WTA structure of *S. agalactiae* DS2242-77 had earlier been discussed to possess the poly(phospho-Gro) chain substituted by Ala and Glc [199]. 2D NMR analysis of this work showed only substitution of the hydrophilic backbone by Ala. Erbing *et al.* described also TA isolated from *S. agalactiae* Type III with the same linkage unit and a poly(phospho-Gro) backbone, but without fatty acids residues and suggested that bacteria are able to release such deacylated TA to the surrounding medium [214].

Gram-positive bacteria are capable to produce the GroP repeating units in the hydrophilic backbones of LTA and WTA [227], but the glycerols of the hydrophilic backbone in this case are

stereochemically opposite to each other. For example the LTA monomeric units of *B. subtilis* contain L-Gro-1-phosphate (S-Gro phosphate) and that of the WTA L-Gro-3-phosphate (R-Gro phosphate) [228]. Sutcliffe *et al.* discussed the enzymes TagB, TagD and TagF which are responsible for the Gro-3-phosphate polymerization. However, these enzymes are absent in *S. agalactiae*, suggesting the impossibility to produce WTA with Gro-3-phosphate units [228, 229]. Furthermore, Kessler *et al.* had demonstrated that the streptococci of Group A possess enzymes which are proposed to be located in the membrane and active in the cytoplasm, and to be capable to deacylate the LTA [230]. In summary, this led to the conclusion that the applied method might be not suitable for the WTA isolation of *S. agalactiae* 0250 and *S. dysgalactiae* 2023, but revealed its dLTA.

In the enzymatic treatment for WTA isolation the lysozyme should have cleaved the PGN, resulting in a WTA which was covalently bound to a MurNAc-GlcNAc disaccharide. Unfortunately the obtained preparations were not pure enough for the investigation. A pure WTA preparation of *Streptococcus* species would be important to prove the Gro stereochemistry, in the case it is present.

## 5.5 CPS

CPS represent a virulence factor of GBS, shielding the pathogens from the host [231] and contributing to a successful internalization by the host and to strategies of the defense against early immune response and host-adaptation processes. The capsules of bovine *S. uberis* and *Staph. aureus* were described to mask the cell, and to be resistant to phagocytosis by PMN [232, 233]. In *S. suis* capsule was shown to protect the bacteria against antimicrobials such as penicillin G and ampicillin, and lead to less production of the cytokines by macrophages compared to non-capsulated bacteria [234]. Pneumococcal 13-valent (*Prevenar13*<sup>®</sup>) or 23-valent (*Pneumovax*<sup>®</sup>) vaccines possess the CPS target of the 13 or 23 most commonly registered capsule types in infection of *S. pneumoniae* [235]. Serotypes Ia, Ib, II, III, V of 10 different serotypes of GBS (classified accordingly different CPS structures) are predominate in neonatal streptococcal diseases [236]. GBS of type III are the causes of invasive neonatal infections and his capsule was shown to be a virulent factor [237]. Streptococcal Group B glycoconjugate vaccines were developed on the basis of CPS type III [238]. The reported capsule switching in pneumococci but also in streptococci can lead to circumvention of applied vaccine targets and represent the next challenge in the vaccination development [239, 240]. All these data point to the importance of this molecule.

Transmission electron micrographs of *S. dysgalactiae* 2023 demonstrated a thick cell envelope. It was presumed that the cells produce CPS or EPS, or both. As CPS is considered as important cell envelope component there were attempts to isolate and characterize CPS from *S. dysgalactiae* 2023 and *S. agalactiae* 0250. However, the isolation of the capsule by 0.9% NaCl and 1% phenol extractions of both streptococci failed. The change of the growth medium from THB to BHI was unsuccessful as well, and supplementation of 2% casein hydrolysate to BHI, which should mimic the conditions of the udder and was successful in case of *S. uberis* [232], was still without any achievement. A next attempt was made by inoculating the large cultures immediately after bacterial growth on the agar plate, omitting growth of pre-cultures. In case of too many passages the bacteria adapt to the laboratory conditions and may not produce virulent factors anymore. The 0.9% NaCl extract of *S. agalactiae* 0250 revealed the rhamnose-rich polysaccharide and the 1% phenol extract the LTA. Both extracts of *S. dysgalactiae* 2023 contained dLTA molecules. Additionally, the lost of the capsule in case of *S. dysgalactiae* during the storage as well as the unsuccessful attempts to initiate the capsule expression were reported [62]. The bovine *S. dysgalactiae* were shown to grow on THB media supplemented with whey, lactose, casein or skim milk and do not express the capsule under laboratory conditions [220].

Since the capsular components could have been present in culture medium, this as well as three supernatants obtained after washing steps were investigated for the presence of capsular polysaccharide, however, nothing could be identified. It has been shown that GCS produce hyaluronic acid capsule [102]. This could not be shown for *S. dysgalactiae* 2023 in this work. Types IV and V were described as the most predominate capsule serotypes in bovine mastitis species, and types Ia, Ib, III, II were also detectable [59]. The recently published study (2013) of Rato *et al.* discovered the *cpsE* gene, and new *cpsD-cpsE-cpsF* sequences of GBS, which are suggestive to code for new CPS serotypes [241]. This shows that the field of studies on streptococci capsules is still not completely well understood.

## 5.6 Rhamnose-rich polysaccharides

### 5.6.1 Rhamnose-rich polysaccharide of *S. agalactiae* 0250

The rhamnose-rich polysaccharides from *S. agalactiae* 0250 were obtained after 0.9% NaCl as well as after TCA treatment. The samples were investigated by chemical analysis, and by 1D and 2D NMR spectroscopy. One branched polymer **1** could be identified with the structure  $\rightarrow 3)\text{-}\alpha\text{-D-GlcNAc-(1}\rightarrow 2)\text{-}\alpha\text{-L-Rhap-(1}\rightarrow 2)\text{-}\alpha\text{-L-Rhap-(1}\rightarrow 3)\text{-}\alpha\text{-D-Galp}$ , which was substituted at C-3 of the second Rha with  $\alpha\text{-L-Rha-(1}\rightarrow 2)\text{-}\alpha\text{-L-Rha-(1}\rightarrow$  disaccharide. The second identified polymer **2** was unbranched and consisted of  $\alpha\text{-L-Rhap-(1}\rightarrow 2)\text{-}\alpha\text{-L-Rha-(1}\rightarrow 3)\text{-}\alpha\text{-D-Galp}$ .

It is known, that GBS species produce the Lancefield Group B antigen, which is bound to PGN and is mainly composed of Rha, Gal, glucitol (Glu) and phosphate. This molecule is extremely complex with one main branch, which is linked to PGN and other two branches. Each of these branches is further branched [242, 243] (Figure 5.1). The investigation of the role of GBS demonstrated that the antigen is important for growth, cell division, separation processes and normal cell morphology. Moreover, abnormalities in PGN synthesis, polymerization of the murein sacculus and altered localization of the PGN hydrolase PcsB (important for cell division of streptococci) were observed in *gbcO* mutants of *S. agalactiae* [244]. Caliot *et al.* discussed the essential function of the GBS antigen as a homolog of WTA of *Staph. aureus* and *B. subtilis* [244].

The complexity of this molecule made it difficult for structural studies. The investigation by 2D NMR spectroscopy and methylation analysis revealed two chains of the molecule which have similar components as GBS antigen, but their sequence was not consistent with the reported structure [242, 243]. However, the published structure of GBS antigen refers to human *S. agalactiae* isolate and structure of bovine isolate could be different. All spin systems in the NMR spectra could not be investigated. The sample requires further investigations to assign the molecule as GBS antigen or other polysaccharide of the cell envelope.

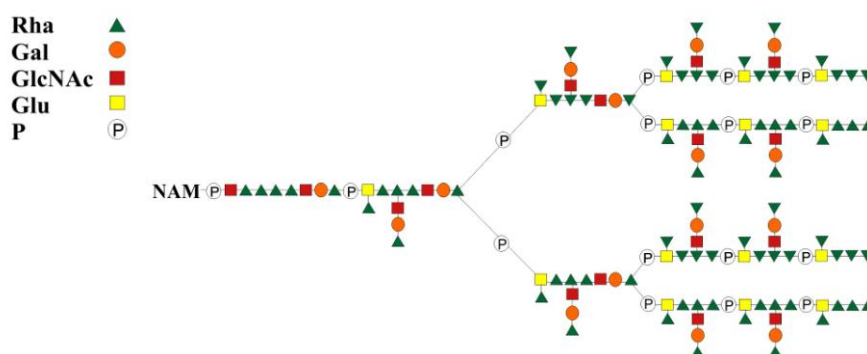


**Figure 5.1** The structure of GBS antigen.

The multiantennary polymer is linked to an *N*-acetyl muramic (NAM) moiety [244].

### 5.6.2 Rhamnose-rich polysaccharide of *S. dysgalactiae* 2023

The investigation of rhamnose-rich polysaccharides of *S. dysgalactiae* 2023 were also obtained using WTA isolation and 1% phenol extraction. First compositional analysis steps revealed Rha and GalNAc as the main constituents. 1D and 2D NMR spectroscopy and methylation analysis identified the composition of the 4 isolated polysaccharides. Polymer 1 contained a branch at C-3 of the second Rha chain [ $\rightarrow 3$ ]- $\alpha$ -L-Rhap-( $1 \rightarrow 2$ )- $\alpha$ -L-Rhap-( $1 \rightarrow$ ] with the GalpNAc-( $1 \rightarrow 3$ )- $\alpha$ -GalpNAc disaccharide. The unbranched polymer 2 consisted of [ $\rightarrow 2$ ]- $\alpha$ -L-Rhap-( $1 \rightarrow 3$ )- $\alpha$ -L-

Rhap-(1→] and two short polymers present the unbranched chains **3**  $\alpha$ -Glc<sub>1</sub>NAc-(1→3)- $\alpha$ -L-Rhap-(1→2)- $\alpha$ -L-Rhap-(1→3)-X and **4** t-L-Rhap-(1→4)- $\beta$ -D-Glc<sub>1</sub>p-(1→2)- $\alpha$ -L-Rhap.

Group C antigen, a typical polysaccharide of their cell envelope, is described for Group C streptococci such as *S. dysgalactiae*. This antigen is composed particularly of Rha and GalNAc. The suggested structure of Group C antigen in 1978 was elucidated applying immunochemical and chemical investigations. The proposed structure contained a main chain [→2)-Rha-(1→3)-Rha-(1→] with the substitution of GalNAc-(1→3)-GalNAc-(1→ on every second Rha [245, 246]. The constituents of the rhamnose-rich polysaccharide of *S. dysgalactiae* 2023 are concordant to the reported components of GCS antigen. This is the first description, yet not complete, of the structure of GCS polysaccharide applying NMR spectroscopy.

## 5.7 Mannose-rich polysaccharides

Mannose-rich polysaccharides were described for a variety of species, e.g. for *Saccharomyces cerevisiae* [247], *Candida* sp. [248], *Phomopsis foeniculi* [249], but also Gram-negative bacteria [250]. All of them possessed nearly the same mannan structure with some modifications in the linkages or in branches.

The NMR investigations of the nutrient medium after the growth of *S. agalactiae* 0250 and *S. dysgalactiae* 2023 and of the medium alone revealed the same <sup>1</sup>H NMR spectrum of a mannose-rich polysaccharide like that of *S. cerevisiae* [247]. No EPS molecule could be observed. Some additional signals, which were not in the blank could probably belong to some metabolism products after the bacterial growth or organic material. This experiment demonstrated the importance of preparing a proper blank sample, which has to be run under the same experimental conditions as the investigated sample(s).

## 5.8 Conclusion

*S. agalactiae* and *S. dysgalactiae* species differ in the replacing niches. *S. agalactiae* species cause human and bovine diseases and a zoonotic pathogen *S. dysgalactiae* is capable to invade different animal hosts and to cause, apart from bovine mastitis in cows, also the summer mastitis. Their phylogenetic relationship was investigated by sequencing of 16S rRNA. Both *Streptococcus* species belong to the same taxonomic tree branch. Thereby both *S. dysgalactiae* subsp. *dysgalactiae* and *S. dysgalactiae* subsp. *equisimilis* originate from *S. agalactiae* and differentiate from it in two sequence pairs [31]. The successful invasion of different hosts and the niches diversity of closely related species reflect in the genes assembly of the *Streptococcus* species like

capability of milk degradation of bovine *S. agalactiae* [60] or exotoxin G (*spegg*) locus, detected in *S. dysgalactiae* subsp. *dysgalactiae* invading fishes, but not in porcine *S. dysgalactiae* [251]. Plasminogen activator PadA was investigated by J. Leigh et al. with herein present *S. dysgalactiae* 2023 and other bovine streptococci. PadA was demonstrated to activate the bovine plasminogen, which helps the strains to hydrolyze milk proteins and to grow well in the cow's udder [69]. The genetic differences of bovine *Streptococcus* isolates make it possible to find out the taxa-specific markers for the rapid detection and distinguishing of bovine common pathogens [252].

In this work the two bovine mastitis isolates GBS *S. agalactiae* 0250 and GCS *S. dysgalactiae* 2023 were investigated with regard to their cell envelope structures and their significance in mastitis infection. The whole cells of both streptococci activated the NF- $\kappa$ B pathway by TLR2-dependent way. The LTAs and the glycolipids of *S. agalactiae* 0250 and *S. dysgalactiae* 2023 were structurally very similar and appeared to be genetically conserved in many streptococci, but also other bacteria, which belong to *Streptococcaceae* produce such cell wall components. The LTA of both *Streptococcus* species were shown to be TLR2 inactive, but it could slight induce IL-6 and TNF- $\alpha$  release in hMNC via an unknown receptor. The LTA was demonstrated to disturb the monocytes and neutrophils in their phagocytosis capability. The stimulation of murine splenocytes by glycolipids was investigated and revealed slight activities, however, these experiments have to be repeated. Bacteria were not observed to produce CPS or EPS in the liquid medium, nevertheless TEM of *S. dysgalactiae* demonstrated the presence of thick cell surroundings in addition to CM and PGN. The WTA of both *Streptococcus* species was shown to possess the same structure like a dLTA.

## 6 Deutsche Zusammenfassung

Rindermastitis ist eine weit verbreitete Krankheit auf Bauernhöfen, die schwer auszurotten ist, da viele der Erreger in der unmittelbaren Umgebung der Kuh vorkommen. In der vorliegenden Arbeit wurden die Zellhüllenkomponenten zweier Gram-positiver Krankheitserreger der Rindermastitis, nämlich *Streptococcus agalactiae* 0250 und *Streptococcus dysgalactiae* 2023 isoliert und strukturell sowie z. T. biologisch untersucht.

Die Isolierung erfolgte mittels bekannter, teilweise modifizierter Methoden und zur strukturellen Analyse wurden biochemischen Komponentenanalysen, NMR Spektroskopie und ESI FT-ICR MS sowie MALDI FT-ICR MS angewendet. Die Untersuchungen der isolierten LTA Moleküle aus *S. agalactiae* 0250 und *S. dysgalactiae* 2023 haben gezeigt, dass die Polymere aus einem poly-(GroP) Rückgrat mit einer durchschnittlichen Länge von 34 (*S. agalactiae* 0250) und 28 Einheiten (*S. dysgalactiae* 2023) bestanden. Der  $\alpha$ -D-Glcp-(1 $\rightarrow$ 2)- $\alpha$ -D-Glcp-(1 $\rightarrow$ 3)-Diacyl-Gro Lipidanker war mit unterschiedlichen Fettsäurenkombinationen von 16:0, 16:1, 18:1 und 18:0 kovalent gebunden. Die hydrophile Kette der LTA war unregelmäßig am O-2 des Gro mit D-Ala substituiert. Die H<sub>2</sub>O<sub>2</sub>-behandelten LTA Proben der beiden Stämme waren nicht TLR2 aktiv, induzierten jedoch leicht eine IL-6 Freisetzung in hMNC. Den Rezeptor, der die LTA als PAMP erkennen kann, gilt es immer noch herauszufinden. Um die möglichen Immunreaktionen im Euter zu prüfen, wurden die H<sub>2</sub>O<sub>2</sub>-behandelten LTA Proben dem Phagozytose-Kapazitätstest mit aus Kühen stammenden Macrophagen und neutrophilen Granulozyten unterzogen. Dabei reduzierte die LTA die Phagozytose-Kapazität der Immunzellen. Ganze Bakterienzellen von *S. agalactiae* 0250 und *S. dysgalactiae* 2023 konnten den NF- $\kappa$ B Weg mittels boTLR2 in den HEK293 Zellen aktivieren.

Die Abspaltung der WTA mittels TCA ergab, dass das isolierte Molekül eine Struktur wie deacylierte LTA der beiden Streptokokken zeigte. Die Strukturanalyse ergab den  $\alpha$ -D-Glcp-(1 $\rightarrow$ 2)- $\alpha$ -D-Glcp-(1 $\rightarrow$ 3)-diacyl-Gro Lipidanker sowie das hydrophile poly-(GroP) Rückgrat, das unregelmäßig am O-2 des Gro mit D-Ala substituiert war. Bakterienstämme, wie z. B. *Bacillus subtilis*, produzieren strukturell gleiche WTA und LTA Polymere, die dabei über umgekehrte Stereochemie von Gro in der hydrophilen Kette verfügen. Die Tatsache, dass die Streptokokken keine Enzyme besitzen in der WTA einen stereochemisch gegenüberliegenden Gro zu dem der LTA zu bilden, schließt jedoch die Möglichkeit nicht aus, dass die Streptokokken anderen Syntheseweg für die WTA Produktion haben können. Anschließend, um eine strukturell andere

WTA von *S. agalactiae* 0250 und *S. dysgalactiae* 2023 mit einem Stück von PGN zu isolieren, wurde die Methode des enzymatischen Verdaus angewandt.

Zusätzlich wurden die Glycolipide der beiden *Streptococcus* Spezies isoliert und nach der Strukturanalyse auf ihre biologische Aktivität überprüft. Die Spezies besaßen die Glycolipide Monoglucosyldiacylglycerol, Diglucosyldiacylglycerol und Phosphatidyldiglucosyldiacylglycerol in größerer Menge. Dabei kann das Diglucosyldiacylglycerol als Lipidanker der LTA fungieren. Glycolipide MGlcDAG und PGro-DGlcDAG konnten die aus der Maus entnommenen Milzzellen leicht stimulieren.

Während der WTA- sowie der Kapsel-Isolierung wurden Rhamnose-reiche Moleküle von beiden *Streptococcus* Spezies co-isoliert und strukturell charakterisiert. Die Auswertung der Methylierungsanalyse und der 1D und 2D NMR Spektren ergab, dass zwei große und zwei kleine Rhamnose-reiche Polymere isoliert wurden. Der erste Polymer hatte die Struktur **1**  $[\rightarrow 3)\text{-}\alpha\text{-L-Rhap-(1}\rightarrow 2)\text{-}\alpha\text{-L-Rhap-(1}\rightarrow ]$  und war dabei am C-3 an der 2. Rhamnose mit GalpNAc-(1 $\rightarrow$ 3)- $\alpha$ -GalpNAc substituiert. Das unverzweigte Polymer **2** bestand aus der *repeating unit*  $[\rightarrow 2)\text{-}\alpha\text{-L-Rhap-(1}\rightarrow 3)\text{-}\alpha\text{-L-Rhap-(1}\rightarrow ]$ . Die kurzen Polymere **3**  $\alpha\text{-GlcPNAc-(1}\rightarrow 3)\text{-}\alpha\text{-L-Rhap-(1}\rightarrow 2)\text{-}\alpha\text{-L-Rhap-(1}\rightarrow 3)\text{-X}$  und **4**  $\text{L-Rhap-(1}\rightarrow 4)\text{-}\beta\text{-D-Glcp-(1}\rightarrow 2)\text{-}\alpha\text{-L-Rhap}$  waren unverzweigt und hatten keine Wiederholungseinheiten. Bei dem Polymer **1** von *S. dysgalactiae* 2023 handelte es sich um das gruppenspezifische Lancefield Antigen C. Dieses wurde bis jetzt chemisch und immunhistochemisch analysiert. Im Fall von *S. agalactiae* ist die sehr komplexe Struktur des GBS Antigens bekannt. Das isolierte und strukturell untersuchte Polymer **1** von *S. agalactiae* 0250 besaß eine Kette  $\rightarrow 3)\text{-}\alpha\text{-D-GlcNAc-(1}\rightarrow 2)\text{-}\alpha\text{-L-Rhap-(1}\rightarrow 2)\text{-}\alpha\text{-L-Rhap-(1}\rightarrow 3)\text{-}\alpha\text{-D-Galp}$ , die am C-3 der 2. Rha mit  $\alpha\text{-L-Rha-(1}\rightarrow 2)\text{-}\alpha\text{-L-Rha-(1}\rightarrow$  substituiert war. Das Polymer **2** enthielt  $\alpha\text{-L-Rhap-(1}\rightarrow 2)\text{-}\alpha\text{-L-Rha-(1}\rightarrow 3)\text{-}\alpha\text{-D-Galp}$ . Beide kurzen Polysaccharide vom Rindermastitis-Isolat waren anders gebaut als die bekannten Polysaccharid-Ketten des GBS Antigens. Um die vollständige Struktur des Rhamnose-reichen Polymers aus den Rindermastitis-Isolaten herauszufinden und ob sie den humanen Isolaten gleich sind, sind weitere strukturelle und biochemische Untersuchungen notwendig.

*S. agalactiae* 0250 und *S. dysgalactiae* 2023 haben keine Kapsel in Flüssigkulturen gebildet und bei beiden *Streptococcus* Spezies konnte kein Exopolysaccharid isoliert werden.

## 7 References

1. Dorland's illustrated medical dictionary. Elsevier W. B. Saunders company Harcourt Brace Jovanovich, Inc., Philadelphia (2007).
2. Biggs, A.: Mastitis in cattle. The Crowood Press Ltd, Ramsbury, Marlborough Wiltshire (2009).
3. Esslemont, R.J., Kossaibati, M.A.: Culling in 50 dairy herds in England. *Vet. Rec.* 140, 36–39 (1997).
4. Hillerton, J.E., Berry, E.A.: Treating mastitis in the cow—a tradition or an archaism. *J. Appl. Microbiol.* 98, 1250–1255 (2005).
5. Lam, T.J.G.M., van den Borne, B.H.P., Jansen, J., Huijps, K., van Veersen, J.C.L., van Schalk, G., Hogeveen, H.: Improving bovine udder health: a national mastitis control program in the Netherlands. *J. Dairy Sci.* 96, 1301–1311 (2012).
6. Sutra, L., Poutrel, B.: Virulence factors involved in the pathogenesis of bovine intramammary infections due to *Staphylococcus aureus*. *J. Med. Microbiol.* 40, 79–89 (1994).
7. Akers, R.M., Nickerson, S.C.: Mastitis and its impact on structure and function in the ruminant mammary gland. *J. Mammary Gland Biol. Neoplasia.* 16, 275–289 (2011).
8. Le Roux, Y., Laurent, F., Moussaoui, F.: Polymorphonuclear proteolytic activity and milk composition change. *Vet. Res.* 34, 629–645 (2003).
9. Åkerstedt, M., Wredle, E., Lam, V., Johansson, M.: Protein degradation in bovine milk caused by *Streptococcus agalactiae*. *J. Dairy Res.* 79, 297–303 (2012).
10. Auldist, M.J., Coats, S., Sutherland, B.J., Mayes, J.J., McDowell, G.H., Rogers, G.L.: Effects of somatic cell count and stage of lactation on raw milk composition and the yield and quality of Cheddar cheese. *J. Dairy Res.* 63, 269–280 (1996).
11. Halasa, T., Huijps, K., Østerås, O., Hogeveen, H.: Economic effects of bovine mastitis and mastitis management: a review. *Vet. Q.* 29, 18–31 (2007).
12. Bengtsson, B., Unnerstad, H.E., Ekman, T., Artursson, K., Nilsson-Ost, M., Waller, K.P.: Antimicrobial susceptibility of udder pathogens from cases of acute clinical mastitis in dairy cows. *Vet. Microbiol.* 136, 142–149 (2009).
13. Roesch, M., Perreten, V., Doherr, M.G., Schaeren, W., Schällibaum, M., Blum, J.W.: Comparison of antibiotic resistance of udder pathogens in dairy cows kept on organic and on conventional farms. *J. Dairy Sci.* 89, 989–997 (2006).
14. Tenhagen, B.-A., Köster, G., Wallmann, J., Heuwieser, W.: Prevalence of mastitis pathogens and their resistance against antimicrobial agents in dairy cows in Brandenburg, Germany. *J. Dairy Sci.* 89, 2542–2551 (2006).

15. Malinowski, E., Gajewski, Z.: Mastitis and fertility disorders in cows. *Pol. J. Vet. Sci.* 13, 555–560 (2010).
16. Blowey, R., Edmondson, P.: *Mastitis Control in Dairy Herds*. CAB International 2010, Oxfordshire OX10 8DE, UK (2010).
17. Bramley, A.J., Dodd, F.H.: Reviews of the progress of dairy science: mastitis control - progress and prospects. *J. Dairy Res.* 51, 481–512 (1984).
18. Kossaibati, M.A., Hovi, M., Esslemont, R.J.: Incidence of clinical mastitis in dairy herds in England. *Vet. Rec.* 143, 649–653 (1998).
19. Bradley, A.J., Leach, K.A., Breen, J.E., Green, L.E., Green, M.J.: Survey of the incidence and aetiology of mastitis on dairy farms in England and Wales. *Vet. Rec.* 160, 253–258 (2007).
20. Olde Riekerink, R.G.M., Barkema, H.W., Kelton, D.F., Scholl, D.T.: Incidence rate of clinical mastitis on Canadian dairy farms. *J. Dairy Sci.* 91, 1366–1377 (2008).
21. Hogeveen, H., Pyorala, S., Waller, K.P., Hogan, J.S., Lam, T.J.G.M., Oliver, S.P., Schukken, Y.H., Barkema, H.W., Hillerton, J.E.: Current status and future challenges in mastitis research. *NMC Annu. Meet. Proc.* 36–48 (2011).
22. Watts, J.L.: Etiological agents of bovine mastitis. *Vet. Microbiol.* 16, 41–66 (1988).
23. Schukken, Y.H., Gunther, J., Fitzpatrick, J., Fontaine, M.C., Goetze, L., Holst, O., Leigh, J., Petzl, W., Schuberth, H.J., Sipka, A., Smith, D.G., Quesnell, R., Watts, J., Yancey, R., Zerbe, H., Gurjar, A., Zadoks, R.N., Seyfert, H.-M.: Host-response patterns of intramammary infections in dairy cows. *Vet. Immunol. Immunopathol.* 144, 270–289 (2011).
24. Leigh, J.A., Egan, S.A., Ward, P.N., Field, T.R., Coffey, T.J.: Sortase anchored proteins of *Streptococcus uberis* play major roles in the pathogenesis of bovine mastitis in dairy cattle. *Vet. Res.* 41, 63 (2010).
25. Bradley, A.J.: Bovine Mastitis: An Evolving Disease. *Vet. J.* 164, 116–128 (2002).
26. Keefe, G.P.: *Streptococcus agalactiae* mastitis: a review. *Can. Vet. J.* 38, 429–437 (1997).
27. Schukken, Y.H., Chuff, M., Moroni, P., Gurjar, A., Santisteban, C., Welcome, F., Zadoks, R.: The “other” gram-negative bacteria in mastitis: *Klebsiella*, *Serratia*, and more. *Vet. Clin. North Am. Food Anim. Pract.* 28, 239–256 (2012).
28. Bal, E.B.B., Bayar, S., Bal, M.A.: Antimicrobial susceptibilities of coagulase-negative staphylococci (CNS) and streptococci from bovine subclinical mastitis cases. *J. Microbiol.* 48, 267–274 (2010).
29. Botrel, M.-A., Haenni, M., Morignat, E., Sulpice, P., Madec, J.-Y., Calavas, D.: Distribution and antimicrobial resistance of clinical and subclinical mastitis pathogens in dairy cows in Rhône-Alpes, France. *Foodborne Pathog. Dis.* 7, 479–487 (2010).
30. Spellenberg, B., Brandt, C., *Bergey’s Manual. Streptococcus*. Springer, 412–429 (2009).

31. Facklam, R.: What happened to the streptococci: overview of taxonomic and nomenclature changes. *Clin. Microbiol. Rev.* 15, 613–630 (2002).
32. Täpp, J., Thollesson, M., Herrmann, B.: Phylogenetic relationships and genotyping of the genus *Streptococcus* by sequence determination of the RNase P RNA gene, *rnpB*. *Int. J. Syst. Evol. Microbiol.* 53, 1861–1871 (2003).
33. Lancefield, R.C.: A serological differentiation of human and other groups of hemolytic streptococci. *J. Exp. Med.* 57, 571–595 (1932).
34. Manning, S.D., Schaeffer, K.E., Springman, C.A., Lehotzky, E., Lewis, M.A., Ouellette, L.M., Wu, G., Moorer, G.M., Whittam, T.S., Davies, D.H.: Genetic diversity and antimicrobial resistance in Group B *Streptococcus* colonizing young, nonpregnant women. *Clin. Infect. Dis.* 47, 388–390 (2008).
35. Schuchat, A.: Epidemiology of Group B streptococcal disease in the United States: shifting paradigms. *Clin. Microbiol. Rev.* 11, 497–513 (1998).
36. Berner, R.: Significance, management and prevention of *Streptococcus agalactiae* infection during the perinatal period. *Expert Rev. Antiinfective Ther.* 2, 427–437 (2004).
37. Schrag, S.J., Zywicki, S., Farley, M.M., Reingold, A., Harrison, L.H., Lewkowitz, L.B., Hadler, J.L., Danila, R., Cieslak, P.R., Schuchat, A.: Group B streptococcal disease in the era of intrapartum antibiotic prophylaxis. *N. Engl. J. Med.* 342, 15–20 (2000).
38. Nocard, E., Mollereau: Sur une mammitte contagieuse des vaches laitieres. *Ann. l'Institut Pasteur, Paris.* 1, 109–126 (1887).
39. Guerreiro, O., Velez, Z., Alvarenga, N., Matos, C., Duarte, N.: Molecular screening of ovine mastitis in different breeds. *J. Dairy Sci.* 96, (2013).
40. Erskine, R.J., Eberhart, R.J., Hutchinson, L.I., Spencer, S.B., Campbell, M.A.: Incidence and types of clinical mastitis in dairy herds with high and low somatic cell counts. *Reports Orig. Stud.* 6, 761–765 (1988).
41. Myllys, V., Asplund, K., Brofeldt, E., Hirvelä-Koski, V., Honkanen-Buzalski, T., Junttila, J., Kulkas, L., Myllykangas, O., Niskanen, M., Saloniemi, H., Sandholm, M., Saranpää, T.: Bovine mastitis in Finland in 1988 and 1995 - changes in prevalence and antimicrobial resistance. *Acta Vet. Scand.* 39, 119–126 (1998).
42. Keefe, G.P., Dohoo, I.R., Spangler, E.: Herd prevalence and incidence of *Streptococcus agalactiae* in the dairy industry of Prince Edward Island. *J. Dairy Sci.* 80, 464–470 (1997).
43. Zadoks, R.N., Middleton, J.R., McDougall, S., Katholm, J., Schukken, Y.H.: Molecular epidemiology of mastitis pathogens of dairy cattle and comparative relevance to humans. *J. Mammary Gland Biol. Neoplasia.* 16, 357–372 (2011).
44. Fehlings, K., Hamann, J., Klawonn, W., Knappstein, K., Mansfeld, R., Wittkowski, G., Zschöck, M.: Leitlinien Bekämpfung der Mastitis des Rindes als Bestandsproblem. DVG service (2012)

45. Pritzlaff, C.A., Chang, J.C., Kuo, S.P., Tamura, G.S., Rubens, C.E., Nizet, V.: Genetic basis for the beta-haemolytic/cytolytic activity of Group B *Streptococcus*. *Mol. Microbiol.* 39, 236–247 (2001).
46. Chen, L., Yang, J., Yu, J., Yao, Z., Sun, L., Shen, Y., Jin, Q.: VFDB: a reference database for bacterial virulence factors. *Nucleic Acids Res.* 33, D325–D328 (2005).
47. Shome, B.R., Bhuvana, M., Mitra, S. Das, Krithiga, N., Shome, R., Velu, D., Banerjee, A., Barbuddhe, S.B., Prabhudas, K., Rahman, H.: Molecular characterization of *Streptococcus agalactiae* and *Streptococcus uberis* isolates from bovine milk. *Trop. Anim. Health Prod.* 44, 1981–1992 (2012).
48. Franken, C., Haase, G., Brandt, C., Weber-Heynemann, J., Martin, S., Lämmler, C., Podbielski, A., Lütticken, R., Spellerberg, B.: Horizontal gene transfer and host specificity of beta-haemolytic streptococci: the role of a putative composite transposon containing scpB and lmb. *Mol. Microbiol.* 41, 925–35 (2001).
49. Lindahl, G., Stalhammar-Carlemalm, M., Areschoug, T.: Surface proteins of *Streptococcus agalactiae* and related proteins in other bacterial pathogens. *Clin. Microbiol. Rev.* 18, 102–127 (2005).
50. Maeland, J.A., Radtke, A., Lyng, R. V, Mavenyengwa, R.T.: Novel aspects of the Z and R3 antigens of *Streptococcus agalactiae* revealed by immunological testing. *Clin. Vaccine Immunol.* 20, 607–612 (2013).
51. Bernheimer, A.W., Linder, R., Avigad, L.S.: Nature and mechanism of action of the CAMP protein of Group B streptococci. *Infect. Immun.* 23, 838–844 (1979).
52. Skalka, B., Smola, J.: Lethal effect of CAMP-Factor and UBERIS-Factor - a new finding about diffusible exosubstances of *Streptococcus agalactiae* and *Streptococcus uberis*. *Zbl. Bakt. Hyg., I. Abt. Orig. A.* 249, 190–194 (1981).
53. Hensler, M.E., Quach, D., Hsieh, C.-J., Doran, K.S., Nizet, V.: CAMP factor is not essential for systemic virulence of Group B *Streptococcus*. *Microb. Pathog.* 44, 84–88 (2008).
54. Chuzeville, S., Puymège, A., Madec, J.-Y., Haenni, M., Payot, S.: Characterization of a new CAMP factor carried by an integrative and conjugative element in *Streptococcus agalactiae* and spreading in streptococci. *PLoS One.* 7, (2012).
55. Puymège, A., Bertin, S., Chuzeville, S., Guédon, G., Payot, S.: Conjugative transfer and cis-mobilization of a genomic island by an integrative and conjugative element of *Streptococcus agalactiae*. *J. Bacteriol.* 195, 1142–1151 (2013).
56. Sharma, P., Lata, H., Arya, D.K., Kashyap, A.K., Kumar, H., Dua, M., Ali, A., Johri, A.K.: Role of pilus proteins in adherence and invasion of *Streptococcus agalactiae* to the lung and cervical epithelial cells. *J. Biol. Chem.* 288, 4023–4034 (2013).
57. Manning, S.D., Springman, A.C., Million, A.D., Milton, N.R., McNamara, S.E., Somsel, P.A., Bartlett, P., Davies, H.D.: Association of Group B *Streptococcus* colonization and bovine exposure: a prospective cross-sectional cohort study. *PLoS One.* 5, (2010).

58. Bisharat, N., Crook, D.W., Leigh, J., Harding, R.M., Ward, P.N., Coffey, T.J., Maiden, M.C., Peto, T., Jones, N.: Hyperinvasive neonatal Group B *Streptococcus* has arisen from a bovine ancestor. *J. Clin. Microbiol.* 42, 2161–2167 (2004).
59. Radtke, A., Bruheim, T., Afset, J.E., Bergh, K.: Multiple-locus variant-repeat assay (MLVA) is a useful tool for molecular epidemiologic analysis of *Streptococcus agalactiae* strains causing bovine mastitis. *Vet. Microbiol.* (2012).
60. Richards, V.P., Lang, P., Pavinski Bitar, P.D., Lefébure, T., Schukken, Y.H., Zadoks, R.N., Stanhope, M.J.: Comparative genomics and the role of lateral gene transfer in the evolution of bovine adapted *Streptococcus agalactiae*. *Infect. Genet. Evol.* 11, 1263–1275 (2011).
61. Rato, M.G., Nerlich, A., Bergmann, R., Bexiga, R., Nunes, S.F., Vilela, C.L., Santos-Sanches, I., Chhatwal, G.S.: Virulence gene pool detected in bovine Group C *Streptococcus dysgalactiae* subsp. *dysgalactiae* isolates by use of a group A *S. pyogenes* virulence microarray. *J. Clin. Microbiol.* 49, 2470–2479 (2011).
62. Calvino, L.F., Almeida, R.A., Oliver, S.P.: Potential virulence factors of *Streptococcus dysgalactiae* associated with bovine mastitis. *Vet. Microbiol.* 61, 93–110 (1998).
63. Leigh, J.A., Hodgkinson, S.M., Lincoln, R.A.: The interaction of *Streptococcus dysgalactiae* with plasmin and plasminogen. *Vet. Microbiol.* 61, 121–135 (1998).
64. Czabańska, A., Neiwert, O., Lindner, B., Leigh, J., Holst, O., Duda, K.A.: Structural analysis of the lipoteichoic acids isolated from bovine mastitis *Streptococcus uberis* 233, *Streptococcus dysgalactiae* 2023 and *Streptococcus agalactiae* 0250. *Carbohydr. Res.* 361, 200–205 (2012).
65. Pyörälä, S., Syväjärvi, J.: Bovine acute mastitis: Part I. Clinical aspects and parameters of inflammation in mastitis caused by different pathogens. *J. Vet. Med. B* 34, 573–584 (1987).
66. Madsen, M., Sdrensen, G.H., Aalbaek, B.: Summer mastitis in heifers: a bacteriological examination of secretions from clinical cases of summer mastitis in Denmark. *Vet. Microbiol.* 22, 319–328 (1990).
67. Chénier, S., Leclère, M., Messier, S., Fecteau, G.: *Streptococcus dysgalactiae* cellulitis and toxic shock-like syndrome in a Brown Swiss cow. *J. Vet. Diagnostic Investig.* 20, 99–103 (2008).
68. Vela, A.I., Falsen, E., Simarro, I., Rollan, E., Collins, M.D., Domínguez, L., Fernandez-Garayzabal, J.F.: Neonatal mortality in puppies due to bacteremia by *Streptococcus dysgalactiae* subsp. *dysgalactiae*. *J. Clin. Microbiol.* 44, 99–103 (2006).
69. Ward, P.N., Abu-Median, A.-B.A.K., Leigh, J.A.: Structural consideration of the formation of the activation complex between the staphylokinase-like streptococcal plasminogen activator PadA and bovine plasminogen. *J. Mol. Biol.* 381, 734–747 (2008).
70. Jonsson, H., Frykberg, L., Rantamäki, L., Guss, B.: MAG, a novel plasma protein receptor from *Streptococcus dysgalactiae*. *Gene.* 143, 85–89 (1994).

71. Song, X., Perez-Casal, J., Bolton, A., Potter, A.A.: Surface-expressed Mig protein protects *Streptococcus dysgalactiae* against phagocytosis by bovine neutrophils. *Infect. Immun.* 69, 6030–6037 (2001).
72. Jonsson, H., Müller, H.P.: The type-III Fc receptor from *Streptococcus dysgalactiae* is also an alpha 2-macroglobulin receptor. *Fed. Eur. Biochem. Soc. J.* 220, 819–826 (1994).
73. Vasi, J., Frykberg, L., Carlsson, L.E., Lindberg, M., Guss, B.: M-like proteins of *Streptococcus dysgalactiae*. *Infect. Immun.* 68, 294–302 (2000).
74. Rato, M.G., Bexiga, R., Nunes, S.F., Vilela, C.L., Santos-Sanches, I.: Human Group A streptococci virulence genes in bovine Group C streptococci. *Emerg. Infect. Dis.* 16, 116–119 (2010).
75. Forster, B.M., Marquis, H.: Protein transport across the cell wall of monoderm Gram-positive bacteria. *Mol. Microbiol.* 84, 405–413 (2012).
76. Schleifer, K.H., Kandler, O.: Peptidoglycan types of bacterial cell walls and their taxonomic implications. *Bacteriol. Rev.* 36, 407–477 (1972).
77. Royet, J., Dziarski, R.: Peptidoglycan recognition proteins: pleiotropic sensors and effectors of antimicrobial defences. *Nat. Rev. Microbiol.* 5, 264–77 (2007).
78. Navarre, W.W., Schneewind, O.: Surface proteins of Gram-positive bacteria and mechanisms of their targeting to the cell wall envelope. *Microbiol. Mol. Biol. Rev.* 63, 174–229 (1999).
79. Vollmer, W., Blanot, D., de Pedro, M.A.: Peptidoglycan structure and architecture. *FEMS Microbiol. Rev.* 32, 149–167 (2008).
80. Brown, S., Meredith, T., Swoboda, J., Walker, S.: *Staphylococcus aureus* and *Bacillus subtilis* W23 make polyribitol wall teichoic acids using different enzymatic pathways. *Chem. Biol.* 17, 1101–1110 (2010).
81. Pooley, H.M., Karamata, D.: Teichoic acid synthesis in *Bacillus subtilis*: genetic organization and biological roles. *Bacterial Cell Wall*. 187–198. Elsevier Science B. V., (1994).
82. Kaya, S., Araki, Y., Ito, E.: Structural studies on the linkage unit between poly(galactosylglycerol phosphate) and peptidoglycan in cell walls of *Bacillus coagulans*. *Eur. J. Biochem.* 147, 41–46 (1985).
83. Tul'skaya, E.M., Streshinskaya, G.M., Naumova, I.B., Shashkov, A.S., Terekhova, L.P.: A new structural type of teichoic acid and some chemotaxonomic criteria of two species *Nocardiosis dassonvillei* and *Nocardiosis antarcticus*. *Arch. Microbiol.* 160, 299–305 (1993).
84. Bracha, R., Glaser, L.: In vitro system for the synthesis of teichoic acid linked to peptidoglycan. *J. Bacteriol.* 125, 872–879 (1976).
85. D'Elia, M.A., Millar, K.E., Beveridge, T.J., Brown, E.D.: Wall teichoic acid polymers are dispensable for cell viability in *Bacillus subtilis*. *J. Bacteriol.* 188, 8313–8316 (2006).

86. Weidenmaier, C., Kokai-Kun, J.F., Kristian, S. a, Chanturiya, T., Kalbacher, H., Gross, M., Nicholson, G., Neumeister, B., Mond, J.J., Peschel, A.: Role of teichoic acids in *Staphylococcus aureus* nasal colonization, a major risk factor in nosocomial infections. *Nat. Med.* 10, 243–245 (2004).
87. Bera, A., Biswas, R., Herbert, S., Kulauzovic, E., Weidenmaier, C., Peschel, A., Götz, F.: Influence of wall teichoic acid on lysozyme resistance in *Staphylococcus aureus*. *J. Bacteriol.* 189, 280–283 (2007).
88. Bertsche, U., Yang, S.-J., Kuehner, D., Wanner, S., Mishra, N.N., Roth, T., Nega, M., Schneider, A., Mayer, C., Grau, T., Bayer, A.S., Weidenmaier, C.: Increased cell wall teichoic acid production and D-alanylation are common phenotypes among daptomycin-resistant methicillin-resistant *Staphylococcus aureus* (MRSA) clinical isolates. *PLoS One* 8, (2013).
89. Morath, S., Von Aulock, S., Hartung, T.: Structure/function relationships of lipoteichoic acids. *J. Endotoxin Res.* 11, 348–356 (2005).
90. Draing, C., Pfitzenmaier, M., Zummo, S., Mancuso, G., Geyer, A., Hartung, T., von Aulock, S.: Comparison of lipoteichoic acid from different serotypes of *Streptococcus pneumoniae*. *J. Biol. Chem.* 281, 33849–33859 (2006).
91. Neuhaus, F.C., Baddiley, J.: A continuum of anionic charge: structures and functions of D-alanyl-teichoic acids in Gram-positive bacteria. *Microbiol. Mol. Biol. Rev.* 67, 686–723 (2003).
92. Greenberg, J.W., Fischer, W., Joiner, K.A.: Influence of lipoteichoic acid structure on recognition by the macrophage scavenger receptor. *Infect. Immun.* 64, 3318–3325 (1996).
93. Schmidt, R.R., Pedersen, C.M., Qiao, Y., Zähringer, U.: Chemical synthesis of bacterial lipoteichoic acids: an insight on its biological significance. *Org. Biomol. Chem.* 9, 2040–2052 (2011).
94. Gisch, N., Kohler, T., Ulmer, A.J., Müthing, J., Pribyl, T., Fischer, K., Lindner, B., Hammerschmidt, S., Zähringer, U.: Structural reevaluation of *Streptococcus pneumoniae* lipoteichoic acid and new insights into its immunostimulatory potency. *J. Biol. Chem.* 288, 15654–15667 (2013).
95. Henneke, P., Morath, S., Uematsu, S., Weichert, S., Pfitzenmaier, M., Takeuchi, O., Müller, A., Poyart, C., Akira, S., Teti, G., Geyer, A., Hartung, T., Trieu-cuot, P., Kasper, D.L., Douglas, T., Mu, A., Berner, R., Golenbock, D.T.: Role of lipoteichoic acid in the phagocyte response to Group B *Streptococcus*. *J. Immunol.* 174, 6449–6455 (2005).
96. Weidenmaier, C., Peschel, A.: Teichoic acids and related cell-wall glycopolymers in Gram-positive physiology and host interactions. *Nat. Rev. Microbiol.* 6, 276–287 (2008).
97. Oku, Y., Kurokawa, K., Matsuo, M., Yamada, S., Lee, B.-L., Sekimizu, K.: Pleiotropic roles of polyglycerolphosphate synthase of lipoteichoic acid in growth of *Staphylococcus aureus* cells. *J. Bacteriol.* 191, 141–151 (2009).
98. Doran, K.S., Engelson, E.J., Khosravi, A., Maisey, H.C., Fedtke, I., Equils, O., Michelsen, K.S., Arditi, M., Peschel, A., Nizet, V.: Blood-brain barrier invasion by Group B

- Streptococcus* depends upon proper cell-surface anchoring of lipoteichoic acid. *J. Clin. Invest.* 115, 2499–2507 (2005).
99. Weidenmaier, C., Peschel, A., Kempf, V.A.J., Lucindo, N., Yeaman, M.R., Bayer, A.S.: DltABCD- and MprF-mediated cell envelope modifications of *Staphylococcus aureus* confer resistance to platelet microbicidal proteins and contribute to virulence in a rabbit endocarditis model. *Infect. Immun.* 73, 8033–8038 (2005).
  100. Seltmann, G., Holst, O.: *The Bacterial Cell Wall*. Springer Verlag, Berlin Heidelberg (2002).
  101. Fischer, W.: Molecular analysis of lipid macroamphiphiles by hydrophobic interaction chromatography, exemplified with lipoteichoic acids. *Anal. Biochem.* 208, 49–56 (1993).
  102. Ovodov, Y.S.: Bacterial capsular antigens. Structural patterns of capsular antigens. *Biochemistry.* 71, 937–954 (2006).
  103. Karakawa, W.W., Fournier, J.M., Vann, W.F., Arbeit, R., Schneerson, R.S., Robbins, J.B.: Method for the serological typing of the capsular polysaccharides of *Staphylococcus aureus*. *J. Clin. Microbiol.* 22, 445–447 (1985).
  104. Skov Sorensen, U.B., Henrichsen, J., Chen, H.-C., Szu, S.C.: Covalent linkage between the capsular polysaccharide and the cell wall peptidoglycan of *Streptococcus pneumoniae* revealed by immunochemical methods. *Microb. Pathog.* 8, 325–334 (1990).
  105. Deng, L., Kasper, D.L., Krick, T.P., Wessels, M.R.: Characterization of the linkage between the type III capsular polysaccharide and the bacterial cell wall of Group B *Streptococcus*. *J. Biol. Chem.* 275, 7497–7504 (2000).
  106. Calix, J.J., Saad, J.S., Brady, A.M., Nahm, M.H.: Structural characterization of *Streptococcus pneumoniae* serotype 9A capsule polysaccharide reveals role of glycosyl 6-O-acetyltransferase wjE in serotype 9V capsule biosynthesis and immunogenicity. *J. Biol. Chem.* 287, 13996–14003 (2012).
  107. Kogan, G., Brisson, J.R., Kasper, D.L., Von Hunolstein, C., Orefici, G., Jennings, H.J.: Structural elucidation of the novel type VII Group B *Streptococcus* capsular polysaccharide by high resolution NMR spectroscopy. *Carbohydr. Res.* 277, 1–9 (1995).
  108. Cieslewicz, M.J., Chaffin, D., Glusman, G., Kasper, D., Madan, A., Rodrigues, S., Fahey, J., Wessels, M.R., Rubens, C.E.: Structural and genetic diversity of Group B *Streptococcus* capsular polysaccharides. *Infect. Immun.* 73, 3096–3103 (2005).
  109. Ward, P.N., Field, T.R., Ditcham, W.G.F., Maguin, E., Leigh, J.A.: Identification and disruption of two discrete loci encoding hyaluronic acid capsule biosynthesis genes hasA, hasB, and hasC in *Streptococcus uberis*. *Infect. Immun.* 69, 392–399 (2001).
  110. Safari, D., Dekker, H.A.T., Rijkers, G.T., van der Ende, A., Kamerling, J.P., Snippe, H.: The immune response to Group B *Streptococcus* type III capsular polysaccharide is directed to the -Glc-GlcNAc-Gal- backbone epitope. *Glycoconj. J.* 28, 557–562 (2011).
  111. Shen, X., Lagergård, T., Yang, Y., Lindblad, M., Fredriksson, M., Holmgren, J.: Systemic and mucosal immune responses in mice after mucosal immunization with Group B

- Streptococcus* type III capsular polysaccharide-cholera toxin B subunit conjugate vaccine. *Infect. Immun.* 68, 5749–5755 (2000).
112. Sára, M., Pum, D., Schuster, B., Sleytr, U.B.: S-layers as patterning elements for application in nanobiotechnology. *J. Nanosci. Nanotechnol.* 5, 1939–1953 (2005).
  113. Sleytr, U.B., Beveridge, T.J.: Bacterial S-layers. *Trends Microbiol.* 7, 253–260 (1999).
  114. Hanson, B.R., Neely, M.N.: Coordinate regulation of Gram-positive cell surface components. *Curr. Opin. Microbiol.* 15, 204–210 (2013).
  115. Theilacker, C., Sanchez-Carballo, P., Toma, I., Fabretti, F., Sava, I., Kropec, A., Holst, O., Huebner, J.: Glycolipids are involved in biofilm accumulation and prolonged bacteraemia in *Enterococcus faecalis*. *Mol. Microbiol.* 71, 1055–1069 (2009).
  116. Wu, D., Fujio, M., Wong, C.-H.: Glycolipids as immunostimulating agents. *Bioorganic Med. Chem.* 16, 1073–1083 (2009).
  117. Belvin, M.P., Anderson, K. V.: A conserved signaling pathway: the *Drosophila* toll-dorsal pathway. *Annu. Rev. Cell Dev. Biol.* 12, 393–416 (1996).
  118. Medzhitov, R.: Toll-like receptors and innate immunity. *Nat. Rev. Immunol.* 1, 135–145 (2001).
  119. Janeway, C.A., Medzhitov, R.: Innate immune recognition. *Annu. Rev. Immunol.* 20, 197–216 (2002).
  120. Roach, J.C., Glusman, G., Rowen, L., Kaur, A., Purcell, M.K., Smith, K.D., Hood, L.E., Aderem, A.: The evolution of vertebrate Toll-like receptors. *Proc. Natl. Acad. Sci. U. S. A.* 102, 9577–9582 (2005).
  121. Schukken, Y.H., Günther, J., Fitzpatrick, J., Fontaine, M.C., Goetze, L., Holst, O., Leigh, J., Petzl, W., Schuberth, H.-J., Sipka, A., Smith, D.G.E., Quesnell, R., Watts, J., Yancey, R., Zerbe, H., Gurjar, A., Zadoks, R.N., Seyfert, H.-M.: Host-response patterns of intramammary infections in dairy cows. *Vet. Immunol. Immunopathol.* 144, 270–289 (2011).
  122. Kumar, H., Kawai, T., Akira, S.: Toll-like receptors and innate immunity. *Biochem. Biophys. Res. Commun.* 388, 621–625 (2009).
  123. Jin, M.S., Lee, J.-O.: Structures of the toll-like receptor family and its ligand complexes. *Immunity.* 29, 182–191 (2008).
  124. Botos, I., Segal, D.M., Davies, D.R.: The structural biology of Toll-like receptors. *Structure.* 19, 447–59 (2011).
  125. O’Neill, L.A.J., Bowie, A.G.: The family of five: TIR-domain-containing adaptors in Toll-like receptor signalling. *Nat. Rev. Immunol.* 7, 353–364 (2007).
  126. Jin, M.S., Kim, S.E., Heo, J.Y., Lee, M.E., Kim, H.M., Paik, S.-G., Lee, H., Lee, J.-O.: Crystal structure of the TLR1-TLR2 heterodimer induced by binding of a tri-acylated lipopeptide. *Cell.* 130, 1071–82 (2007).

127. Kang, J.Y., Nan, X., Jin, M.S., Youn, S.-J., Ryu, Y.H., Mah, S., Han, S.H., Lee, H., Paik, S.-G., Lee, J.-O.: Recognition of lipopeptide patterns by Toll-like receptor 2-Toll-like receptor 6 heterodimer. *Immunity*. 31, 873–884 (2009).
128. Ohnishi, H., Tochio, H., Kato, Z., Orii, K.E., Li, A., Kimura, T., Hiroaki, H., Kondo, N., Shirakawa, M.: Structural basis for the multiple interactions of the MyD88 TIR domain in TLR4 signaling. *PNAS*. 106, 1–6 (2009).
129. Lin, S.-C., Lo, Y.-C., Wu, H.: Helical assembly in the MyD88-IRAK4-IRAK2 complex in TLR/IL-1R signalling. *Nature*. 465, 885–90 (2010).
130. Jones, K.J., Perris, A.D., Vernallis, A.B., Worthington, T., Lambert, P. a, Elliott, T.S.J.: Induction of inflammatory cytokines and nitric oxide in J774.2 cells and murine macrophages by lipoteichoic acid and related cell wall antigens from *Staphylococcus epidermidis*. *J. Med. Microbiol.* 54, 315–321 (2005).
131. Takeuchi, O., Hoshino, K., Kawai, T., Sanjo, H., Takada, H., Ogawa, O., Takeda, K., Akira, S.: Differential roles of TLR2 and TLR4 in recognition of gram-negative and gram-positive cell wall components. *Immunity*. 11, 443–451 (1999).
132. Pedersen, C.M., Figueroa-Perez, I., Boruwa, J., Lindner, B., Ulmer, A.J., Zähringer, U., Schmidt, R.R.: Synthesis of the core structure of the lipoteichoic acid of *Streptococcus pneumoniae*. *Chem. - A Eur. J.* 16, 12627–12641 (2010).
133. Hashimoto, M., Furuyashiki, M., Kaseya, R., Fukada, Y., Akimaru, M., Aoyama, K., Okuno, T., Tamura, T., Kirikae, T., Kirikae, F., Eiraku, N., Morioka, H., Fujimoto, Y., Fukase, K., Takashige, K., Moriya, Y., Kusumoto, S., Suda, Y.: Evidence of immunostimulating lipoprotein existing in the natural lipoteichoic acid fraction. *Infect. Immun.* 75, 1926–1932 (2007).
134. Graham, F.L., Smiley, J., Russell, W.C., Nairn, R.: Characteristics of a human cell line transformed by DNA from human adenovirus type 5. *J. Gen. Virol.* 36, 59–74 (1977).
135. Shaw, G., Morse, S., Ararat, M., Graham, F.L.: Preferential transformation of human neuronal cells by human adenoviruses and the origin of HEK 293 cells. *FASEB J.* 16, 869–871 (2002).
136. Farhat, K., Sauter, K.S., Brcic, M., Frey, J., Ulmer, A.J., Jungi, T.W.: The response of HEK293 cells transfected with bovine TLR2 to established pathogen-associated molecular patterns and to. *Vet. Immunol. Immunopathol.* 125, 326–336 (2008).
137. Godfrey, D.I., MacDonald, H.R., Kronenberg, M., Smyth, M.J., Van Kaer, L.: NKT cells: what's in a name? *Nat. Rev. Immunol.* 4, 231–237 (2004).
138. Brennan, P.J., Brigl, M., Brenner, M.B.: Invariant natural killer T cells: an innate activation scheme linked to diverse effector functions. *Nat. Rev. Immunol.* 13, 101–117 (2013).
139. Wu, L., Van Kaer, L.: Natural killer T cells in health and disease. *Front. Biosci.* 3, 236–251 (2011).

140. Simoni, Y., Diana, J., Ghazarian, L., Beaudoin, L., Lehuen, A.: Therapeutic manipulation of natural killer (NK) T cells in autoimmunity: are we close to reality? *Clin. Exp. Immunol.* 171, 8–19 (2013).
141. Aspeslagh, S., Nemcovic, M., Pauwels, N., Venken, K., Wang, J., Van Calenbergh, S., Zajonc, D.M., Elewaut, D.: Enhanced TCR footprint by a novel glycolipid increases NKT-dependent tumor protection. *J. Immunol.* doi:10.404, (2013).
142. Uldrich, A.P., Patel, O., Cameron, G., Pellicci, D.G., Day, E.B., Sullivan, L.C., Kyparissoudis, K., Kjer-Nielsen, L., Vivian, J.P., Cao, B., Brooks, A.G., Williams, S.J., Illarionov, P., Besra, G.S., Turner, S.J., Porcelli, S.A., McCluskey, J., Smyth, M.J., Rossjohn, J., Godfrey, D.I.: A semi-invariant V $\alpha$ 10+ T cell antigen receptor defines a population of natural killer T cells with distinct glycolipid antigen-recognition properties. *Nat. Immunol.* 12, 616–623 (2011).
143. Moody, D.B., Zajonc, D.M., Wilson, I. A.: Anatomy of CD1-lipid antigen complexes. *Nat. Rev. Immunol.* 5, 387–399 (2005).
144. Im, J.S., Arora, P., Bricard, G., Molano, A., Venkataswamy, M.M., Baine, I., Jerud, E.S., Goldberg, M.F., Baena, A., Yu, K.O.A., Ndongue, R.M., Howell, A.R., Yuan, W., Cresswell, P., Chang, Y.-T., Illarionov, P.A., Besra, G.S., Porcelli, S.A.: Kinetics and cellular site of glycolipid loading control the outcome of natural killer T cell activation. *Immunity.* 30, 888–898 (2009).
145. Venkataswamy, M.M., Porcelli, S.A.: Lipid and glycolipid antigens of CD1d-restricted natural killer T cells. *Semin. Immunol.* 22, 68–78 (2010).
146. Riollet, C., Rainard, P., Poutrel, B.: Cells and cytokines in inflammatory secretions of bovine mammary gland. *Adv. Exp. Med. Biol.* 480, 247–258 (2000).
147. Elazar, S., Gonen, E., Livneh-Kol, A., Rosenshine, I., Shpigel, N.Y.: Neutrophil recruitment in endotoxin-induced murine mastitis is strictly dependent on mammary alveolar macrophages. *Vet. Res.* 41, (2010).
148. Jiang, Z., Georgel, P., Du, X., Shamel, L., Sovath, S., Mudd, S., Huber, M., Kalis, C., Keck, S., Galanos, C., Freudenberg, M., Beutler, B.: CD14 is required for MyD88-independent LPS signaling. *Nat. Immunol.* 6, 565–570 (2005).
149. Sladek, Z., Rysanek, D.: The role of CD14 during resolution of experimentally induced *Staphylococcus aureus* and *Streptococcus uberis* mastitis. *Comp. Immunol. Microbiol. Infect. Dis.* 29, 243–262 (2006).
150. Sladek, Z., Ryznarova, H., Rysanek, D.: Macrophages of the bovine heifer mammary gland: morphological features during initiation and resolution of the inflammatory response. *Anat. Histol. Embryol.* 35, 116–124 (2006).
151. Paape, M.J.P., Bannerman, D.D.B., Zhaob, X., Lee, J.-W.: The bovine neutrophil: structure and function in blood and milk. *Vet. Res.* 34, 597–627 (2003).
152. Thielen, M.A., Mielenz, M., Hiss, S., Zerbe, H., Petzl, W., Schuberth, H.-J., Seyfert, H.-M., Sauerwein, H.: Cellular localization of haptoglobin mRNA in the experimentally infected bovine mammary gland. *J. Dairy Sci.* 90, 1215–1219 (2007).

153. Pyörälä, S., Hovinen, M., Simojoki, H., Fitzpatrick, J., Eckersall, P.D., Orro, T.: Acute phase proteins in milk in naturally acquired bovine mastitis caused by different pathogens. *Vet. Rec.* 168, 535 (2011).
154. Pyörälä, S.: Mastitis in post-partum dairy cows. *Reprod. Domest. Anim. Zuchthygiene.* 43 Suppl 2, 252–259 (2008).
155. Goldammer, T., Zerbe, H., Molenaar, A., Schuberth, H., Brunner, R.M., Kata, S.R., Seyfert, H.M.: Mastitis increases mammary mRNA abundance of  $\beta$ -defensin 5, but not TLR9 in cattle. *Clin. Diagn. Lab. Immunol.* 11, 174–185 (2004).
156. Petzl, W., Zerbe, H., Günther, J., Yang, W., Seifert, H.-M., Nürnberg, G., Schuberth, H.-J.: *Escherichia coli*, but not *Staphylococcus aureus* triggers an early increased expression of factors contributing to the innate immune defense in the udder of the cow. *Vet. Res.* 39, (2008).
157. Schukken, Y.H., Hertl, J., Bar, D., Bennett, G.J., González, R.N., Rauch, B.J., Santisteban, C., Schulte, H.F., Tauer, L., Welcome, F.L., Gröhn, Y.T.: Effects of repeated gram-positive and gram-negative clinical mastitis episodes on milk yield loss in Holstein dairy cows. *J. Dairy Sci.* 92, 3091–3105 (2009).
158. Bannerman, D.D., Paape, M.J., Lee, J.-W., Zhao, X., Hope, J.C., Rainard, P.: *Escherichia coli* and *Staphylococcus aureus* elicit differential innate immune responses following intramammary infection. *Clin. Diagn. Lab. Immunol.* 11, 463–472 (2004).
159. Lutzow, Y.C.S., Donaldson, L., Gray, C.P., Vuocolo, T., Pearson, R.D., Reverter, A., Byrne, K.A., Sheehy, P.A., Windon, R., Tellam, R.L.: Identification of immune genes and proteins involved in the response of bovine mammary tissue to *Staphylococcus aureus* infection. *BMC Vet. Res.* 4, (2008).
160. Jensen, K., Günther, J., Talbot, R., Petzl, W., Zerbe, H., Schuberth, H.-J., Seyfert, H.-M., Glass, E.J.: *Escherichia coli*- and *Staphylococcus aureus*- induced mastitis differentially modulate transcriptional responses in neighbouring uninfected bovine mammary gland quarters. *BMC Genomics.* 14, (2013).
161. Lara-Zárate, L., López-Meza, J.E., Ochoa-Zarzosa, A.: *Staphylococcus aureus* inhibits nuclear factor kappa B activation mediated by prolactin in bovine mammary epithelial cells. *Microb. Pathog.* 51, 313–318 (2011).
162. Bannerman, D.D., Paape, M.J., Goff, J.P.G., Kimura, K.K., Lippolis, J.D., Hope, J.C.: Innate immune response to intramammary infection with *Serratia marcescens* and *Streptococcus uberis*. *Vet. Res.* 35, 681–700 (2004).
163. Melchior, M.B., Fink-Gremmels, J., Gaastra, W.: Comparative assessment of the antimicrobial susceptibility of *Staphylococcus aureus* isolates from bovine mastitis in biofilm versus planktonic culture. *J. Vet. Med. B.* 53, 326–332 (2006).
164. Almeida, R.A., Dunlap, J.R., Oliver, S.P.: Binding of host factors influences internalization and intracellular trafficking of *Streptococcus uberis* in bovine mammary epithelial cells. *Vet. Med. Int.* (2010).

165. Calvino, L.F., Oliver, S.P.: Characterization of mechanisms involved in uptake of *Streptococcus dysgalactiae* by bovine mammary epithelial cells. *Vet. Microbiol.* 63, 261–274 (1998).
166. Correa, A.B.A., Americo, M.A., Oliviera, I.C.M., Silva, L.G., de Mattos, M.C., Ferreira, A.M.M., Couceiro, J.N.S.S., Fracalanza, S.E.L., Benchetrit, L.C.: Virulent characteristics of genetically related isolated of Group B streptococci from bovines and humans. *Vet. Microbiol.* 143, 429–433 (2010).
167. White, L.J., Schukken, Y.H., Dogan, B., Green, L., Döpfer, D., Chappell, M.J., Medley, G.F.: Modelling the dynamics of intramammary *E. coli* infections in dairy cows: understanding mechanisms that distinguish transient from persistent infections. *Vet. Res.* 41, (2010).
168. Ostensson, K., Lam, V., Sjögren, N., Wredle, E.: Prevalence of subclinical mastitis and isolated udder pathogens in dairy cows in Southern Vietnam. *Trop. Anim. Health Prod.* DOI 10.1007/s11250-012-0320-0 (2012).
169. Mungube, E.O., Tenhagen, B.A., Regassa, F., Kyule, M.N., Shiferaw, Y., Kassa, T., Baumann, M.P.O.: Reduced milk production in udder quarters with subclinical mastitis and associated economic losses in crossbred dairy cows in Ethiopia. *Trop. Anim. Health Prod.* 37, 503–512 (2005).
170. Hill, A.W., Finch, J.M., Field, T.R., Leigh, J.A.: Immune modification of the pathogenesis of *Streptococcus uberis* mastitis in the dairy cow. *FEMS Immunol. Med. Microbiol.* 8, 109–117 (1994).
171. Finch, J.M., Hill, A.W., Field, T.R., Leigh, J.A.: Local vaccination with killed *Streptococcus uberis* protects the bovine mammary gland against experimental intramammary challenge with the homologous strain. *Infect. Immun.* 62, 3599–3603 (1994).
172. Leigh, J.A., Finch, J.M., Field, T.R., Real, N.C., Winter, A., Walton, A.W., Hodgkinson, S.M.: Vaccination with the plasminogen activator from *Streptococcus uberis* induces an inhibitory response and protects against experimental infection in the dairy cow. *Vaccine.* 17, 851–7 (1999).
173. Pereira, U.P., Oliveira, D.G.S., Mesquita, L.R., Costa, G.M., Pereira, L.J.: Efficacy of *Staphylococcus aureus* vaccines for bovine mastitis: a systematic review. *Vet. Microbiol.* 148, 117–124 (2011).
174. Use, I.: Brain Heart Infusion (Broth Media). BD, Difco™ & BBL™ Manual, 2nd Edition.
175. Todd, E.W.: Antigenic streptococcal hemolysin. *J. Exp. Med.* 55, 267–280 (1932).
176. Todd Hewitt Broth. Acumedia NEOGEN Corp. PI 7161, Rev 04. (2010).
177. RPMI 1640 liquid and powder medium. Biochrom Product Information Catalog. pp. 62–63 (2012).
178. Cell Culture Media. ATCC® Animal Cell Culture Guide. pp. 13–14. American Type Culture Collection (2013).

179. Dittmar, K., Mamat, U., Whiting, M., Goldmann, T., Reinhard, K., Guillen, S.: Techniques of DNA-studies on prehispanic ectoparasites (*Pulex* sp., *Pulicidae*, Siphonaptera) from Animal mummies of the Chiribaya culture, southern Peru. Mem. Inst. Oswaldo Cruz. 98 Suppl 1, 53–58 (2003).
180. Morath, S., Geyer, A., Hartung, T.: Structure-function relationship of cytokine induction by lipoteichoic acid from *Staphylococcus aureus*. J. Exp. Med. 193, 393–398 (2001).
181. Fischer, W., Koch, H.U., Haas, R.: Improved preparation of lipoteichoic acids. Fed. Eur. Biochem. Soc. J. 133, 523–530 (1983).
182. Lowry, O.H., Roberts, N.R., Leiner, K.Y., Wu, M.-L., Farr, A., Albers, R.W.: The quantitative histochemistry of brain. J. Biol. Chem. 207, 1–17 (1954).
183. Bligh, E.G., Dyer, W.J.: A rapid method of total lipid extraction and purification. Can. J. Biochem. Physiol. 37, 911–917 (1959).
184. Dittmer, J.C., Lester, R.L.: A simple, specific spray for the detection of phospholipids on thin-layer chromatograms. J. Lipid Res. 15, 126–127 (1964).
185. Sánchez Carballo, P.M., Vilen, H., Palva, A., Holst, O.: Structural characterization of teichoic acids from *Lactobacillus brevis*. Carbohydr. Res. 345, 538–542 (2010).
186. Bychowska, A., Theilacker, C., Czerwicka, M., Marszewska, K., Huebner, J., Holst, O., Stepnowski, P., Kaczyński, Z.: Chemical structure of wall teichoic acid isolated from *Enterococcus faecium* strain U0317. Carbohydr. Res. 346, 2816–2819 (2011).
187. Kamerling, J.P., Gerwig, G.J.: Strategies for the structural analysis of carbohydrates. Introduction to Glycoscience; Synthesis of Carbohydrates, Oxford, UK (2007).
188. Hakomori, S.: A rapid permethylation of glycolipid, and polysaccharide catalyzed by methylsulfinyl carbanion in dimethyl sulfoxide. J. Biochem. 55, 205–208 (1964).
189. Holst, O.: Deacylation of lipopolysaccharides and isolation of oligosaccharide phosphates. Methods in Molecular Biology. 345–353. Clifton, N.J. (2000).
190. Yang, W., Molenaar, A., Kurts-Ebert, B., Seyfert, H.-M.: NF-kappaB factors are essential, but not the switch, for pathogen-related induction of the bovine  $\beta$ -defensin 5-encoding gene in mammary epithelial cells. Mol. Immunol. 43, 210–225 (2006).
191. Zähringer, U., Lindner, B., Knirel, Y.A., Van Den Akker, W.M.R., Hiestand, R., Heine, H., Dehio, C.: Structure and biological activity of the short-chain lipopolysaccharide from *Bartonella henselae* ATCC 49882T. J. Biol. Chem. 279, 21046–21054 (2004).
192. Zähringer, U., Lindner, B., Inamura, S., Heine, H., Alexander, C.: TLR2 - promiscuous or specific? A critical re-evaluation of a receptor expressing apparent broad specificity. Immunobiology. 213, 205–224 (2008).
193. Morr, M., Takeuchi, O., Akira, S., Simon, M.M., Mühradt, P.F.: Differential recognition of structural details of bacterial lipopeptides by toll-like receptors. Eur. J. Immunol. 32, 3337–3347 (2002).

194. Böyum, A.: Separation of leukocytes from blood and bone marrow. Introduction. Scand. J. Clin. Lab. Investig. Suppl. 97, 7 (1968).
195. Bezbradica, J.S., Stanic, A.K., Joyce, S.: Characterization and functional analysis of mouse invariant natural T (iNKT) cells. Curr. Protoc. Immunol. Chapter 14, 14.13.1–14.13.27 (2006).
196. Kinjo, Y., Pei, B., Bufali, S., Raju, R., Richardson, S.K., Imamura, M., Fujio, M., Wu, D., Khurana, A., Kawahara, K., Wong, C.-H., Howell, A.R., Seeberger, P.H., Kronenberg, M.: Natural *Sphingomonas* glycolipids vary greatly in their ability to activate natural killer T cells. Chem. Biol. 15, 654–664 (2008).
197. Kinjo, Y., Illarionov, P., Vela, J.L., Pei, B., Girardi, E., Li, X., Li, Y., Imamura, M., Kaneko, Y., Okawara, A., Miyazaki, Y., Gómez-Velasco, A., Rogers, P., Dahesh, S., Uchiyama, S., Khurana, A., Kawahara, K., Yesilkaya, H., Andrew, P.W., Wong, C.-H., Kawakami, K., Nizet, V., Besra, G.S., Tsuji, M., Zajonc, D.M., Kronenberg, M.: Invariant natural killer T cells recognize glycolipids from pathogenic Gram-positive bacteria. Nat. Immunol. 12, 966–74 (2011).
198. Mancuso, G., Midiri, A., Beninati, C., Biondo, C., Galbo, R., Akira, S., Henneke, P., Golenbock, D., Teti, G.: Dual role of TLR2 and myeloid differentiation factor 88 in a mouse model of invasive Group B streptococcal disease. J. Immunol. 172, 6324–6329 (2004).
199. Goldschmidt, J.C., Panos, C.: Teichoic acids of *Streptococcus agalactiae*: chemistry, cytotoxicity, and effect on bacterial adherence to human cells in tissue culture. Infect. Immun. 43, 670–677 (1984).
200. Fischer, K., Stein, K., Ulmer, A.J., Lindner, B., Heine, H., Holst, O.: Cytokine-inducing lipoteichoic acids of the allergy-protective bacterium *Lactococcus lactis* G121 do not activate via Toll-like receptor 2. Glycobiology. 21, 1588–95 (2011).
201. Fischer, W.: Phosphocholine of pneumococcal teichoic acids: role in bacterial physiology and pneumococcal infection. Res. Microbiol. 151, 421–427 (2000).
202. Fabretti, F., Theilacker, C., Baldassarri, L., Kaczynski, Z., Kropec, A., Holst, O., Huebner, J.: Alanine esters of enterococcal lipoteichoic acid play a role in biofilm formation and resistance to antimicrobial peptides. Infect. Immun. 74, 4708–4714 (2006).
203. Theilacker, C., Kaczynski, Z., Kropec, A., Fabretti, F., Sange, T., Holst, O., Huebner, J.: Opsonic antibodies to *Enterococcus faecalis* strain 12030 are directed against lipoteichoic acid. Infect. Immun. 74, 5703–5712 (2006).
204. Perego, M., Glaser, P., Minutello, A., Strauch, M.A., Leopold, K., Fischer, W.: Incorporation of D-alanine into lipoteichoic acid and wall teichoic acid in *Bacillus subtilis*. Identification of genes and regulation. J. Biol. Chem. 270, 15598–15606 (1995).
205. Silhavy, T.J., Kahne, D., Walker, S.: The bacterial cell envelope. Cold Spring Harb. Perspect. Biol. 2, 1–16 (2010).
206. Ludwig, W., Seewaldt, E., Kilpper-Bälz, R., Schleifer, K.H., Magrum, L., Woese, C.R., Fox, G.E., Stackebrandt, E.: The phylogenetic position of *Streptococcus* and *Enterococcus*. J. Gen. Microbiol. 131, 543–551 (1985).

207. Atilano, M.L., Pereira, P.M., Yates, J., Reed, P., Veiga, H., Pinho, M.G., Filipe, S.R.: Teichoic acids are temporal and spatial regulators of peptidoglycan cross-linking in *Staphylococcus aureus*. *Proc. Natl. Acad. Sci. U. S. A.* 107, 18991–18996 (2010).
208. Reichmann, N.T., Gründling, A.: Location, synthesis and function of glycolipids and polyglycerolphosphate lipoteichoic acid in Gram-positive bacteria of the *Phylum firmicutes*. *FEMS Microbiol. Lett.* 9999, 1–9 (2011).
209. Nealon, T.J., Mattingly, S.J.: Kinetic and chemical analyses of the biologic significance of lipoteichoic acids in mediating adherence of serotype III Group B streptococci. *Infect. Immun.* 50, 107–115 (1985).
210. Loos, M., Clas, F., Fischer, W.: Interaction of purified lipoteichoic acid with the classical complement pathway. *Infect. Immun.* 53, 595–599 (1986).
211. Lynch, N.J., Roscher, S., Hartung, T., Morath, S., Matsushita, M., Maennel, D.N., Kuraya, M., Fujita, T., Schwaeble, W.J.: L-ficolin specifically binds to lipoteichoic acid, a cell wall constituent of Gram-positive bacteria, and activates the lectin pathway of complement. *J. Immunol.* 172, 1198–1202 (2004).
212. Zelová, H., Hošek, J.: TNF- $\alpha$  signaling and inflammation: interactions between old acquaintances. *Inflamm. Res.* 62, 641–651 (2013).
213. Heinrich, P.C., Behrmann, I., Haan, S., Hermanns, H.M., Müller-Newen, G., Schaper, F.: Principles of interleukin (IL)-6-type cytokine signaling and its regulation. *Biochem. J.* 374, 1–20 (2003).
214. Erbing, B., Kenne, L., Lindberg, B., Helting, T., Hammerschmid, F.: Structural studies of a teichoic acid from *Streptococcus agalactiae* type III. *Carbohydr. Res.* 156, 147–155 (1986).
215. Cumley, N.J., Smith, L.M., Anthony, M., May, R.C.: The CovS/CovR acid response regulator is required for intracellular survival of Group B *Streptococcus* in macrophages. *Infect. Immun.* 80, 1650–1661 (2012).
216. Domenech, M., Ramos-Sevillano, E., García, E., Moscoso, M., Yuste, J.: Biofilm formation avoids complement immunity and phagocytosis of *Streptococcus pneumoniae*. *Infect. Immun.* 81, 2606–2615 (2013).
217. Kristian, S.A., Datta, V., Weidenmaier, C., Kansal, R., Fedtke, I., Peschel, A., Gallo, R.L., Nizet, V.: D-alanylation of teichoic acids promotes Group A *Streptococcus* antimicrobial peptide resistance, neutrophil survival, and epithelial cell invasion. *J. Bacteriol.* 187, 6719–6725 (2005).
218. Valentin-Weigand, P., Traore, M.Y., Blobel, H., Chhatwal, G.S.: Role of alpha 2-macroglobulin in phagocytosis of Group A and C streptococci. *FEMS Microbiol. Lett.* 58, 321–324 (1990).
219. Schuberth, H.-J., Dahnke, J., Leibold, W., Seyfert, H.-M., Zerbe, H.: Bacterial pathogen associated molecular pattern and superantigens indirectly induce the accelerated death of bovine neutrophilic granulocytes. *Berl. Munch. Tierarztl. Wochenschr.* 117, 464–471 (2004).

220. Calvino, L.F., Almeida, R.A., Oliver, S.: Influence of *Streptococcus dysgalactiae* surface hydrophobicity on adherence to mammary epithelial cells and phagocytosis by mammary macrophages. *J. Vet. Med. Ser. B.* 43, (1996).
221. Fischer, W., Nakano, M., Laine, R.A., Bohrer, W.: On the relationship between glycerophosphoglycolipids and lipoteichoic acids in Gram-positive bacteria. I. The occurrence phosphoglycolipids. *Biochim. Biophys. Acta.* 528, 288–297 (1978).
222. Czabańska, A.: Immunochemical investigations of the cell envelope components isolated from *Streptococcus uberis*. PhD Work. (2013).
223. Melchior, M.B., Vaarkamp, H., Fink-Gremmels, J.: Biofilms: a role in recurrent mastitis infections? *Vet. J.* 171, 398–407 (2006).
224. Schröder, N.W., Opitz, B., Lamping, N., Michelsen, K.S., Zähringer, U., Göbel, U.B., Schumann, R.R.: Involvement of lipopolysaccharide binding protein, CD14, and Toll-like receptors in the initiation of innate immune responses by *Treponema* glycolipids. *J. Immunol.* 165, 2683–2693 (2000).
225. Kawano, T., Cui, J., Koezuka, Y., Toura, I., Kaneko, Y., Sato, H., Kondo, E., Harada, M., Koseki, H., Nakayama, T., Tanaka, Y., Taniguchi, M.: Natural killer-like nonspecific tumor cell lysis mediated by specific ligand-activated Valpha14 NKT cells. *Proc. Natl. Acad. Sci. U. S. A.* 95, 5690–5693 (1998).
226. Joyce, S., Girardi, E., Zajonc, D.M.: NKT cell ligand recognition logic: molecular basis for a synaptic duet and transmission of inflammatory effectors. *J. Immunol.* 187, 1081–1089 (2011).
227. Fischer, W., Behr, T., Hartmann, R., Peter-Katalinić, J., Egge, H.: Teichoic acid and lipoteichoic acid of *Streptococcus pneumoniae* possess identical chain structures. A reinvestigation of teichoid acid (C polysaccharide). *Fed. Eur. Biochem. Soc. J.* 215, 851–857 (1993).
228. Bhavsar, A.P., Brown, E.D.: Cell wall assembly in *Bacillus subtilis*: how spirals and spaces challenge paradigms. *Mol. Microbiol.* 60, 1077–1090 (2006).
229. Sutcliffe, I.C., Black, G.W., Harrington, D.J.: Bioinformatic insights into the biosynthesis of the Group B carbohydrate in *Streptococcus agalactiae*. *Microbiology.* 154, 1354–1363 (2008).
230. Kessler, R.E., van de Rijn, I., McCarty, M.: Characterization and localization of the enzymatic deacylation of lipoteichoic acid in Group A streptococci. *J. Exp. Med.* 150, 1498–1509 (1979).
231. Kallman, J., Schollin, J., Schalen, C., Erlandsson, A., Kihlstrom, E.: Impaired phagocytosis and opsonisation towards Group B streptococci in preterm neonates. *Arch. Dis. Child. Fetal Neonatal Ed.* 78, F46–F50 (1998).
232. Leigh, J.A., Field, T.R.: *Streptococcus uberis* resists the bactericidal action of bovine neutrophils despite the presence of bound immunoglobulin. *Infect. Immun.* 62, 1854–1859 (1994).

233. Sutra, L., Rainard, P., Poutrel, B.: Phagocytosis of mastitis isolates of *Staphylococcus aureus* and expression of type 5 capsular polysaccharide are influenced by growth in the presence of milk. *J. Clin. Microbiol.* 28, 2253–2258 (1990).
234. Tanabe, S.-I., Bonifait, L., Fittipaldi, N., Grignon, L., Gottschalk, M., Grenier, D.: Pleiotropic effects of polysaccharide capsule loss on selected biological properties of *Streptococcus suis*. *Can. J. Vet. Res.* 74, 65–70 (2010).
235. Sanders, M.E., Taylor, S., Tullos, N., Norcross, E.W., Moore, Q.C., Thompson, H., King, L.B., Marquart, M.E.: Passive immunization with Pneumovax® 23 and pneumolysin in combination with vancomycin for pneumococcal endophthalmitis. *BMC Ophthalmol.* 13, 8 (2013).
236. Edmond, K.M., Kortsalioudaki, C., Scott, S., Schrag, S.J., Zaidi, A.K.M., Cousens, S., Heath, P.T.: Group B streptococcal disease in infants aged younger than 3 months: systematic review and meta-analysis. *Lancet.* 379, 547–556 (2012).
237. Rubens, C.E., Wessels, M.R., Heggen, L.M., Kasper, D.L.: Transposon mutagenesis of type III Group B *Streptococcus*: correlation of capsule expression with virulence. *Proc. Natl. Acad. Sci. U. S. A.* 84, 7208–7212 (1987).
238. Jones, C.: Vaccines based on the cell surface carbohydrates of pathogenic bacteria. *An. Acad. Bras. Cienc.* 77, 293–324 (2005).
239. Martins, E.R., Melo-Cristino, J., Ramirez, M.: Evidence for rare capsular switching in *Streptococcus agalactiae*. *J. Bacteriol.* 192, 1361–1369 (2010).
240. Bellais, S., Six, A., Fouet, A., Longo, M., Dmytruk, N., Glaser, P., Trieu-Cuot, P., Poyart, C.: Capsular switching in Group B *Streptococcus* CC17 hypervirulent clone: a future challenge for polysaccharide vaccine development. *J. Infect. Dis.* 206, 1745–1752 (2012).
241. Rato, M.G., Bexiga, R., Florindo, C., Cavaco, L.M., Vilela, C.L., Santos-Sanches, I.: Antimicrobial resistance and molecular epidemiology of streptococci from bovine mastitis. *Vet. Microbiol.* 161, 286–294 (2013).
242. Michon, F., Katzenellenbogen, E., Kasper, D.L., Jennings, H.J.: Structure of the complex group-specific polysaccharide of Group B *Streptococcus*. *Biochemistry.* 26, 476–486 (1987).
243. Michon, F., Brisson, J.-R., Dell, A., Kasper, D.L., Jennings, H.J.: Multiantennary group-specific polysaccharide of Group B *Streptococcus*. *Biochemistry.* 27, 5341–5351 (1988).
244. Caliot, É., Dramsi, S., Chapot-Chartier, M.-P., Courtin, P., Kulakauskas, S., Péchoux, C., Trieu-Cuot, P., Mistou, M.-Y.: Role of the Group B antigen of *Streptococcus agalactiae*: a peptidoglycan-anchored polysaccharide involved in cell wall biogenesis. *PLoS Pathog.* 8, 1–12 (2012).
245. Coligan, J.E., Schnute, W.C., Kindt, T.J.: Immunochemical and chemical studies on streptococcal group-specific carbohydrates. *J. Immunol.* 114, 1654–1658 (1975).
246. Coligan, J.E., Kindt, T.J., Krause, R.M.: Structure of the streptococcal Groups A, A-variant and C carbohydrates. *Immunochemistry.* 15, 755–760 (1978).

247. Vinogradov, E., Petersen, B., Bock, K.: Structural analysis of the intact polysaccharide mannan from *Saccharomyces cerevisiae* yeast using  $^1\text{H}$  and  $^{13}\text{C}$  NMR spectroscopy at 750 MHz. *Carbohydr. Res.* 307, 177–183 (1998).
248. Shibata, N., Kobayashi, H., Suzuki, S.: Immunochemistry of pathogenic yeast, *Candida* species, focusing on mannan. *Proc. Japan Acad. Ser. B.* 88, 250–265 (2012).
249. Corsaro, M.M., De Castro, C., Evidente, A., Lanzetta, R., Molinaro, A., Mugnai, L., Parrilli, M., Surico, G.: Chemical structure of two phytotoxic exopolysaccharides produced by *Phomopsis foeniculi*. *Carbohydr. Res.* 308, 349–357 (1998).
250. Sandal, I., Inzana, T.J., Molinaro, A., De Castro, C., Shao, J.Q., Apicella, M.A., Cox, A.D., St Michael, F., Berg, G.: Identification, structure, and characterization of an exopolysaccharide produced by *Histophilus somni* during biofilm formation. *BMC Microbiol.* 11, (2011).
251. Abdelsalam, M., Chen, S.-C., Yoshida, T.: Dissemination of streptococcal pyrogenic exotoxin G (*spegg*) with an IS-like element in fish isolates of *Streptococcus dysgalactiae*. *FEMS Microbiol. Lett.* 309, 105–113 (2010).
252. Almeida, A., Albuquerque, P., Araujo, R., Ribeiro, N., Tavares, F.: Detection and discrimination of common bovine mastitis-causing streptococci. *Vet. Microbiol.* 164, 370–377 (2013).



## Curriculum vitae



## List of publications contributing to this study

### Printed publications:

Duda, K. A., Neiwert, O., Seyfert, H.-M., Dobrindt, U., Engelmann, S., Holst, O.: Characterization of pathogen associated molecular patterns isolated from the causative agents of bovine mastitis. *Glycoconj. J.* 28, 301-302 (2011)

Czabańska, A., Neiwert, O., Lindner, B., Leigh, J., Holst, O., Duda, K. A.: Structural analysis of the lipoteichoic acids isolated from bovine mastitis *Streptococcus uberis* 233, *Streptococcus dysgalactiae* 2023 and *Streptococcus agalactiae* 0250. *Carbohydr. Res.* 361, 200-205 (2012)

### Selected poster presentations:

Neiwert, O., Duda, K. A., Leigh, J., Holst, O.: The structure of the lipoteichoic acids of *Streptococcus agalactiae* 0250 and *Streptococcus dysgalactiae* 2023 bovine mastitis isolates. 22<sup>nd</sup> Joint Glycobiology Meeting, November 22 – 29, 2011, Lille, France

Neiwert, O., Duda, K. A., Leigh, J., Holst, O.: Structural analysis of the wall teichoic acids of *Streptococcus agalactiae* 0250 and *Streptococcus dysgalactiae* 2023. 5<sup>th</sup> Baltic Meeting on Microbial Carbohydrates, September 2 – 6, 2012, Suzdal, Russia

Neiwert, O., Duda, K. A., Lindner, B., Leigh, J., Holst, O.: Structural investigation of the cell envelope components isolated from *Streptococcus agalactiae* 0250 and *Streptococcus dysgalactiae* 2023 bovine mastitis isolates. EuroCarb17, July 7 – 11, 2013, Tel-Aviv, Israel



## Acknowledgements

I would like to express my gratitude to my Supervisor Prof. Dr. Otto Holst for giving me the opportunity to carry out this PhD thesis in his lab, for showing me the fascinating world of carbohydrates, for fruitful discussions and support during all phases of the work.

I am very grateful to my Co-Supervisor Prof. Dr. Hans-Joachim Schuberth from the Veterinary Institute of Hannover for the great support and discussions of immunological part in the PhD thesis. Special thanks to Prof. Dr. Hans-Joachim Schuberth and Dr. Jamal Hussen for the great performance of the phagocytosis experiments.

Thanks to Prof. Dr. James Leigh from the University of Nottingham for the idea of the structural investigation of the bovine mastitis streptococci, for kindly proving of the bacterial isolates, and for the sharing of his knowledge in the bovine mastitis pathogenesis research.

I am very grateful to Dr. Katarzina A. Duda for teaching me to analyze the 2D NMR spectra, for her competent support and advice in experimental and publishing skills.

I thank Prof. Dr. Holger Heine and Ina Goroncy from the Division of Innate Immunity, RCB for good cooperation and their excellent work of the HEK293 *in vitro* tests, and Prof. Dr. Hans-Martin Seyfert and Dr. Juliane Günther from FBN of Dummerstorf for the tests with HEK293 cells transfected with boTLR2. I am grateful to Dr. Nestor Gonzalez Roldan from the Division of Immunobiology, RCB for the investigation of the recognition of the glycolipids by NKT cells.

I thank Prof. Dr. Buko Lindner, Helga Lüthje und Brigitte Kunst for performance of ESI/MS and MALDI-TOF experiments. I am grateful to Heiko Käßner und Dr. Nicolas Gisch for excellent performance of NMR experiments and Dr. Nicolas Gisch also for some fruitful discussions.

I thank Dr. Uwe Mamat for the help with anion-exchange chromatography. Jasmin Tiefenbach and Prof. Dr. Goldmann are acknowledged for the performance of TEM pictures.

I am grateful to Prof. Dr. Tamás Laskay for the examination of this thesis as a second referee. I also want to thank Prof. Dr. Thomas Peters for taking the chair of the doctoral examination.

Moreover, I wish to thank Regina Engel and Herman Moll for the great performance of MS experiments and for the good explanations of their biochemistry. I am grateful to my colleagues Katharina Jakob and Sylvia Düpow for the technical support and advice in the lab, Kathleen Fischer and Anna Czabanska for help and advice in the lab, Volker Grote for amino acids determination and Rainer Bartels for technical support of the computer. I am very grateful to Natalja Redinger for her friendship and her support in the PhD time.

I am very thankful to my family, my husband, my children Sophia and Linus and my friends for their love and support. I appreciate you all for being an important part of my life!



## **Erklärung**

Die Arbeit wurde unter der Betreuung von Herrn Prof. Dr. Otto Holst (Forschungszentrum Borstel, Asthma und Allergie, Strukturbiochemie) von August 2010 bis Juli 2013 durchgeführt.

Ich versichere, dass ich die Dissertation ohne fremde Hilfe angefertigt und keine anderen als die angegebenen Hilfsmittel verwendet habe. Weder vorher noch gleichzeitig habe ich andernorts einen Zulassungsantrag gestellt oder diese Dissertation vorgelegt. Ich habe mich bisher noch keinem Promotionsverfahren unterzogen.

Lübeck, den 09.10.2013

Olga Neiwert